

**Investigating the regulation of tumour associated
lipogenesis using the model organism,
Saccharomyces cerevisiae.**

By

Alexander Agius BSc (Hons)

A thesis submitted in partial fulfilment of the requirements for the degree of: **MSc (by
Research)** at the University of Central Lancashire

January 2018

Student declaration form



Concurrent registration for two or more academic awards

*I declare that while registered as a candidate for the research degree, I have not been a registered candidate or enrolled student for another award of the University or other academic or professional institution.

Material submitted for another award

*I declare that no material contained in the thesis has been used in any other submission for an academic award and is solely my own work

Collaboration

Where a candidate's research programme is part of a collaboration project, the thesis must indicate in addition clearly the candidate's individual contribution and the extent of the collaboration. Please state below: N/A.

Signature of candidate

A handwritten signature in black ink, appearing to read "A. Agius", is written over a horizontal dashed line.

Type of award: Master of Science by Research

School: Pharmacy and Biomedical Sciences.

Contents

Student declaration form.....	2
List of tables and illustrative material	4
Abstract	6
Acknowledgements.....	8
Abbreviations	8
1. Introduction.....	12
1.1 Cancer	12
1.2 Signalling pathways.....	12
1.2.1 AMP-activated protein kinase (AMPK).....	13
1.2.2 Mechanistic target of rapamycin (mTOR)	14
1.2.3 Mitogen activated protein kinases (MAPK)	15
1.2.4 Sterol regulatory element-binding proteins (SREBP).....	18
1.3 Lipids including lipogenesis	19
1.3 Metabolic switch in cancer.....	20
1.4 Neutral lipids	21
1.4.1 Lipid Droplet formation	24
1.5 Use of yeast as a model organism	24
1.5.1 MAPK in <i>Saccharomyces cerevisiae</i>	25
1.5.2 Lipogenesis in <i>Saccharomyces cerevisiae</i>	28
2. Materials and Methods.....	30
2.1 Yeast strains	30
2.1.1 Growth Media.....	32
2.1.2 Growth curves	32
2.2 Nile red lipid screening	33
2.3 Yeast genomic DNA extraction.....	34
2.3.1 Polymerase chain reaction (PCR)	34
2.3.1.1 Amplification of the <i>SCH9</i> gene from <i>S. cerevisiae</i> gDNA by PCR	35
2.3.1.2 Amplification of <i>SCH9</i> Deletion and 3HA tagging cassettes.....	36
2.3.1.3 Amplification of <i>DGA1</i> from <i>S. cerevisiae</i> gDNA by PCR.....	37
2.3.1.4 Mutagenesis of <i>DGA1</i>	37
2.4.1 Cloning PCR products into vectors.....	40
2.4.1.1 Cloning PCR products into a TOPO vector.....	41
2.4.1.2 Cloning PCR products into pRS vectors	41
2.4.1.3 Transformation of cassettes into <i>S. cerevisiae</i>	42
2.5 SDS-PAGE and western blotting	43
2.5.1 Denatured protein extraction	43
2.5.2 Gels of protein extractions.....	44

2.5.3 Western blotting	44
2.5.4 Phos-tag™	45
3.0 Results.....	46
3.1. The MAPK Hog1 is required for neutral lipid accumulation	46
3.2 Hog1p phosphorylation is seen as cells began to accumulate neutral lipid	53
3.3 Hog1p activation appears to be Pbs2p independent.....	54
3.4 Sch9p is required for neutral lipid accumulation	61
3.5 Hog1p is a potential target of the protein kinase, Sch9p.....	67
3.6 Deletion of <i>MSN2/4</i> and <i>DGA1</i> result in a reduction of neutral lipid levels	69
3.7 Dga1p appears to be a downstream target of Hog1	74
3.8 Dga1p contains 4 potential MAPK sites.....	78
3.9 Tagged <i>DGA1</i> is not detectable by Western Blotting	79
4.0 Discussion	84
The MAPK Hog1 is required for neutral lipid accumulation.....	84
Regulation of neutral lipid accumulation via Hog1p is Pbs2p independent.	87
Sch9p is required for neutral lipid accumulation	93
Hog1p is a potential target of the protein kinase, Sch9p.....	95
In neutral lipid accumulation, Msn2/4p and Dga1 are potential downstream targets of Hog1p	99
5.0 Appendix.....	109
6.0 References	112

List of tables and illustrative material

Figure 1.1 AMPK promotes cell survival.	16
Figure 1.2. mTORC1 promotes de novo lipogenesis through the activation of SREBP-1.....	17
Figure 1.3. The Ras/Raf/MEK/ERK cascade.....	19
Figure 1.4 The process of mammalian lipogenesis.	22
Figure 1.5 TAG metabolism via different pathways (Athenstaedt et al 2006).	25
Figure 1.6 Conservation of the p38 MAPK pathway between mammals and <i>S. cerevisiae</i>	28
Figure 1.7 The HOG MAPK pathway of <i>S. cerevisiae</i> (Rostron 2015).....	29
Figure 1.8 Comparison of lipid biosynthesis and its regulation in mammals and yeast.....	31
Table 2.1: <i>S. cerevisiae</i> strains used.	32
Table 2.2: Table of primers designed and utilised for PCR.	36
Table 2.3: Table of plasmids utilised in this study	42
Figure 3.1. Growth curve of <i>S. cerevisiae</i> wild type and <i>ssk2Δ</i> under normal conditions in yeast nitrogen base medium (YNB).....	50

Figure 3.2. Growth curve of <i>S. cerevisiae</i> wild type and <i>ste11Δ</i> under normal conditions in yeast nitrogen base medium (YNB).....	50
Figure 3.3. Growth curve of <i>S. cerevisiae</i> wild type and <i>pbs2Δ</i> under normal conditions in yeast nitrogen base medium (YNB).....	51
Figure 3.4. Growth curve of <i>S. cerevisiae</i> wild type and <i>hog1Δ</i> under normal conditions in yeast nitrogen base medium (YNB).....	51
Figure 3.5. Growth curve of <i>S. cerevisiae</i> wild type and <i>Iro1Δ</i> under normal conditions in yeast nitrogen base medium (YNB).....	52
Figure 3.6. Growth curve of <i>S. cerevisiae</i> wild type and <i>fat1Δ</i> under normal conditions in yeast nitrogen base medium (YNB).....	52
Figure 3.7. Neutral lipid fluorescence intensity of Nile Red stained <i>S. cerevisiae</i> wild type and the HOG component mutants.....	53
Figure 3.8. Neutral lipid fluorescence intensity of Nile Red stained <i>S. cerevisiae</i> wild type and <i>hog1Δ</i> mutant with pRS313 and pRS313 <i>HOG1</i> transformed into both.	54
Figure 3.9. Western blot of protein extractions from wild type <i>S. cerevisiae</i> cells over a time course of 6 to 10 hours of growth in YNB media and incubated with shaking, 180rpm, at 30°C.	55
Figure 3.10. Growth curve of <i>S. cerevisiae</i> wild type and <i>hog1Δpbs2Δ</i> under normal conditions in yeast nitrogen base medium (YNB).....	57
Figure 3.11. Neutral lipid fluorescence intensity of Nile Red stained <i>S. cerevisiae</i> wild type and <i>pbs2Δ</i> , <i>hog1Δ</i> and <i>hog1Δpbs2Δ</i> mutants.....	58
Figure 3.12. Duplicate Western blot of protein extractions from wild type and <i>pbs2Δ</i> <i>S. cerevisiae</i> cells over a time course of 8 to 10 hours of growth in YNB media and incubated with shaking, 180rpm, at 30°C.....	59
Figure 3.13.1 Western blot of Phos-tag™ gel.....	61
Figure 3.13.2. Western blot of Phos-tag™ gel.....	62
Figure 3.14. (A) Amplification of SCH9 deletion cassettes.	64
(B) Testing of integration of cassette into wild type <i>S. cerevisiae</i>	64
(C) Testing of integration of cassette into <i>hog1Δ</i> and <i>pbs2Δ</i> <i>S. cerevisiae</i>	64
Figure 3.15. Growth curve of <i>S. cerevisiae</i> wild type and <i>sch9Δ</i> under normal conditions in yeast nitrogen base medium (YNB).....	65
Figure 3.16. Neutral lipid fluorescence intensity of Nile Red stained <i>S. cerevisiae</i> wild type and <i>msn2/4Δ</i> , <i>sch9Δ</i> , <i>Iro1Δ</i> and <i>fat1Δ</i> mutants.	66
Figure 3.17. Complementation of <i>sch9Δ</i> phenotype.....	66
Figure 3.18. Growth curve of <i>S. cerevisiae</i> wild type and <i>hog1Δsch9Δ</i> under normal conditions in yeast nitrogen base medium (YNB).....	69
Figure 3.19. Growth curve of <i>S. cerevisiae</i> wild type and <i>pbs2Δsch9Δ</i> under normal conditions in yeast nitrogen base medium (YNB).....	70
Figure 3.20. Neutral lipid fluorescence intensity of Nile Red stained <i>S. cerevisiae</i> wild type and <i>sch9Δ</i> , <i>hog1Δ</i> and <i>pbs2Δ</i> single and double delete mutants.	70
Figure 3.21. Deletion of genomic copy of <i>DGA1</i>	72
Figure 3.22. Growth curve of <i>S. cerevisiae</i> wild type and <i>msn2/4Δ</i> under normal conditions in yeast nitrogen base medium (YNB).....	73

Figure 3.23. Growth curve of <i>S. cerevisiae</i> wild type and <i>dga1Δ</i> under normal conditions in yeast nitrogen base medium (YNB).....	73
Figure 3.24. Neutral lipid fluorescence intensity of Nile Red stained <i>S. cerevisiae</i> wild type and <i>HOG</i> component mutants.....	74
Figure 3.25. Cloning of <i>DGA1</i>	76
Figure 3.26. Growth curve of <i>S. cerevisiae</i> wild type and <i>hog1Δdga1Δ</i> under normal conditions in yeast nitrogen base medium (YNB).....	77
Figure 3.27. Growth curve of <i>S. cerevisiae</i> wild type and <i>pbs2Δdga1Δ</i> under normal conditions in yeast nitrogen base medium (YNB).....	78
Figure 3.28. Neutral lipid fluorescence intensity of Nile Red stained <i>S. cerevisiae</i> wild type and <i>HOG</i> component mutants.....	79
Figure 3.29. Potential MAPK phosphorylation sites (S/T P) in the N terminus of Dga1p.....	80
Figure 3.30. Genomic tagging of <i>DGA1</i>	83
Figure 3.31. A) Western blot of protein extractions from <i>dga1-3HA</i> tagged <i>S. cerevisiae</i>	84
Figure 4.1 Sequence alignments between <i>DGA1</i> and <i>LRO1</i> + 1Kb.....	103
Figure 4.2 <i>DGA1</i> + 1Kb sequence.....	103
Figure 4.3 Proposed topology model of ScDGAT2.....	105

Abstract

The highly conserved mitogen activated protein kinase (MAPK) high-osmolarity glycerol (HOG) pathway plays a vital role in the ability of *Saccharomyces cerevisiae* cells to respond to stress conditions, primarily hyperosmotic stress. In addition, there is also evidence that the HOG pathway is involved in lipid accumulation, which occurs in nitrogen depleted cells as they enter stationary phase. Understanding this lipogenic switch is important both for the biotechnology industry (for example biofuels) and understanding human disease, where cancer cells accumulate cellular lipid.

To investigate the role of the HOG1 pathway in neutral lipid accumulation, a Nile red assay was undertaken to measure lipid accumulation in stationary phase of genomic deletion strains of key HOG pathway proteins. Deletion of the majority of HOG components had no effect on lipid accumulation. However, the *hog1Δ* mutant showed a significant decrease in neutral lipids levels when compared to the wildtype. Hog1p is

the key MAPK in the HOG pathway and this data suggests that it may also be a regulator of neutral lipid accumulation.

Hog1p is activated by phosphorylation, as such, a western blot analysis was performed to monitor dual phosphorylation of Hog1p during the lipogenic switch. This showed an increase in Hog1p phosphorylation between 9 – 10 hours of growth, which corresponds to the transitional period between late exponential phase and early stationary phase and accumulation of neutral lipids.

Regulation of Hog1 is classically believed to be via dual phosphorylation by the MAPKK Pbs2. However, results from the Nile red assay of the *pbs2Δ* mutant, demonstrated that accumulation of neutral lipids is not affected in this strain when compared to the wildtype. Further, a *hog1Δpbs2Δ* double deletion showed no additive effect when compared to the individual deletion strains. This suggests that Pbs2p is not involved in the accumulation of neutral lipids, and, therefore, Hog1p is being activated by an alternative regulator. This was further investigated by monitoring Hog1p phosphorylation during the lipogenic switch in the absence of Pbs2p.

To investigate how Hog1 is regulating lipid accumulation, a number of potential neutral lipid downstream targets were investigated. One potential target is Dga1p, an enzyme that catalyses the terminal step of triacylglycerol formation in lipid production. Deletion of this protein results in reduction in neutral lipid levels as measured by the Nile red assay. A similar reduction in neutral lipid levels was observed in a *hog1Δdga1Δ* double deletion indicating the proteins may be involved in the same pathway. Dga1 being a target of Hog1 is supported by bioinformatics analysis, which identified four potential MAPK sites (S/T followed by P) within the protein.

This work indicates a potential novel role for Hog1p in regulating lipid accumulation in *S. cerevisiae* which may have wider implications for the study of lipid related diseases and for the biotechnological application of cellular lipids.

Acknowledgements

I would like to thank my supervisor, Dr Clare Lawrence. She has supported me throughout this project, giving sound advice and guidance in both the practical lab skills needed to do this work, but also in the writing and academic advice needed to write this thesis. I would also like to thank my director of studies, Dr Steve Beeton, and my secondary supervisor Dr Jane Alder who both helped me in this project. I'd also like to thank the numerous people in the Darwin building labs who helped me over the year.

Abbreviations

Abs	Absorbance
AcCoA	Acetyl Coenzyme A
AceAcCoA	Acetacetyl Coenzyme A
AGC	A group of kinases named after the protein kinase A, G and C families; it consists of 16 families of kinases
Akt	Protein kinase B
AMPK	Adenosine monophosphate-activated protein kinase
ANOVA	Analysis of variance
Atf1	Activating transcription factor 1
Atf2	Activating transcription factor 2
ATP	Adenosine triphosphate
cDNA	Complementary deoxyribonucleic acid

ChIP	Chromatin immunoprecipitation
DAG	Diacylglycerol
DGA1	Diacylglycerol O-acyltransferase 1
DMSO	Dimethyl Sulphoxide
DNA	Deoxyribonucleic acid
dNTPs	Deoxyribonucleotide triphosphates
ECL	Enhanced chemiluminescence
EDTA	Ethylenediaminetetraacetic acid
ER	Endoplasmic reticulum
ERK	Extracellular signal-regulated kinase
Euroscarf	European <i>Saccharomyces cerevisiae</i> Archive for Functional Analysis
FAs	Fatty acids
FAS	Fatty acid synthase
FASN	Fatty acid synthase N
GFP	Green fluorescent protein
GPAT	Glycerol-3-phosphate-acyltransferase
HOG	High osmolarity glycerol
JNK	c-Jun NH ₂ -terminal kinase
LRO1	Phospholipid diacylglycerol acyltransferase
MAPK	Mitogen-activated protein kinase
MAPKK/MAP2K/MEK	Mitogen-activated protein kinase kinase
MAPKKK/MAP3K	Mitogen-activated protein kinase kinase kinase
MAP4K	Mitogen-activated protein kinase kinase kinase kinase
mRNA	Messenger ribonucleic acid

MS	Mass spectrometry
<i>MSN2</i>	Multicopy suppressors of the <i>snf1</i> defect 2
<i>MSN4</i>	Multicopy suppressors of the <i>snf1</i> defect 4
<i>mTOR</i>	Mechanistic target of rapamycin
<i>mTORC1</i>	Mechanistic target of rapamycin complex 1
<i>mTORC2</i>	Mechanistic target of rapamycin complex 2
NADH	Nicotinamide adenine dinucleotide
NADPH	Nicotinamide adenine dinucleotide phosphate
NAT	Nourseothricin
NBRP	National BioResource Project
Nile red	9-diethylamino-5H-benzo[a]phenoxazine- 5-one
OD	Optical density
ORF	Open reading frame
PA/ PtdOH	Phosphatidic acid
PBS	Phosphate buffered saline
PCR	Polymerase chain reaction
PEG	Polyethylene glycol
PL	Phospholipid
RNA	Ribonucleic acid
<i>S. cerevisiae</i> <i>S. cerevisiae</i>	<i>Saccharomyces cerevisiae</i>
<i>S. pombe</i>	<i>Schizosaccharomyces pombe</i>

SAPK	Stress-activated protein kinase
SD	Standard deviation
SDS	Sodium dodecyl sulphate
SDS-PAGE	Sodium dodecyl sulphate polyacrylamide electrophoresis
SEs	Sterol esters
SORB	Sorbitol Buffer
SREBPs	Sterol regulatory element binding proteins
STRE	Stress response elements
TAGs	Triacylglycerol's
TBST	Tris buffered saline tween
TCA	Tricarboxylic acid
TFs	Transcription factors
TOPO <i>gene</i>	A gene in a TOPO vector, e.g. TOPO <i>dga1</i>
TOR	Target of rapamycin
TORC1	Target of rapamycin complex 1
TORC2	Target of rapamycin complex 2
Tris-HCl	Tris-hydrachloride
WEs	Wax esters
YNB	Yeast nitrogen base
YPD	Yeast extract peptone dextrose

1. Introduction

1.1 Cancer

Cancer is a disease state of cells in the body in which cells undergo uncontrolled proliferation. Irrespective of the cause, the result is cellular genetic changes leading to the acquisition of certain characteristics (hallmarks of the disease) that define cancer (Hanahan and Weinburg 2011).

In normal tissues, cellular growth is tightly controlled. Growth promoting signals and cell cycle checkpoints, which control entry and progression through the cell cycle, are key components in this regulation. Cancer cells can avoid these regulatory mechanisms, via a series of methods including overexpression of intracellular pathways and mutation of key proteins, resulting in uncontrolled cell proliferation (Hanahan and Weinburg 2011).

Another key characteristic of cancer cells is their altered metabolism, which results in cells accumulating more lipid and undergoing aerobic glycolysis, due to the Warburg effect (Warburg 1925; Warburg 1956; Diaz-Ruiz *et al* 2011; Walther and Farese 2012; Baenke *et al* 2013; Liberti *et al* 2016). This altered metabolism provides the cancer cells with both energy and increased lipid synthesis required to support their proliferation with many cancers undergoing increased *de novo* fatty acid synthesis (Esechie *et al* 2009; Liberti *et al* 2016).

1.2 Signalling pathways

Lipid accumulation is regulated by several signal transduction pathways (Zaidi *et al* 2013). These pathways are predominantly what become dysregulated in cancer (Zaidi *et al* 2013; Sever *et al* 2015). Cells need to be able to be aware of their changing environment by detecting and responding to external stimuli to survive. Cell sensing

and signalling pathways are the mechanisms by which the cell can respond to change by communicating with cytoplasmic and nuclear targets to elicit a phenotypical response to stimuli (e.g. the osmotic stress response to external salt concentrations) (Marshall 1994; Waskiewicz *et al* 1995; Lawrence *et al* 2007).

1.2.1 AMP-activated protein kinase (AMPK)

AMPK is a key pathway involved in regulating numerous cellular processes within the cell including lipid metabolism (Krebs *et al* 1979), with its deletion causing Warburg effect phenotype in cells (Faubert *et al* 2013). AMPK activation requires phosphorylation (primarily performed by liver kinase B1) at the threonine residue Thr172 within the activation loop of the catalytic subunit (Hawley *et al* 1996); this can be in response to several factors which deplete cellular ATP supplies (Hurley *et al* 2006). Once activated, the AMPK pathway can perform many functions (Figure 1.1) such as decreasing fatty acid synthesis by phosphorylating (and so inactivating) the acetyl-CoA carboxylase enzymes (ACC1 and ACC2) resulting in no malonyl-CoA production, which is needed to produce palmitate (Jeon *et al* 2012). This generally occurs in states of glucose starvation and hypoxia, AMPK will promote the breakdown of fatty acids by promoting their mitochondrial uptake where they are broken down by β -oxidation. In cancer this process can be disrupted as intact mitochondrial function is required, which can be limited in cancer (Liang *et al* 2013).

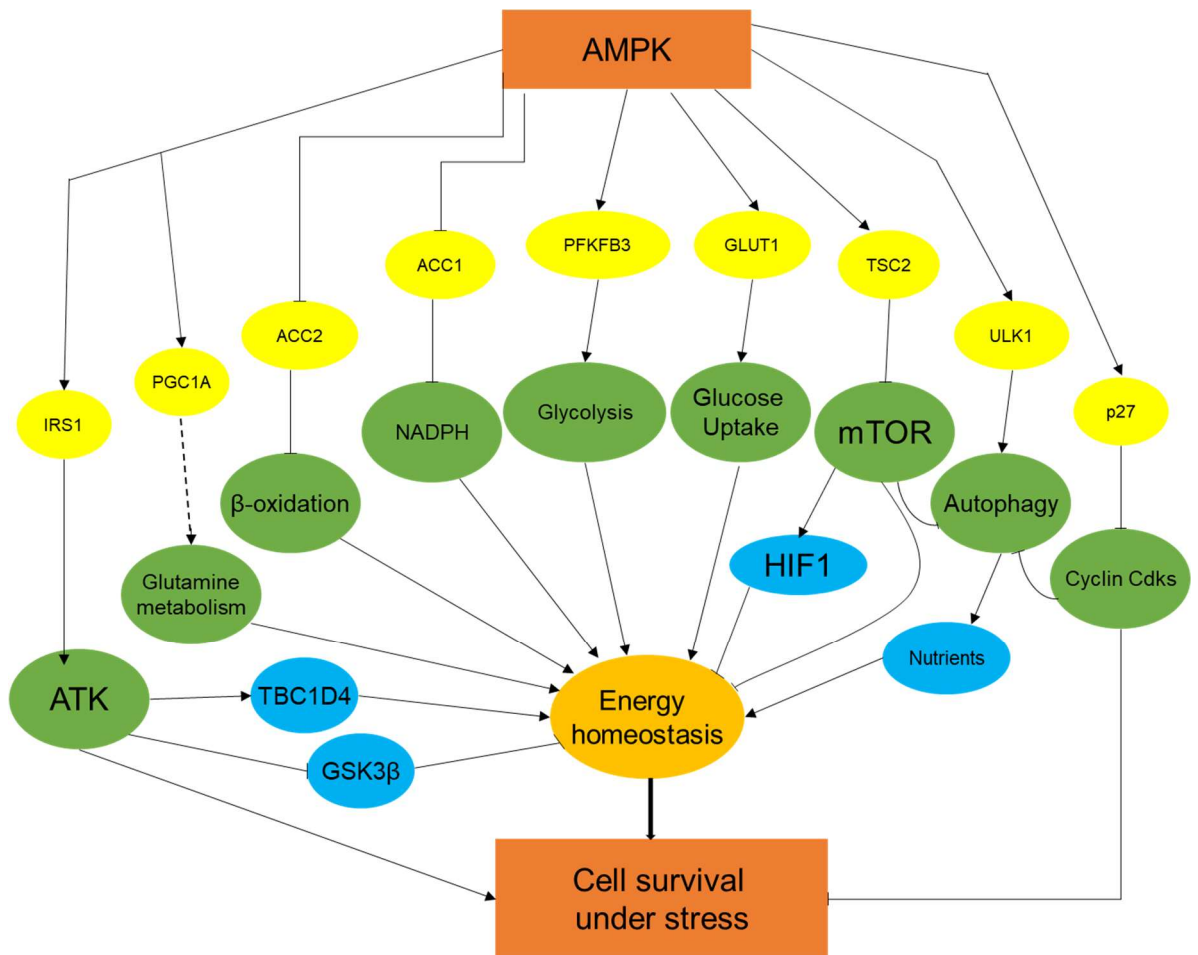


Figure 1.1 AMPK promotes cell survival. Adenosine monophosphate-activated protein kinase (AMPK), acetyl-CoA carboxylase isoform 1 (ACC1), acetyl-CoA carboxylase isoform 2 (ACC2), peroxisome proliferator-activated receptor gamma coactivator 1-alpha (PGC1A), insulin receptor substrate 1 (IRS1), 6-phosphofructo-2-kinase/fructose-2,6-biphosphatase 3 enzyme (PFKFB3), Glucose transporter 1 (GLU1), Tuberous Sclerosis Complex 2 (TSC2), serine/threonine-protein kinase ULK1, Hypoxia-inducible factor 1 (HIF1), TBC1 domain family member 4 (TBC1D4), glycogen synthase kinase 3 beta (GSK3 β). Adapted from Liang *et al* 2013

1.2.2 Mechanistic target of rapamycin (mTOR)

mTOR consists of two separate complexes, mTORC1/mTORC2, and serves as part of a signal transduction pathway which is a central regulator of cell growth, proliferation, metabolism and survival (Laplante *et al* 2009a). mTOR is implicated in the regulation of

lipogenesis by its ability to promote activation of sterol regulatory element-binding protein 1a (SREBP-1a) (Porstmann *et al* 2008; Laplante *et al* 2009b) which has been implicated in the regulation of lipid biosynthesis (Liang *et al*, 2002). Once active SREBP-1a translocates to the nucleus where it activates SREBP responsive genes including include *FASN* (Laplante *et al* 2009b); *FASN* encodes the fatty acid synthase (FASM) enzyme (Jeon *et al* 2012; Krycer *et al* 2010). Figure 1.2 displays the role of mTOR in lipid biosynthesis.

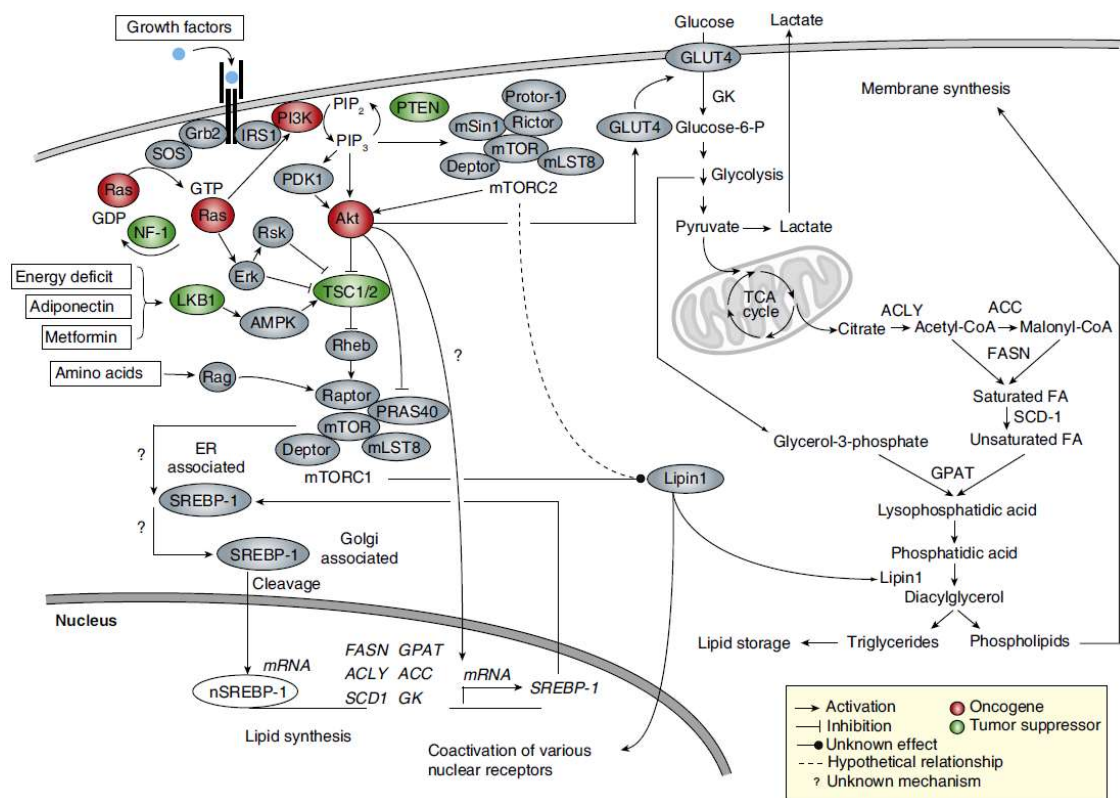


Figure 1.2. mTORC1 promotes *de novo* lipogenesis through the activation of SREBP-1. Acetyl-CoA carboxylase (ACC), acyl-CoA lyase (ACLY), fatty acid synthase (FASN), glycerol-3-phosphate acyltransferase (GPAT), glucokinase (GK) and stearoyl-CoA desaturase-1 (SCD-1). Taken from Laplante *et al* 2009b.

1.2.3 Mitogen activated protein kinases (MAPK)

There are many MAPK pathways. These pathways mediate intracellular signalling that it associated with cellular activities including cell proliferation, differentiation, survival,

transformation, migration and apoptosis (Dhillon *et al* 2007). p38 and ERK are two mammalian MAPK pathways.

ERK 1/2 MAPK are part of the Ras-Raf-MEK-ERK signal transduction cascade, which is involved in many processes including the cell cycle, and cellular metabolism (Roskoski 2012). This cascade is initiated by the G protein RAS (Shaul *et al* 2007) as shown in Figure 1.3. MAPKs are involved in the metabolic switch that occurs in cancer with implications that increased signalling via the Ras/Raf/MEK/ERK cascade leads to increased *FASN* expression (and so increased lipogenesis) via SREBP-1 (Yang *et al* 2002).

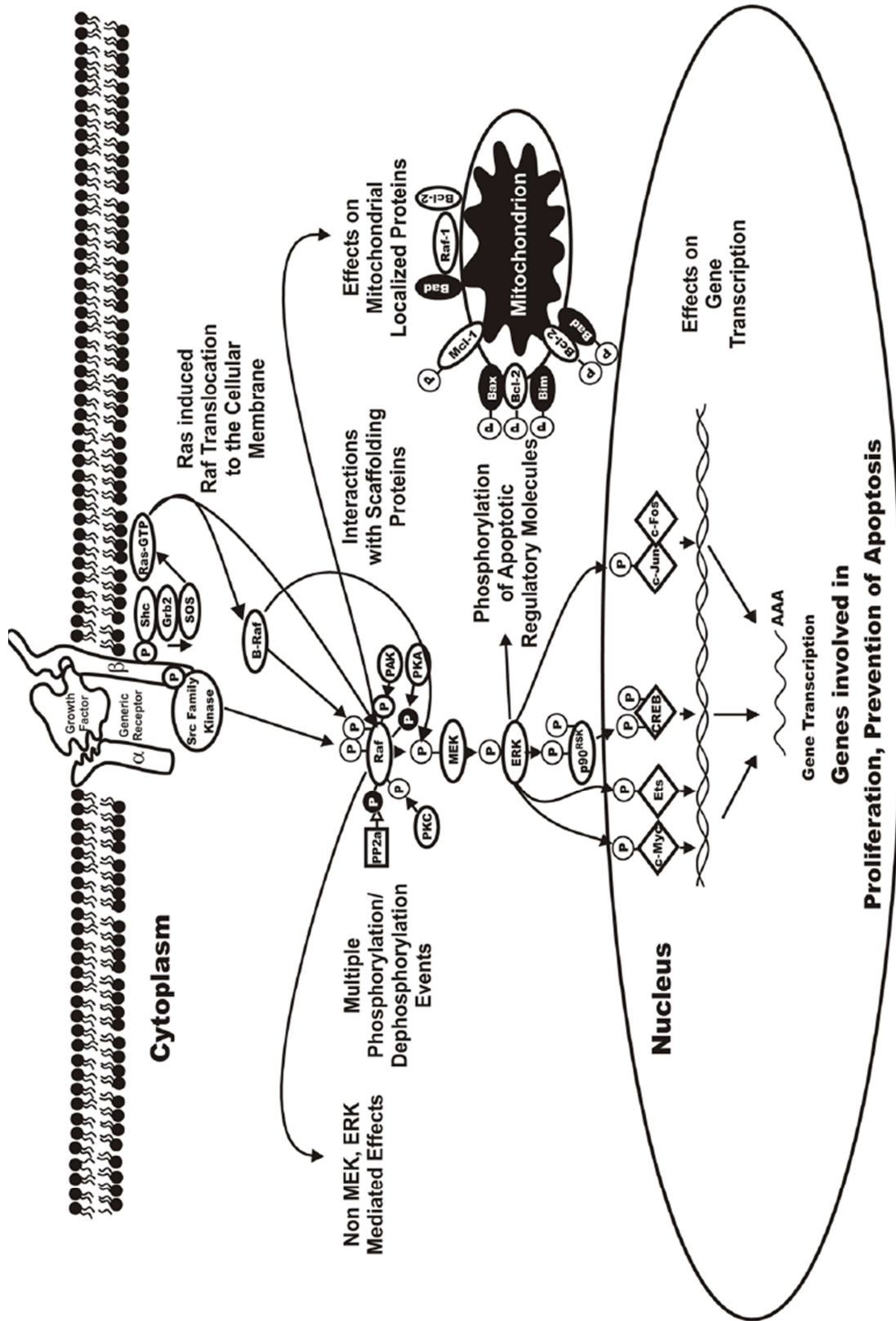


Figure 1.3. The Ras/Raf/MEK/ERK cascade. Phosphorylation that enhances activity - P in black circle, inhibitory phosphorylation - P in white circle. Taken from **McCubrey et al 2006**

p38 has 4 isoforms and is involved in many cellular processes such as (but not limited to) apoptosis, the cell cycle and in in senescence and tumour suppression (Roux *et al*

2004; Zarubin *et al* 2005). There is evidence to suggest that the p38 pathway is involved in lipogenesis, with SREBP-1c dependent genes being transcribed as a result of p38- and JNK-mediated phosphorylation cascades (Guijas *et al* 2012).

1.2.4 Sterol regulatory element-binding proteins (SREBP)

The AMPK and MAPK pathways interact with SREBP (Yang *et al* 2002; Liang *et al* 2013). SREBP are transcription factors that regulate expression of genes required to maintain cellular lipid homeostasis (Jeon *et al* 2012). There are 3 SREBPs SREBP-1a, SREBP-1c and SREBP-2. SREBP-1a targets genes that transcribe elements involved in fatty acid metabolism such as *FASN* (Jeon *et al* 2012; Krycer *et al* 2010). Studies have shown the involvement of SREBP-1a and SREBP-1c in the regulation of lipid biosynthesis (Liang *et al*, 2002).

SREBP-2 targets genes involved with cholesterol such as 3-hydroxy-3- methylglutaryl coenzyme A (HMG-CoA) reductase, which acts as a catalyst in cholesterol biosynthesis, acting as a rate limiting enzyme in the mevalonate pathway (Mullen *et al* 2016). SREBP-1a targets both sets of genes, and so if upregulated can cause an increase in the expression of both sets of genes. SREBPs can be activated through the AMPK pathway via Phosphatidylinositol 3'-kinase (PI3K) and Akt (Protein kinase B). In numerous cases of cancer mutations cause Akt to become overactive and so increase SREBP activity (Krycer *et al* 2010). SREBPs are conserved between mammals and *S. cerevisiae* (Jeon *et al* 2012). It should be noted that *S. cerevisiae* uses ergosterol where mammalian cells would use cholesterol (van Meer *et al* 2008).

These signal transduction pathways are required for normal cell function, with their dysregulation causing a disease phenotype, such as that seen in cancer (Downward 2003). The mitogen activated protein kinase (MAPK) and mammalian target of rapamycin (mTOR) signalling pathways are especially related to disease phenotype

due to their involvement in cell growth, motility, proliferation and survival, processes (Hsu *et al* 2011) Dysregulation of these pathways are often involved in cancer and, as such, are under intense investigation (Masui *et al* 2012).

1.3 Lipids including lipogenesis

Lipogenesis is a highly regulated metabolic process, whereby acetyl-CoA is converted to fatty acids (Zaidi *et al* 2013). The regulatory pathways involved include the adenosine monophosphate-activated protein kinase (AMPK), mechanistic target of rapamycin (mTOR) and mitogen-activated protein kinase (MAPK).

De novo fatty acids synthesis starts with the carboxylation of acetyl-CoA to malonyl-CoA, malonyl-CoA is then used by fatty acid synthase (FAS) to form palmitate. These are either used as an energy store (so incorporated into triacylglycerols) or used to form phospholipid membranes (Ameer *et al* 2014). Figure 1.4 displays lipogenesis in mammalian cells.

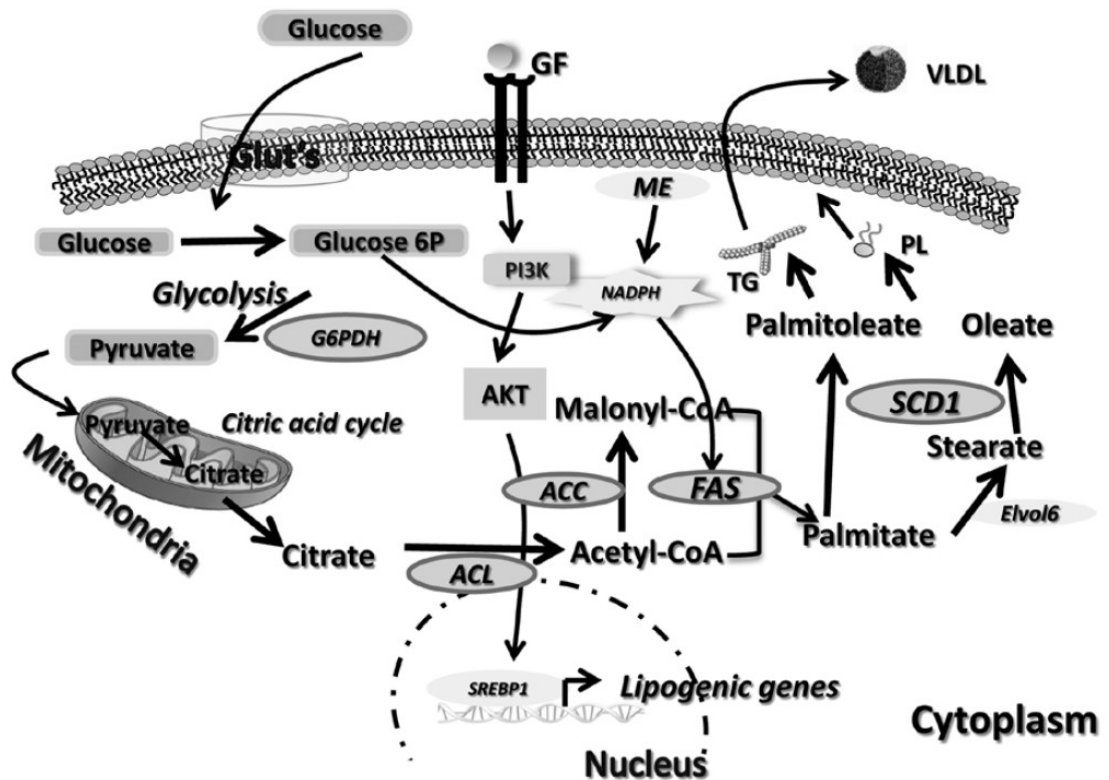


Figure 1.4 The process of mammalian lipogenesis. ATP citrate lyase (ACL), acetyl CoA carboxylase (ACC), fatty acid synthase (FAS), malic enzyme (ME), stearoyl CoA desaturase (SCD1), phospholipids (PL), triglycerides (TG), growth factors (GF), very-low-density lipoproteins (VLDL), protein kinase B (AKT). Taken from **Mounier et al 2014**.

FAS is a multi-enzyme protein, which under normal conditions converts excess carbohydrate into FAs to allow for esterification to storage triacylglycerols, these can then be used in times of need to provide energy through β -oxidation. In cases of cancer, FAS is used by the cell for *de novo* fatty acid synthesis using excess pyruvate produced from glycolysis (Menendez et al 2007).

1.3 Metabolic switch in cancer

The Warburg effect is a metabolic change that occurs in cancer cells (Warburg 1925; Warburg 1956). It results in what is known as “aerobic glycolysis” with cells primarily undergoing glycolysis despite ample oxygen; normally glycolysis only becomes the

primary energy source under anaerobic conditions; resulting in the production of lactic acid (Hanahan *et al* 2011). The prevailing theory behind the rationale for this change, and why it is viable for cells despite being far less efficient an energy source when compared to oxidative phosphorylation (Hanahan *et al* 2011), is that cells redirect glycolytic intermediates into other synthesis pathways (Heiden *et al* 2009) allowing cells to produce the macromolecules and organelles needed for the rapid proliferation of cancer cells. This theory is supported by evidence that some rapidly proliferating embryonic cells display a Warburg-like metabolism (Hanahan *et al* 2011).

The mechanism of *de novo* fatty acids synthesis (Figure 1.4) explains the need for cancer cells to produce high level of NADPH and comparatively less ATP (Liberti *et al* 2016). In order to produce the large amounts of lipids (phospholipids and triglycerides) required, the FAS enzyme needs to synthesise palmitate from acetyl CoA and malonyl CoA, which requires NADPH (Figure 1.4). Palmitate is a synthetic intermediate in lipogenesis and its formation acts as the rate limiting step in *de novo* fatty acids synthesis (Ameer *et al* 2014).

As lipid accumulation does not occur in most healthy mammalian cells (adipocytes being a notable exception) but does occur in cancer cells (Walther and Farese 2012), understanding the metabolic differences that contribute to this change will allow us to better understand cancer progression. This may enable us to develop ways to prevent it from happening (e.g. inhibitors of a particular protein) or target the altered metabolism (e.g. target lipid accumulation itself) (Vander Heiden 2011; Sun *et al* 2014). This is especially of interest in cancers that are difficult to remove via surgery, such as gliomas (Yang *et al* 2013).

1.4 Neutral lipids

Neutral lipids are lipid molecules that lack charged groups (and so are hydrophobic) and do not form part of the phospholipid bilayers of the cell, instead forming lipid

droplets and lipid bodies (Czabany *et al* 2007). Neutral lipids can be divided into three groups, triacylglycerols (TAGs), steryl esters (SEs) and wax esters (WEs), with TAGs and SEs being the most common neutral lipids in yeast and mammalian cells, acting as energy stores within the cell (Athenstaedt *et al* 2006).

Due to their hydrophobic nature, combined with the high water content within the cell, neutral lipids form the core of lipid droplets, with phospholipids surrounding the neutral lipid core (Athenstaedt *et al* 2006). Figure 1.5 details TAGs synthesis.

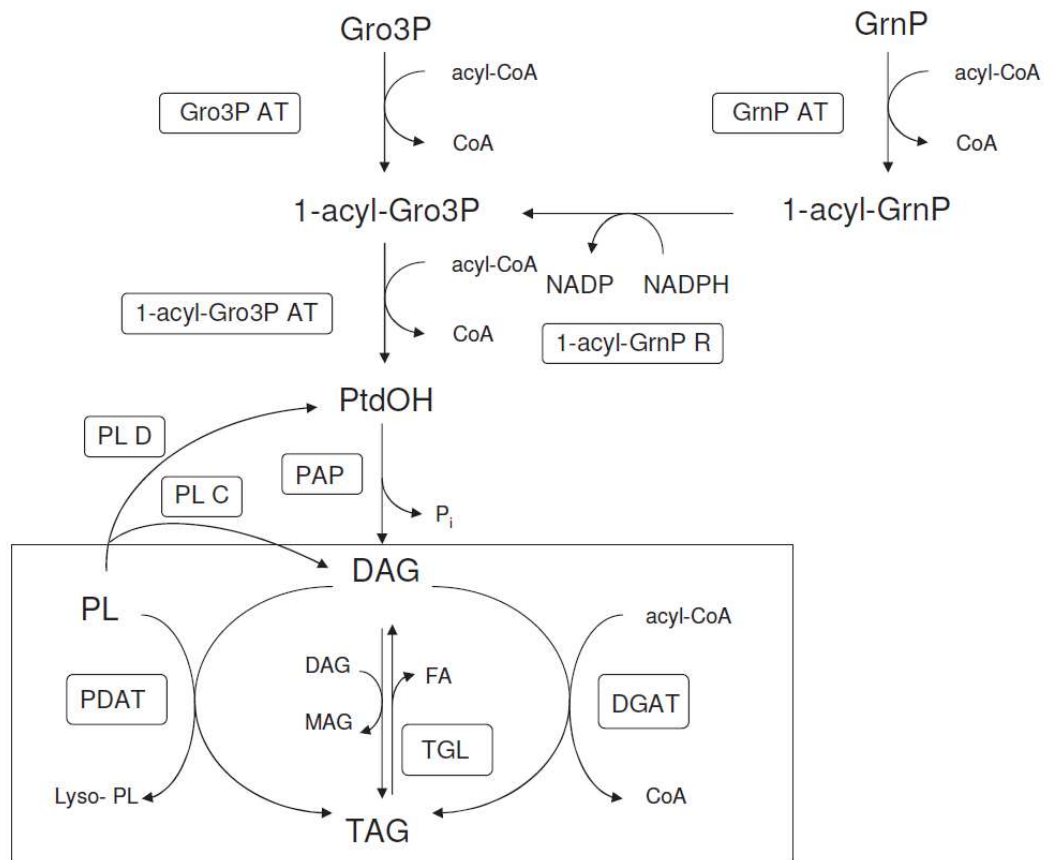


Figure 1.5 TAG metabolism via different pathways (Athenstaedt *et al* 2006). In the upper part of the figure, enzymatic reactions leading to the synthesis of diacylglycerol(DAG) via the intermediate phosphatidic acid (PtdOH) are shown. The framed, lower part of the figure shows the different possibilities for the final reactions yielding TAG. Enzymes: 1-acyl-GrnP R, 1-acyldihydroxyacetone phosphate reductase; 1-acyl-Gro3P AT, 1-acyl glycerol-3-phosphate acyltransferase; DGAT, diacylglycerol acyltransferase; GrnP AT, dihydroxyacetone phosphate acyltransferase; Gro3P AT, glycerol-3-phosphate acyltransferase; PAP, phosphatidate phosphatase; PDAT, phospholipid:diacylglycerol acyltransferase; PL C, phospholipase C; PL D, phospholipase D; TGL, triacylglycerol lipase. Substrates: 1-acyl-GrnP, 1-acyl dihydroxyacetone phosphate; 1-acyl-Gro3P, 1-acyl glycerol-3-phosphate; DAG: diacylglycerol; FA, fatty acid; GrnP, dihydroxyacetone phosphate; Gro3P, glycerol-3-phosphate; MAG, monoacylglycerol; PL, phospholipid; PtdOH, phosphatidic acid; TAG, triacylglycerol. Diagram taken from Athenstaedt *et al* 2006.

1.4.1 Lipid Droplet formation

While previously thought to be nothing but energy stores, lipid droplets are in fact involved in many functions in lipid metabolism and the production of energy (e.g. with the peroxisome via peroxisome protrusions which extend from the peroxisome to the core of the lipid droplet) (Beller *et al* 2010). Several models of lipid droplet formation have been proposed. For example, the Lensing model where neutral lipids are deposited between endoplasmic reticulum (ER) membrane leaflets. Once enough lipid has accumulated this lipid core pushes outwards and releases from the ER, surrounded by the phospholipids from the ER which encapsulate the hydrophobic core (Martin *et al* 2006). Other methods have also been suggested including the “bicelle” and “vesicle-budding” models, although there is little evidence to support either of them, (Wilfling *et al* 2013). The bicelle model is similar to that of the lensing model but rather than a single layer of phospholipid membrane forming the monolayer of the lipid droplet both layers do (Ploegh 2007). This would leave holes in the ER membrane, comprising the ER membrane (Walther and Farese 2009).

The “vesicle-budding” model proposes that lipid droplets form within a bilayer vesicle which remains attached to the membrane of the ER, lipids accumulate within the vesicle, filling the space between the two membranes. This squeezes the lumen of the vesicle and results in the membrane bulging outward from the ER membrane similarly to that of the lensing model (Walther and Farese 2009).

1.5 Use of yeast as a model organism

The budding yeast, *Saccharomyces cerevisiae* (*S. cerevisiae*), is an excellent model organism as the *S. cerevisiae* cells are easily grown in low cost media (relative to mammalian cells) and have a (comparatively) simple genotype/phenotype relationship which is well characterised. This is especially important when one wishes to study the consequences of inactivation or overexpression of a gene (Mager *et al* 2005, Botstein

et al 2011). As such, to understand complex processes in mammalian cells we can utilise model organisms which contain highly conserved pathways.

S. cerevisiae has been long established as a model organism (Zhang *et al* 2003; Henry *et al* 2012) and has been used to increase our understanding of many cellular and molecular processes (Mager *et al* 2005); for example, much of our understanding of lipid biosynthesis and its regulation in higher eukaryotes was determined using yeast models (Diaz-Ruiz *et al* 2011; Schmidt *et al* 2013; Koch *et al* 2014). Also of interest the fatty acid synthase structure was first elucidated in yeast (Lomakin *et al* 2007). This is because many processes and regulatory elements are conserved, with many human genes having orthologues in *S. cerevisiae* (Siepel *et al* 2005; Hamza *et al* 2015), including components of the lipogenic, MAPK and mTOR pathways (Figure 1.2; The mammalian mTOR has the *S. cerevisiae* homologues Tor1 and Tor2) (Hay *et al* 2004; Dann and Thomas 2006; Loewith *et al* 2011).

1.5.1 MAPK in *Saccharomyces cerevisiae*

There are multiple MAPK pathways in yeast, including the pheromone, the partial nutrient deprivation, the hyperosmolarity, the cell wall stress and the nutrient starvation pathways (Chen *et al* 2006). The hyperosmolarity (HOG) pathway is both structurally and functionally conserved to the mammalian p38 MAPK pathway as shown in Figure 1.6 (Waskiewicz *et al* 1995; Banuett 1998; Wagner *et al* 2009).

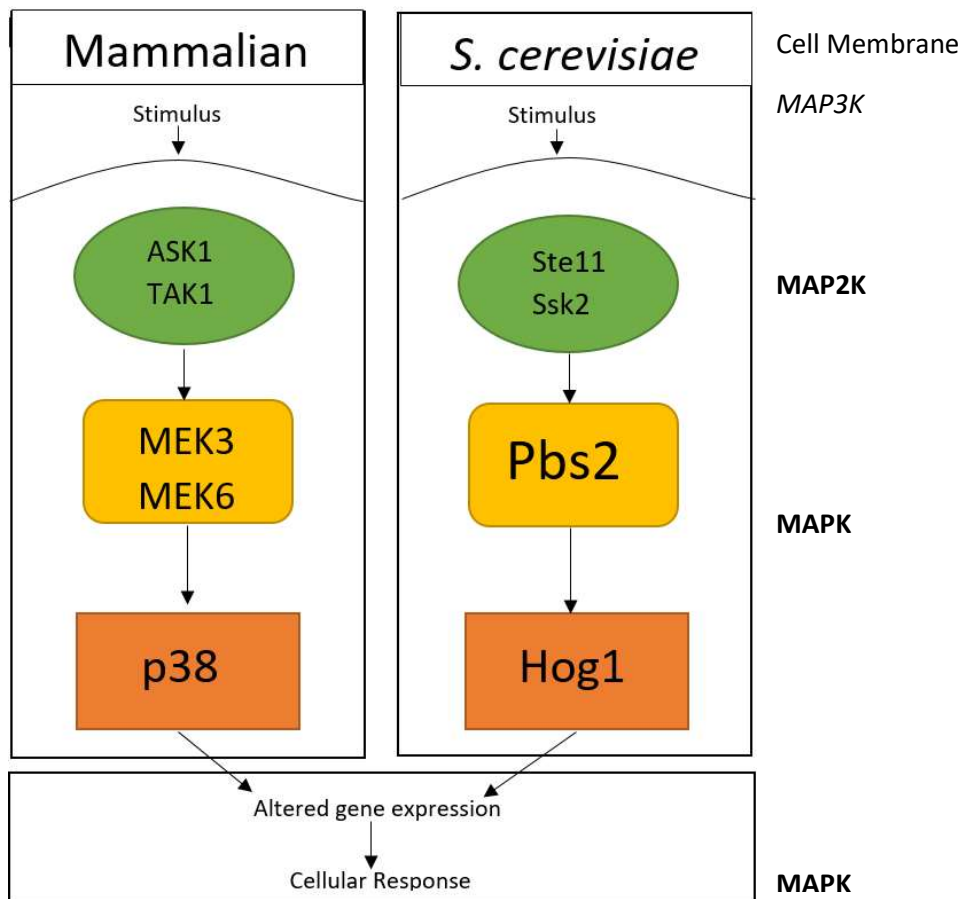


Figure 1.6 Conservation of the p38 MAPK pathway between mammals and *S. cerevisiae*. Adapted from Banuett, 1998.

The high osmolarity glycerol (HOG) pathway is a stress response pathway which is activated in response to high osmolarity, citric acid, ethanol, heat shock and pH (Kapteyn *et al* 2001; Lawrence *et al* 2004; Saito and Posas 2012). This results in the activation (via phosphorylation) and translocation of the MAPK protein Hog1p to the nucleus where it mediates the cell's adaptive response, acting directly or indirectly to cause transcription of genes. (Ferrigno *et al* 1998; de Nadal *et al* 2010). In addition to phosphorylating targets, Hog1p is also required for activation of stress response genes by recruiting RNA polymerase II to the gene promoter (Alepuz *et al*. 2001).

It is well accepted that Hog1p is activated by Pbs2p phosphorylation, however Pbs2p independent activation of Hog1p has been suggested (Rodriguez-Pena *et al* 2010; Qi

et al 2005; Maayan *et al* 2012). Pbs2p dependent activation of Hog1p is displayed in Figure 1.7.

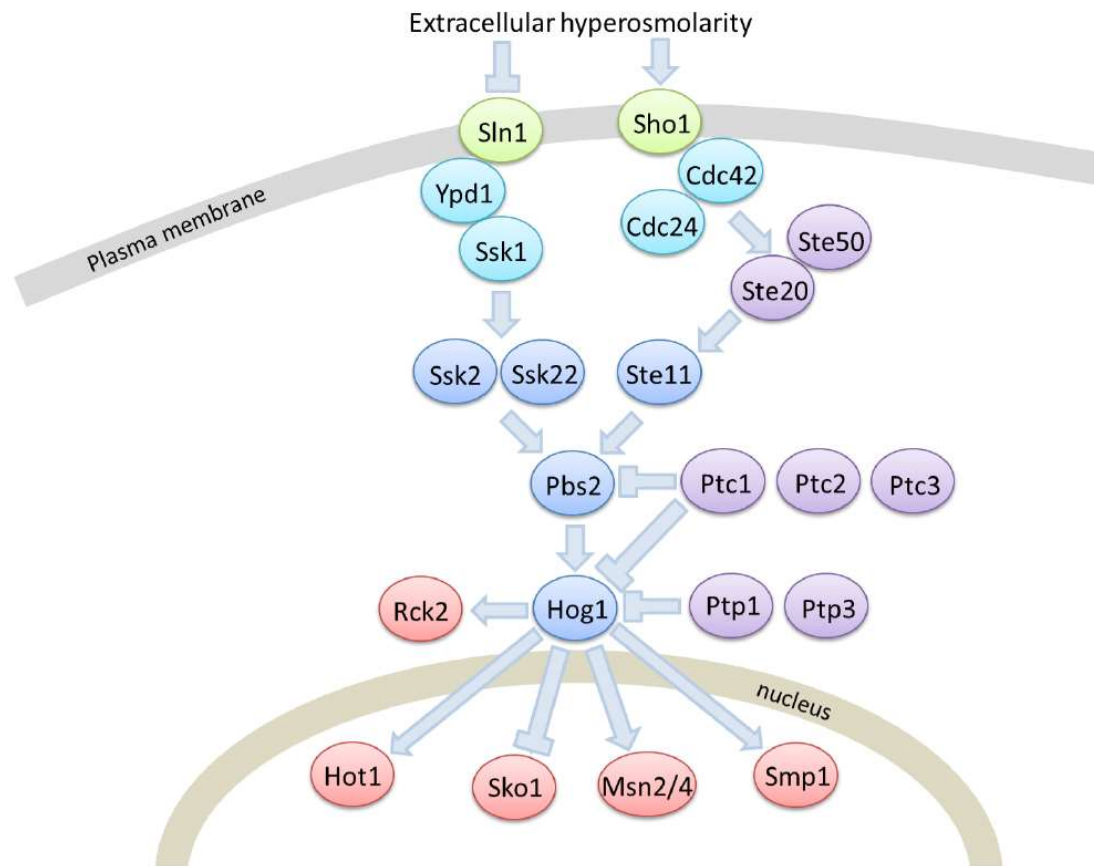


Figure 1.7 The classical HOG MAPK pathway of *S. cerevisiae* (Rostron 2015)

There are two main pathways which activate the MAP2K Pbs2, the Sln1 and Sho1 pathways, this leads to the dual phosphorylation of Hog1p at residues Thr174 and Ty176 allowing its nuclear localisation where it then acts on transcription factors such as Hot1 and Msn2/4. Arrow indicate stimulation of, blunt ended arrow indicate inhibition of. Taken from Rostron 2015.

There is evidence to suggest that a Pbs2p independent mechanism exists, although not one involving a direct activator. For example, there is evidence of autophosphorylation of Hog1p in response to osmotic pressure (Maayan *et al* 2012).

1.5.2 Lipogenesis in *Saccharomyces cerevisiae*

By changing the growth conditions of *S. cerevisiae*, nitrogen limitation or media exhaustion of nitrogen, it can be used to simulate cancer cells; primarily through the Crabtree effect that occurs in yeast (RodrigoDiaz-Ruiz, *et al* 2011). Cells are able to undergo aerobic glycolysis; in cancer cells this is termed Warburg effect (Warburg 1925; Warburg 1956; Arlia-Ciommo *et al* 2016). Cells also accumulate lipid in the stationary phase of growth in response to nitrogen limitation in the media (Henry *et al* 1973; Behalova *et al* 1992; Natter *et al* 2013); performing lipogenesis (like that of cancer cells) accumulating lipid (Diaz-Ruiz *et al* 2011; Walther and Farese 2012; Baenke *et al* 2013; Natter *et al* 2013; Arlia-Ciommo *et al* 2016; Liberti *et al* 2016).

S. cerevisiae can perform *de novo* fatty acid synthesis (Bessoule *et al* 1987), starting with acetyl-CoA carboxylation by acetyl-CoA carboxylase to malonyl-CoA. Elongases and desaturases in the endoplasmic reticulum act to elongate and desaturate the products in a cyclical manner resulting in the formation triglycerides and steryl esters (Han *et al* 2002; Rossler *et al* 2003).

S. cerevisiae synthesises the same general classes of lipids found in mammals and via pathways with high homology to that of mammalian systems. It should be noted however that there are differences, specifically in the composition of lipids, the simpler fatty acids and the yeast's synthesis of ergosterol where mammalian cells would synthesise cholesterol (van Meer *et al* 2008); there is also a slight difference in the synthesis of phospholipids with mammalian cells incorporating poly-unsaturated fatty acids into some phospholipids (Figure 1.8) (Carman *et al* 2007; Nielsen 2009).

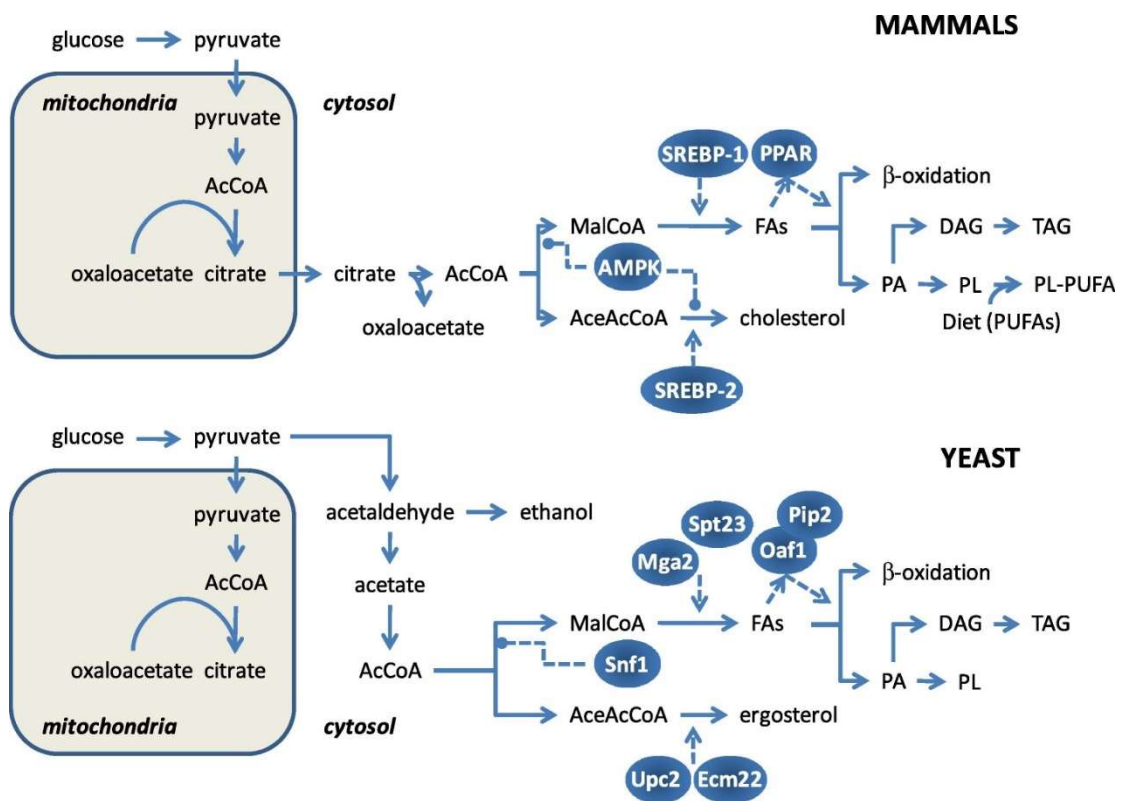


Figure 1.8 Comparison of lipid biosynthesis and its regulation in mammals and yeast. Acetyl-CoA (AcCoA), malonyl-CoA (MalCoA), acetoacetyl-CoA (AceAcCoA), fatty acids (FAs), phosphatidic acid (PA), diacylglycerols (DAG), triacylglycerols (TAG), phospholipids (PL), phospholipids containing poly-unsaturated fatty acids (PL-PUFA). Taken from Rostron 2015.

1.6 Aims of this study

The aim of this study is to investigate the role of the MAPK pathway in the regulation of (tumour associated) lipogenesis using the model organism *Saccharomyces cerevisiae*. First the role of key components of the HOG MAPK pathway (Ste11p, Ssk2p, Pbs2p, and Hog1p) in regulating lipid accumulation was investigated. This was followed by the investigation of the regulation of the Hog1 MAPK in lipid accumulation following nitrogen limitation. Finally, potential downstream lipogenic targets (Dga1) of the HOG MAPK pathway were investigated, their interaction with Hog1p would suggest its involvement in lipogenesis regulation.

Based on previous work it seems likely that the HOG MAPK pathway is involved in the regulation of lipogenesis, and given the known function of Dga1 it is possible that these two proteins may interact.

2. Materials and Methods

2.1 Yeast strains

Details of the *Saccharomyces cerevisiae* (*S. cerevisiae*) strains utilised are detailed in table 2.1.

Strains were maintained at 4°C on agar plates, either yeast peptone dextrose (YPD) or yeast nitrogen base (YNB). For non wild type strains a selection media was used, either G418 (100 µg/ml from 1000x stock in water), NAT (1 g/ml) or YNB lacking the appropriate amino acids to maintain the deletion. All plates were made and maintained in duplicate. See section 2.1.1 for media composition.

Table 2.1: *S. cerevisiae* strains used. Strain information for wildtype and deletion (Δ) strains used. National BioResource Project of the Ministry of Education, Culture, Sports, Science and Technology is abirritated to NBRP of the MEXT, Japan. CLL followed by a number is the strain collection number for the laboratory this work was performed in.

Yeast	Strain	Genotype	Reference
wildtype	BY4741a (derivative of S288C)	MATa <i>his3Δ1 leu2Δ0 met15Δ0</i> <i>ura3Δ0</i>	Brachmann <i>et al.</i> (1998)

<i>hog1Δ</i>	BY23209	MAT α <i>leu2 his3 trp1 ura3</i> <i>hog1::URA3</i>	NBRP of the MEXT, Japan
<i>msn2/4Δ</i>	BYP23752	MAT α <i>msn2::HIS3 msn4::URA3</i> <i>ade2-1 his3-11,15 leu2-3,112 trp1-1</i> <i>ura3-1 can1-100</i>	NBRP of the MEXT, Japan
<i>fat1Δ</i>	BYP5648	MAT α <i>fat1::HIS3 ade2-1 leu2-1,112</i> <i>ura3-1 trp1-1 his3-11,15 can1-100</i> <i>ssd1-d2 rad3-535</i>	NBRP of the MEXT, Japan
<i>pbs2Δ</i>	Y07101	BY4741; MAT α ; <i>his3Δ1; leu2Δ0;</i> <i>met15Δ0; ura3Δ0; pbs2::kanMX4</i>	Euroscarf
<i>dga1Δ</i>	Y02501	BY4741; MAT α ; <i>his3Δ1; leu2Δ0;</i> <i>met15Δ0; ura3Δ0; dga1::kanMX4</i>	Euroscarf
<i>ste11Δ</i>	Y05271	BY4741; MAT α ; <i>his3Δ1; leu2Δ0;</i> <i>met15Δ0; ura3Δ0; ste11::kanMX4</i>	Euroscarf
<i>lro1Δ</i>	Y05383	BY4741; MAT α ; <i>his3Δ1; leu2Δ0;</i> <i>met15Δ0; ura3Δ0; lro1::kanMX4</i>	Euroscarf
<i>sch9 Δ</i>	CLL130	BY4741; MAT α ; <i>his3Δ1; leu2Δ0;</i> <i>met15Δ0; ura3Δ0; sch9::natMX4</i>	This study
<i>pbs2Δsch9Δ</i>	CLL134	BY4741; MAT α ; <i>his3Δ1; leu2Δ0;</i> <i>met15Δ0; ura3Δ0; pbs2::kanMX4</i> <i>sch9::natMX4</i>	This study
<i>hog1Δsch9Δ</i>	CLL137	MAT α <i>leu2 his3 trp1 ura3</i> <i>hog1::URA3 sch9::natMX4</i>	This study

<i>dga1-3HA</i>	CLL126	BY4741; MATa; <i>his3Δ1</i> ; <i>leu2Δ0</i> ; <i>met15Δ0</i> ; <i>ura3Δ0</i> ; <i>dga1-3HA-natMX6</i>	This study
-----------------	--------	--	------------

2.1.1 Growth Media

All media and agar was prepared in distilled water and autoclaved.

The *S. cerevisiae* strains used were initially pre-cultured in YPD [2% glucose, 1% peptone, 1% yeast extract], with relevant selections added as relevant for each strain to maintain mutations on agar plates.

The minimal media used was YNB [0.67% yeast nitrogen base without amino acids (ForMedium™, UK) 2% glucose and 0.002%, appropriate amino acids except for threonine, uracil, tyrosine, lysine at 0.001% and 0.005% leucine], amino acid deficient media were also prepared for use as selection media for some deletions or plasmids insertions. Cells were grown at 30°C at 180 rpm in 250ml conical flasks.

For growth of DH5- α *Escherichia coli* (*E. coli*) Luria Broth (LB) [1% tryptone, 0.5% yeast extract, 1% NaCl] was utilised with growth conditions of 37°C with 200rpm shaking in 50ml falcon tubes. LB with 100 μ g/ml ampicillin was used to select for cells with successfully transformed plasmids or vectors. LB agar (2% agar and 100 μ g/ml ampicillin) was used to select for cells with successfully transformed plasmids or vectors after transformation.

2.1.2 Growth curves

Growth curves were conducted in YNB in duplicate, yeast was pre-cultured in YPD overnight before resuspending to a density of $\sim 2.0 \times 10^6$ cells/ml ($OD_{595nm} \sim 0.1$).

Growth rates of all yeast strains used were monitored hourly using a spectrophotometer at a wavelength of 595nm.

2.2 Nile red lipid screening

Method used was as Rostron *et al* 2015.

Stationary phase cells were harvested by centrifugation at 2000rpm for 2 mins. The cell pellet that formed was washed twice in phosphate buffered saline (PBS) [8% NaCl, 0.2% KCl, 1.44% Na₂HPO₄, 0.24% KH₂PO₄] (Fisher, UK), to remove the high background fluorescence of the medium, before being resuspended in PBS; the optical density (at 595nm) was recorded following resuspension of the pellet.

To a black clear bottomed 96-well plate each well had 25µl of DMSO/PBS (1:1 v/v) added, followed by 250µl of the suspended cell pellets in triplicate (in the case of the control this was replaced with PBS) and finally 25µl of Nile red in acetone (with a final concentration of 5 µg/ml). Wavelengths of excitation 485 nm emission 535 nm, for determining the amount of neutral lipid, were utilised on a Tecan Genios Pro plate reader.

The data was processed to account for the background fluorescence of the PBS and to account for any variations in optical density after washing and resuspension in PBS. To combine the triplicate data the processed well data (for each triplicate) was averaged.

Where relevant, statistical analyses were performed by means of one way ANOVA with Tukey post hoc comparisons using GraphPad Prism 7.0 software. A significant result was determined to have a p value of <0.05.

2.3 Yeast genomic DNA extraction

Genomic DNA extractions were carried out as described by Lööke *et al.* 2011 and was done from both liquid media and directly from fresh plates. From liquid 200µl of exponential culture (OD₅₉₅ ~ 0.4) was harvested and centrifuged at 2000rpm for 2 minutes, from plates, single colonies were harvested, cells were resuspended in 100µl of lysis buffer [0.2M LiAc, 1% SDS solution] and incubated for 5 minutes at 70°C. 300µl 100% ethanol was added and samples vortexed before centrifuging at 15 000 x g for 3 minutes. The resultant pellet was then washed with 70% ethanol before resuspension in 100µl of TE buffer [10 mM Tris-HCL pH 8, 1 mM EDTA].

2.3.1 Polymerase chain reaction (PCR)

Primers utilised in this study are listed in table 2.2 and were synthesised by integrated DNA technologies (IDT, UK).

Table 2.2: Table of primers designed and utilised for PCR.

Primer	Sequence	Restriction sites
Dga1+promoter FP XhoI	5' ATA TAT CTC GAG GAT GAG ATT GCC TTT ACT GCG 3'	XhoI
Dga1 Rev SacI	5' ATA TAT GAG CTC GCA GAA TTG AAG ATA GTT GGG TAA 3'	SacI
Dga1 S2	5' TAA AAA ATC CTT ATT TAT TCT AAC ATA TTT TGT GTT TTC CAA TGA ATT CAT TAT TAA TCG ATG AAT TCG AGC TCG 3'	
Dga1 S3	5' TAC GAA AAT AGA GAA AAA TAT GGG GTA CCG GAT GCA GAA TTG AAG ATA GTT GGG TCG TAC GCT GCA GGT CGA C -3'	
Dga1 S17 F	5' GGA AGA AGG AAG GAG CCC CTA CAG CCG GTA TTA C 3'	
Dga1 S17 R	5' GTA ATA CCG GCT GTA GGG GCT CCT TCT TCC TTC C 3'	

Dga1 T53 F	5' CAT GCT GTC CAT TGG CGG CCC CTT TTG AAA GAA G 3'	
Dga1 T53 R	5' CTT TCA AAA GGG GCC AAT GGA CAG CAT G 3'	
Sch9 For 100bp UP	5' CTC ACA TAA TCA CCT AAG GGC ATC 3'	
Sch9 Rev 150bp Down	5' GTG ATA AAC TAG AAA TTT GCA GGA ACA ATT ATT C 3'	
Sch9 For ORF + Prom BamHI	5' ACA CAC GGA TCC ATG ATG AAT TTT TTT ACA TC 3'	BamHI
Sch9 Rev ORF XbaI	5' GTG TGT TCT AGA TCA TAT TTC GAA TCT TCC ACT-3	XbaI
Nat FOR	5' GAG GCC CAG AAT ACC CTC 3'	
Nat REV	5' GGG CAG ATG ATG TCG AGG 3'	
Dga1 Seq F	5' CCA AGC ACG ACA GTG GTC TAT C 3'	
Dga1 Seq2	5' CTA GAG TCA TGC TGT CCA TTG G 3'	
Dga1 T84 For	5' ATT TGC AAT CTC GGC ACC AGC ACT GTG GGT 3'	
Dga1 T84 Rev	5' ACC CAC AGT GCT GGT GCC GAG ATT GCA AAT 3'	
Dga1 S103 For	5' TTT TCG ATA GGG CTC CTG CAA CTG GC 3'	
Dga1 S103 Rev	5' GCC AGT TGC AGG AGC CCT ATC GAA AA 3'	
Sch9 S1	5'AAA AGA AAA GGA AAA GAA GAG GAA GGG CAA GAG GAG CGA TTG AGA AAT CAA TC	
Sch9 S2	5' TCT GAG AAT TAT ACT CGT ATA AGC AAG AAA TAA AGA TAC GAA TAT ACA ATA TGC GTA CGC TGC AGG TCG AC 3'	
M13 For	5' GTA AAA CGA CGG CCA GT '3	
M13 Rev	5' AAC AGC TAT GAC CAT G '3	

2.3.1.1 Amplification of the *SCH9* gene from *S. cerevisiae* gDNA by PCR

Primers Sch9 For ORF + Prom BamHI and Sch9 Rev ORF XbaI were used to amplify *SCH9* ORF, including 1000 bp upstream of start, from *S. cerevisiae* genomic DNA (gDNA).

A 1x reaction consisted of 1x Biomix Red, 0.2 μ M primers and ~250ng template gDNA from wild type *S. cerevisiae*.

PCR conditions were as follows;

1. Initial denaturation	95°C, 5 minutes		
2. Denaturation	95°C, 30 seconds	}	30 cycles
3. Annealing	45°C, 30 seconds		
4. Extension	72°C, 2 minutes 30 seconds		
5. Final Extension	72°C, 7 minutes		

2.3.1.2 Amplification of *SCH9* Deletion and 3HA tagging cassettes

Primers Sch9 S1 and Sch9 S2 were used to create and amplify an *SCH9* deletion cassette, using NAT as a selector, a 1x reaction consisted of; 1x HF Buffer, 200 μ M dNTPs, 1 μ M of each primer 50ng template DNA (pFA6aNatMX), 1 μ M MgCl₂ and 0.02U/ μ l Phusion polymerase.

Primers Dga1 S2 and Dga1 S3 were used to create and amplify a 3' 3HA tagged *DGA1*. A 1x reaction consisted of 1x HF Buffer, 200 μ M dNTPs, 0.2 μ M of each primer 50ng template DNA (pFA6aNatMX), 1 μ M MgCl₂ and 0.02U/ μ l Phusion polymerase.

PCR conditions were as follows;

1. Initial denaturation	98°C, 3 minutes		
2. Denaturation	98°C, 1 minute	}	35 cycles
3. Annealing	58°C, 1 minute		
4. Extension	72°C, 1 minute		

5. Final Extension 72°C, 7 minutes

SCH9 deletion cassette products were pooled and ethanol precipitated before transformation into *S. cerevisiae* strains.

Ten PCR reactions of the *dga1*-3HA tagging cassette were pooled prior to transformation into *S. cerevisiae* strains.

2.3.1.3 Amplification of *DGA1* from *S. cerevisiae* gDNA by PCR

Primers Dga1+promoter FP XhoI and Dga1 Rev SacI were used to amplify DGA1 ORF, including 1000bp upstream of the start, from *S. cerevisiae* gDNA. A 1x reaction (for 50µl) consisted of 1x HF Buffer, 200 µM dNTPs, 1µM of each primer 50ng template gDNA, 1 µM MgCl₂ and 0.02U/µl Phusion polymerase.

PCR conditions were as follows;

1. Initial denaturation	98°C, 3 minutes	
2. Denaturation	98°C, 1 minute	} 35 cycles
3. Annealing	59°C, 1 minute	
4. Extension	72°C, 2 minutes 30 seconds	
5. Final Extension	72°C, 7 minutes	
6. Hold at 21°C		

2.3.1.4 Mutagenesis of *DGA1*

Primers were used to create and amplify *Dga1* mutants of. *Dga1* mutations all result in a substitution of serine or threonine to alanine, at positions S17 (S17 For, S17 Rev), T53 (T53 For, T53 Rev), T84 (T84 For, T84 Rev) and S103 (S103 For, S103 Rev) using mutagenesis primers (see brackets for primers in relation to the mutation they

cause; E.g. substitution of serine to alanine at position 17 (S17) will utilise the S17 For and S17 Rev primers.

Two different methods of PCR were attempted, first a QuikChange method was used (as detailed in the “QuikChange II Site-Directed Mutagenesis Kit” by Agilent Technologies), and extended primer (or “SOEing”) PCR; this was done due to the failure of the QuikChange method to generate a product that was able to transform properly into DH5α cells.

QuikChange Method is a single method using TOPO*dga1* (*dga1* in a TOPO vector) as a template. The whole plasmid is copied using the PCR primers, resulting in a plasmid with the point mutation integrated into the *DGA1* in the plasmid. A 1x reaction consisted of 1× reaction buffer, 50 ng of dsDNA template, 125 ng of Dga1 S17 F, 125 ng of Dga1 S17 R, 200 μM dNTPs and 0.02U/μl Pfu polymerase. This was then digested with the restriction endonuclease *DpnI* as per the manufactures instructions (Thermo Scientific) to remove parental DNA

PCR conditions were as follows;

1. Initial denaturation	95°C, 30 seconds	
2. Denaturation	95°C, 30 seconds	} 12 cycles
3. Annealing	55°C, 1 minute	
4. Extension	68°C, 14 minutes	
5. Hold at 21°C		

The Extended primer PCR method consisted of 3 reactions, the products of the first two being the template of the third.

Mutagenesis 1 and 2 PCRs were performed with a normal Dga1 primer and a mutagenesis primer that was in the inverse direction, (e.g. a Forward Dga1 primer and a reverse mutagenesis primer such as Dga1+promoter FP XhoI and S17 Rev)

A 1x reaction consisted of 1x HF Buffer, 200 μ M dNTPs, 1 μ M of each primer 1ng template DNA (pTOPO-*DGA1*) and 0.02U/ μ l Phusion polymerase.

PCR conditions were as follows;

1. Initial denaturation	98°C, 30 seconds	
2. Denaturation	98°C, 30 seconds	} 35 cycles
3. Annealing	59°C, 30 seconds	
4. Extension	72°C, 2 minutes 30 seconds	
5. Final Extension	72°C, 7 minutes	
6. Hold at 21°C		

The products were then gel extracted and then used in mutagenesis 3.

A 1x reaction consisted of 1x HF Buffer, 200 μ M dNTPs, 1 μ M of each primer, 2ng template DNA (R1 + R2), 3% DMSO and 0.02U/ μ l Phusion polymerase

PCR conditions were as follows;

1. Initial denaturation	98°C, 30 seconds	
2. Denaturation	98°C, 30 seconds	} 10 cycles
3. Annealing	69°C, 30 seconds (-1°C every cycle)	
4. Extension	72°C, 1 minute 30 seconds	
5. Denaturation	98°C, 30 seconds	

6. Annealing	59°C, 30 seconds	} 30 cycles
7. Extension	72°C, 1 minute 30 seconds	
8. Final Extension	72°C, 7 minutes	
9. Hold at 21°C		

2.4.1 Cloning PCR products into vectors

Table 2.3: Table of plasmids utilised in this study

Plasmid name	Base vector	Selectable markers/promoter	Construction	Source
pRS313	pRS313	Amp/HIS3	N/A	Lab stock
pRS316	pRS316	Amp/URA3	N/A	Lab stock
pFA6a-natMX6	pFA6a-natMX6	Amp/NatMX	N/A	Lab stock
pRS313 <i>SCH9</i>	pRS313	Amp/HIS3	<i>SCH9</i> upstream of ATG cloned into BamHI and XbaI sites of pRS313	This Study
pRS316 <i>DGA1</i>	pRS316	Amp/URA3	<i>DGA1</i> upstream of ATG cloned into XbaI and SacI sites of pRS316	This Study
pRS313 <i>HOG1</i>	pRS313	Amp/HIS3	<i>HOG1</i> upstream of ATG cloned into BamHI and XbaI sites of pRS313	Lab stock

TOPO	TOPO	Amp/Kan	N/A	Invitrogen
------	------	---------	-----	------------

2.4.1.1 Cloning PCR products into a TOPO vector

Taq polymerase PCR products, were cloned into TOPO as per manufacturer's instructions (Invitrogen). These were left overnight and were transformed into DH5 α *E. coli*.

For PCR products from proofreading enzymes a poly-A tail had to first be added before they could be cloned into TOPO. Reactions consisted of 1 x Taq buffer, 66 μ M dATP, ~20ng DNA and 0.025U/ μ l Taq polymerase. Samples were incubated at 70°C for 15minutes before being using directly in TOPO ligation.

2.4.1.2 Cloning PCR products into pRS vectors

First both PCR products and the vector were digested with relevant fast digest restriction enzymes (as per the restriction enzyme sites on the primers used in the PCR; these were chosen to not cut the amplified gene at any position, the restriction sites alone would be cut and allow for insertion into the vector) [Thermo Scientific]. Digests were performed as per manufacturer's instructions but were left for 1 hour at 37°C. These were then cleaned with a NucleoSpin® Gel and PCR Clean-up kit (Macherey-Nagel) to remove the enzyme and any unreacted reactants from PCR left over, they were both eluted into the minimum volume allowed for by the kit.

These were then ligated with T4 Ligase (Thermo Scientific) as per manufacturer's instructions for sticky-end ligation but were left overnight at RT; the manufacturer

recommended a 1 hour ligation, instead ligations were performed over night to ensure the best chance of successful ligation (a 1 hour ligation proved to be unreliable).

5µl of the ligation was added to 50µl of chemically competent DH5α *E. coli* cells and incubated on ice for 1 hour. This was heat shocked at 42°C for 2 minutes and left on ice for 2 minutes. 1ml of LB was added and the cells left to recover for 1 hour at 37°C with shaking at 200rpm. This was centrifuged at 11,000 g for 30 seconds, 800µl of LB is removed, the pellet is resuspended in the remaining 200µl and spread onto an LB plate with 100µg/ml ampicillin and grown overnight at 37°C. Colonies were resuspended in 10µl of sterile distilled water, a colony PCR was performed using M13 forward and reverse primers. Reactions consisted of 1 x BioMix™ red, 1µM of each primer and 5µl of resuspended *E. coli* cells per 25µl reaction.

PCR conditions were as follows;

1. Initial denaturation	95°C, 5 minutes	
2. Denaturation	95°C, 30 seconds	} 30 cycles
3. Annealing	45°C, 30 seconds	
4. Extension	72°C, 2 minutes 30 seconds	
5. Final Extension	72°C, 7 minutes	

Those colonies that gave successful amplification of a product of the correct size were resuspended in 10ml of LB ampicillin and allowed to grow overnight 37°C to allow for plasmid preparation the following day.

2.4.1.3 Transformation of cassettes into *S. cerevisiae*

Preparation and transformation of *S. cerevisiae* competent cells was carried out as detailed in Janke *et al.* 2004. Mid exponentially growing cells (7 hours) were harvested

by centrifugation at 492 x g for 5 minutes and washed once with 0.5 volumes of sterile water and once with 0.2 volumes of SORB [100mM LiAc, 10mM Tris-HCl pH 8, 1mM EDTA/NaOH pH 8, 1M sorbitol; adjusted to pH 8 with dilute acetic acid].

SORB was removed by aspiration and cells resuspended in 360µl SORB per 50ml culture and 1mg/ml salmon sperm carrier DNA added (Invitrogen, UK). The cells were stored at 80°C until needed for transformation. They were defrosted prior to use.

50µl of prepared competent cells were added to 4µg plasmid DNA and mixed well before addition of a six-fold volume of PEG [100mM LiAc, 10mM Tris-HCl pH 8, 1mM EDTA/NaOH pH 8, 40% PEG 4000 (Fisher, UK)]. The suspension was incubated for 30 minutes at room temperature, mixing throughout. 10% DMSO was added before heat shocking the cells at 42°C for 15 minutes. Cells were pelleted by centrifugation for 2 minutes at 300 x g, the supernatant removed and cells resuspended in 1000µl of YPD liquid medium and left to grow overnight at 30°C at 180 rpm before plating onto selective medium.

2.5 SDS-PAGE and western blotting

2.5.1 Denatured protein extraction

Denatured protein extractions were carried out as described by Lawrence *et al* 2007.

Cells were harvested at 492 x g from samples frozen in liquid nitrogen (LN) before resuspension in 1ml of 0.3M NaOH followed by the addition of 150µl of 55% (w/v) trichloroacetic acid. Samples were centrifuged at 4°C at 19000g for 1 minutes before aspiration of supernatant. The pellet was then resuspended in 30µl SDS sample buffer [50 mM Tris-Cl (pH 6.8), 2% SDS (w/v), 0.1% bromophenol blue, 10% (v/v) glycerol]

per Abs_{595nm} 0.1 of cells. Proteins were denatured at 95°C for 10 minutes and allowed to cool before having 1µl of Dithiothreitol (DTT) added per 100µl of overall volume.

2.5.2 Gels of protein extractions

12% polyacrylamide gels were prepared [for running portion; 12% acrylamide, 0.39M Tris (pH 8.8), 0.1% Sodium dodecyl sulphate (SDS), 0.1 % Tetramethylethylenediamine (TEMED), and 0.1% Ammonium persulphate (APS). For stacking portion; 5.1% acrylamide, 0.13M Tris (pH 6.8), 0.1% SDS, 0.1% TEMED, and 0.1% APS], protein extraction samples were then loaded into the wells. Gels were run in pairs at 300 volts at 20 mA per gel in a running buffer [0.033M Tris base, 0.3M glycine, and 0.0035M SDS].

2.5.3 Western blotting

Proteins were transferred from the 12% polyacrylamide gel to nitrocellulose membrane by application of a constant voltage (90 volts) for 1 hour in transfer buffer [25 mM Tris-HCl (pH 7.6), 192 mM glycine, 20% methanol). This was then blocked with 10% milk in Tris buffered saline tween (TBST) [50 mM Tris HCl, pH 7.4, 150 mM NaCl, 0.1% Tween 20] for one hour before applying the primary antibody and leaving overnight at 4°C. Three washes of 15 minutes in TBST were done to remove the excess primary antibody. Secondary antibody was added and incubated at room temperature for 45 minutes, before another three washes of 15 minutes TBST to remove excess secondary antibody.

Antibodies utilised by the present study were: α-Hog1p to detect total amounts of Hog1p (Santa Cruz Biotechnology), 1:1000 dilution in TBST. α-P-p38 to detect dually phosphorylated Hog1p (Cell Signalling Technology), 1:1000 dilution in TBST. Rabbit IgG, HRP-linked secondary antibody (from donkey) was used at a dilution of 1:10000 in

TBST for α -Hog1p and α -P-p38. HA primary antibody was used in a 1:1000 dilution in TBST with mouse IgG, HRP-linked secondary antibody (from donkey) was used at a dilution of 1:10000 in TBST.

Westerns were visualised using ECL prime solutions (GE Healthcare) as per manufacturer's instructions.

2.5.4 Phos-tag™

Phos-Tag™ gels were run to try to separate proteins by their phosphorylation status (e.g. how many times a protein is phosphorylated). Phos-Tag™ gels were prepared as per 2.5.2 but with the addition of a final concentration of 0.05mM Phos-tag tag™ AAL Solution and 0.1 mM MnCl₂ solution (a 0.2 mM MnCl₂ solution was used when a 0.1 mM MnCl₂ solution failed to transfer properly). These were run as 2.5.2 but for a minimum of 2 hours. Western blotting was as per 2.5.3 but prior to transfer Phos-tag™ gels were washed in transfer buffer with 1 mM EDTA for 10 minutes and in normal transfer buffer for 10 minutes. Transfer was done for 2.5 hours at 90 volts.

3.0 Results

3.1. The MAPK Hog1 is required for neutral lipid accumulation

Lipogenesis is a metabolic process whereby lipids are formed from fatty acids, these fatty acids are themselves formed through a series of biosynthetic reactions starting which use acetyl-CoA as their starting point. Cancer cells undergo many changes to their cellular metabolism, so the process of lipogenesis becomes dysregulated. This results in cancer cells have altered lipid metabolism (Walther and Farese 2012) which, due to the Warburg effect (Diaz-Ruiz *et al*, 2011; Liberti *et al*, 2016), results in cells accumulating more lipid (Baenke *et al*, 2013). This altered metabolism provides the cancer cells with both energy and increased lipid synthesis required to support their proliferation (Liberti *et al*, 2016). This altered lipid metabolism makes cancer cells distinct from healthy body cells, an altered phenotype may allow for treatments which select for that phenotype, in effect for cancer.

In mammalian cells, mTOR has a well-established role in regulating lipid metabolism (Laplante *et al*, 2009a, Laplante *et al* 2012b) but there is also some evidence that the MAPK, p38, might also have a role in lipid metabolism regulation, with p38 implicated in cancer cell proliferation, angiogenesis and metastasis (Leelahavanichkul *et al* 2014, Mao *et al* 2010).

S. cerevisiae is a well-established model organism (Henr *et al*, 2012; Zhang *et al*, 2003) and has been previously used to characterise lipid metabolism in mammalian cells (Schmidt *et al*, 2013; Koch *et al*, 2014; Diaz-Ruiz *et al*, 2011). *S. cerevisiae* is easy to work with, cells accumulate neutral lipid when nitrogen in the media has been expended and cells enter stationary phase (Kolouchova *et al*, 2016, Natteret *et al*, 2013). Once in stationary phase neutral lipid levels can be assessed using the Nile Red method (Rostron *et al*, 2015).

It also has highly conserved MAPK pathways, Hog1p is the *S. cerevisiae* orthologue of the mammalian MAPK p38 (Banuett 1998), acting primarily as the cellular response to osmotic stress. Previous unpublished work suggests a link between the MAPK Hog1 and neutral lipid accumulation. *S. cerevisiae*.

To determine the role of the MAPK pathway in neutral lipid accumulation in yeast, a series of HOG MAPK *S. cerevisiae* genomic deletion mutants were investigated; *ssk2Δ*, *ste11Δ*, *pbs2Δ*, *hog1Δ* (Figure 1.7). Initially, growth curves were undertaken to investigate whether the deletions affected overall cell growth and to determine the time point for entry into stationary phase. Growth curves (Figures 3.1 – 3.6) indicate that the HOG pathway mutants have similar growth rates when compared to the wild type *S. cerevisiae*. Further, all strains enter stationary phase at a similar time indicating that 18hrs was an appropriate time point to measure neutral lipid levels as used in Rostron *et al*, 2015. Levels of neutral lipid in stationary phase for each mutant was then determined using a Nile Red assay, previously described by Rostron *et al*, 2015. Two additional mutants, *lro1Δ* and *fat1Δ*, were used as negative and positive controls, respectively; *lro1Δ* and *fat1Δ* would accumulate less and more lipid respectively (Rostron *et al*, 2015) and so were used as controls to ensure that the assay was properly functioning.

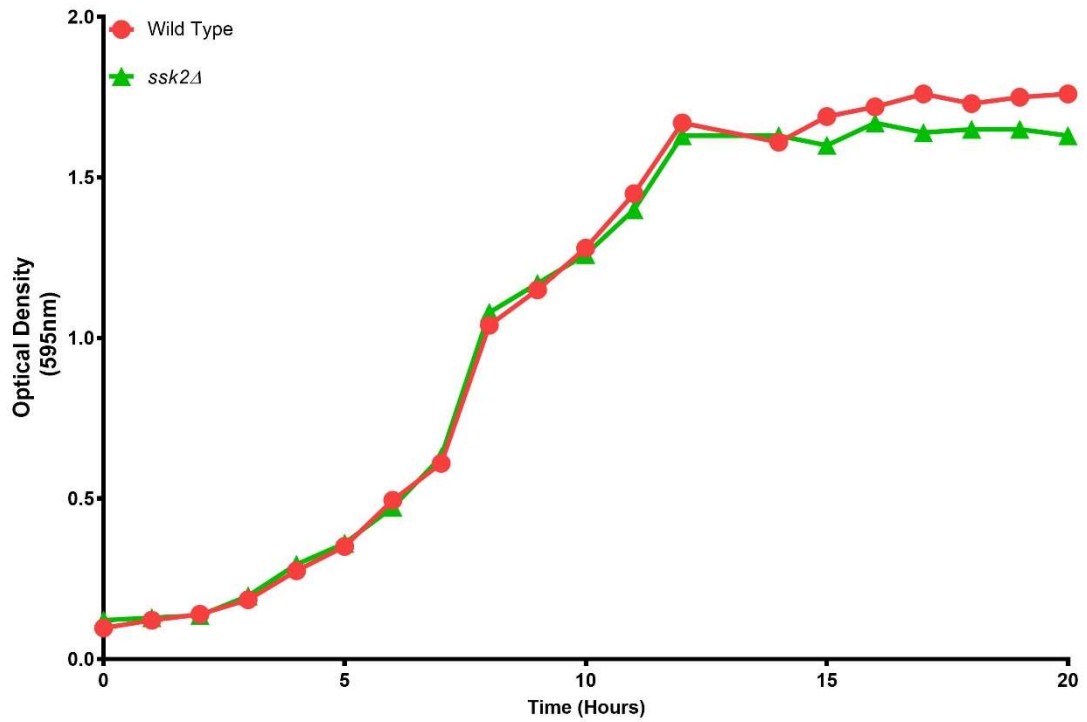


Figure 3.1. Growth curve of *S. cerevisiae* wild type and *ssk2*Δ under normal conditions in yeast nitrogen base medium (YNB). Cultures were diluted to 2×10^6 cells ($OD_{595} \sim 0.1$) and incubated with shaking, 180rpm, at 30°C. Optical density readings at 595nm were taken hourly until mid to late stationary phase was reached.

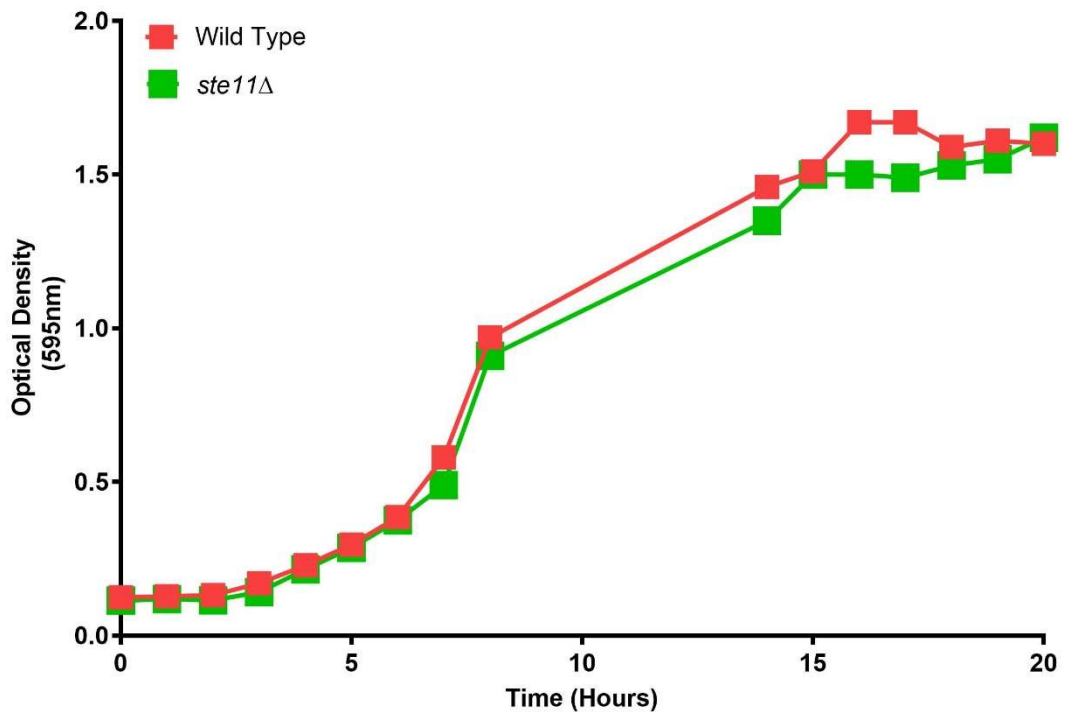


Figure 3.2. Growth curve of *S. cerevisiae* wild type and *ste11*Δ under normal conditions in yeast nitrogen base medium (YNB). Cultures were diluted to 2×10^6 cells ($OD_{595} \sim 0.1$) and incubated with shaking, 180rpm, at 30°C. Optical density readings at 595nm were taken hourly until mid to late stationary phase was reached.

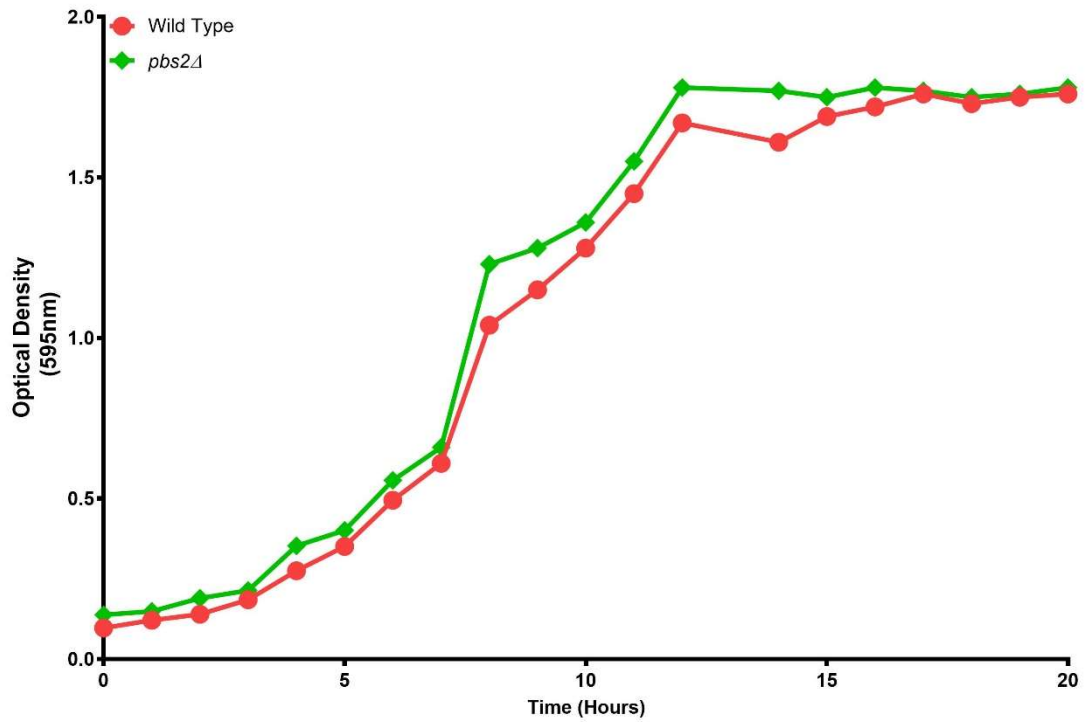


Figure 3.3. Growth curve of *S. cerevisiae* wild type and *pbs2Δ* under normal conditions in yeast nitrogen base medium (YNB). Cultures were diluted to 2×10^6 cells ($OD_{595} \sim 0.1$) and incubated with shaking, 180rpm, at 30°C. Optical density readings at 595nm were taken hourly until mid to late stationary phase was reached.

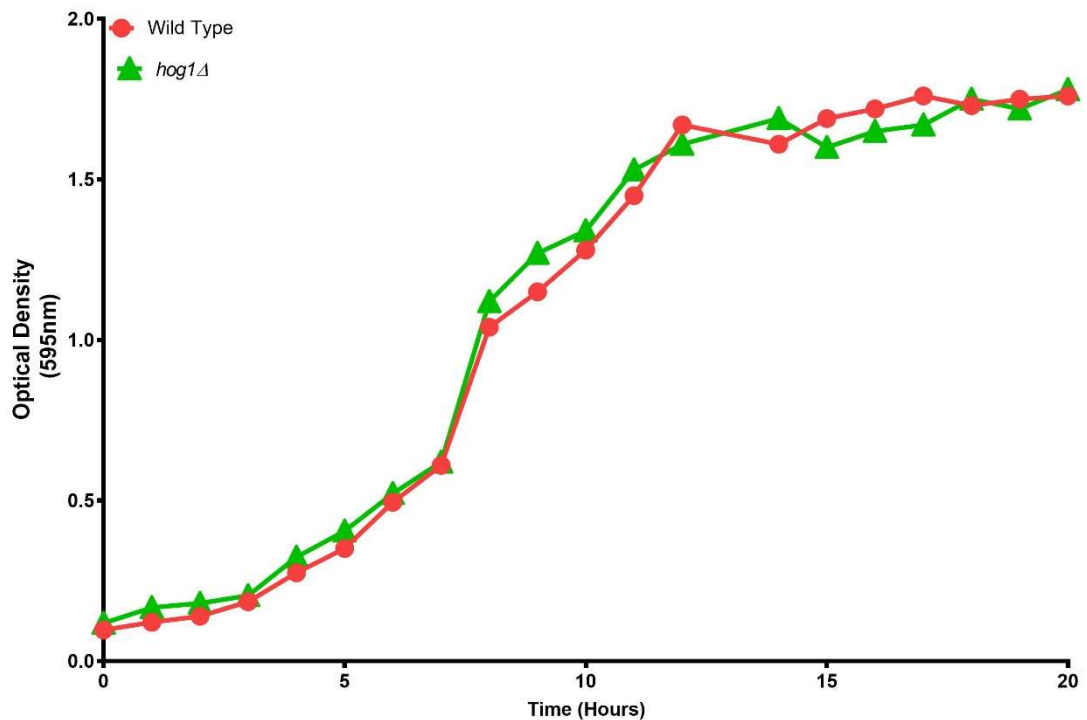


Figure 3.4. Growth curve of *S. cerevisiae* wild type and *hog1Δ* under normal conditions in yeast nitrogen base medium (YNB). Cultures were diluted to 2×10^6 cells ($OD_{595} \sim 0.1$) and incubated with shaking, 180rpm, at 30°C. Optical density readings at 595nm were taken hourly until mid to late stationary phase was reached.

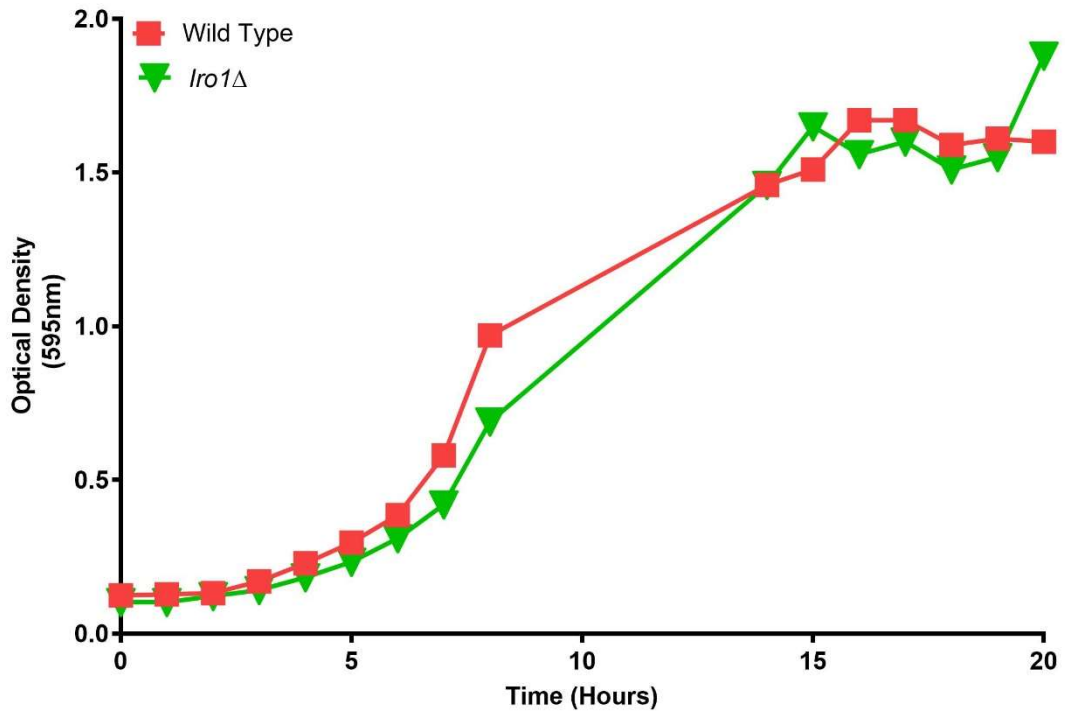


Figure 3.5. Growth curve of *S. cerevisiae* wild type and *Iro1*Δ under normal conditions in yeast nitrogen base medium (YNB). Cultures were diluted to 2×10^6 cells ($OD_{595} \sim 0.1$) and incubated with shaking, 180rpm, at 30°C. Optical density readings at 595nm were taken hourly until mid to late stationary phase was reached.

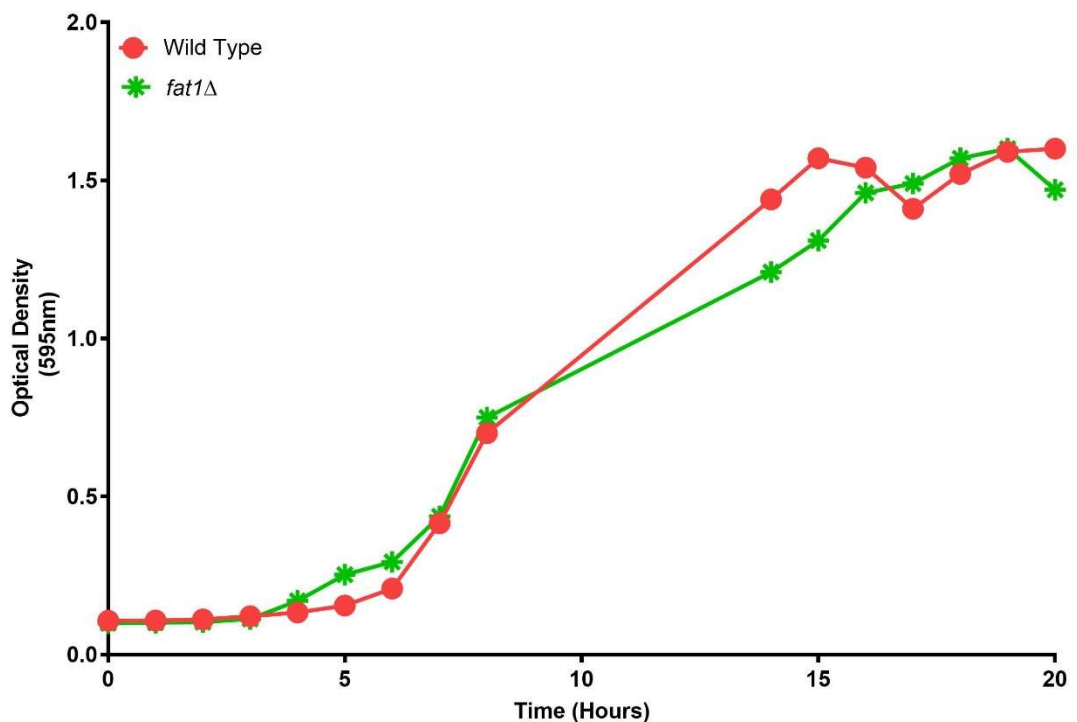


Figure 3.6. Growth curve of *S. cerevisiae* wild type and *fat1*Δ under normal conditions in yeast nitrogen base medium (YNB). Cultures were diluted to 2×10^6 cells ($OD_{595} \sim 0.1$) and incubated with shaking, 180rpm, at 30°C. Optical density readings at 595nm were taken hourly until mid to late stationary phase was reached.

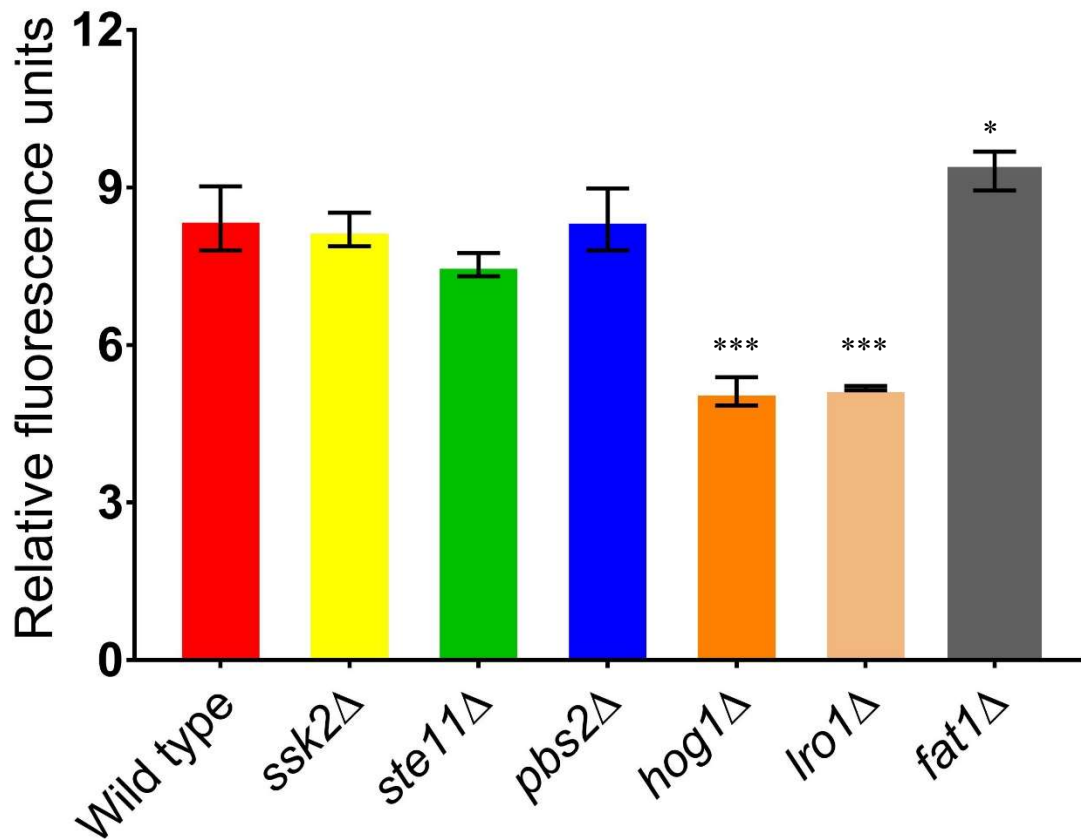


Figure 3.7. Neutral lipid fluorescence intensity of Nile Red stained *S. cerevisiae* wild type and the HOG component mutants *ssk2Δ*, *ste11Δ*, *pbs2Δ*, *hog1Δ*, *lro1Δ* and *fat1Δ*. Cells were harvested 18 hrs post resuspension in YNB. Cells were washed twice in PBS before adjusting to a cell density of 2×10^7 cells/ml. 5×10^6 cells were transferred to the wells of black 96-well plates in triplicate. $25 \mu\text{l}$ PBS/DMSO (1:1 v/v) and $5 \mu\text{g/ml}$ Nile red were added to each sample. Plates were screened using the wavelengths: excitation 485nm, emission 535nm. Data shown as means of duplicates \pm SD. Significance indicated between wild type and *hog1Δ* and *lro1Δ* and *fat1Δ*. * $p \leq 0.01$ *** $p \leq 0.001$. Data analysed by one way ANOVA with Tukey *post hoc* test.

Nile Red results (Figure 3.7) show no significant difference in neutral lipid accumulation in *ssk2Δ*, *ste11Δ* and *pbs2Δ* when compared to the wildtype. However, a significant decrease of 1.6-fold was observed in the *hog1Δ* strain when compared to the wildtype. The controls *lro1Δ* and *fat1Δ* accumulated 1.6-fold less and 1.13-fold more neutral lipid respectively as previously described (Rostron *et al*, 2015).

To confirm that the loss of *HOG1* was causing the reduction in neutral lipid accumulation, *HOG1* was cloned into pRS316 and introduced into the *hog1Δ* strain. Neutral lipid levels were then measured and compared to the control, wild type and *hog1Δ* strain containing the vector pRS316 alone.

Figure 3.8 shows a restoration of neutral lipid accumulation phenotype once *HOG1* is reintroduced into cells on a plasmid, with *hog1Δ*pRS313*HOG1* accumulating neutral lipid at a similar level to the wild type.

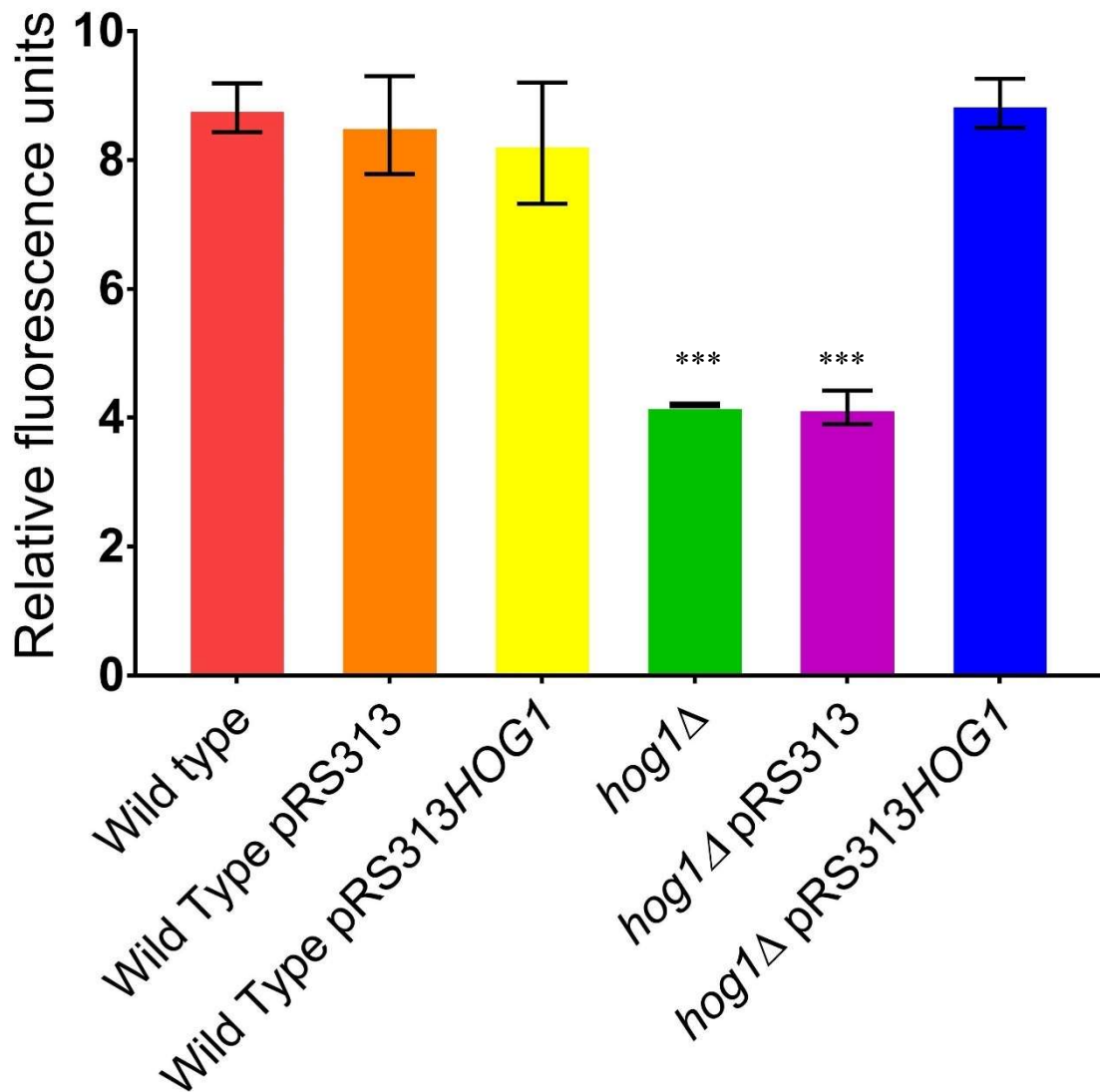


Figure 3.8. Neutral lipid fluorescence intensity of Nile Red stained *S. cerevisiae* wild type and *hog1Δ* mutant with pRS313 and pRS313HOG1 transformed into both. Cells were harvested 18 hrs post resuspension in YNB. Cells were washed twice in PBS before adjusting to a cell density of 2×10^7 cells/ml. 5×10^6 cells were transferred to the wells of black 96-well plates in triplicate. 25 μ l PBS/DMSO (1:1 v/v) and 5 μ g/ml Nile red were added to each sample. Plates were screened using the wavelengths: excitation 485nm, emission 535nm. Data shown as means of duplicates \pm SD. Significance indicated between wild type and the *hog1Δ* and *hog1Δ*pRS313 mutants. **** $p \leq 0.0001$. Data analysed by one way ANOVA with Tukey *post hoc* test.

These data suggest that Hog1p is involved in neutral lipid accumulation. This cause to further investigate Hog1p, its activation may be a good place to start.

3.2 Hog1p phosphorylation is seen as cells began to accumulate neutral lipid

Hog1p is activated via a dual phosphorylation on Thr174 and Ty176 (Maayan *et al.* 2012), therefore, if Hog1p is important for neutral lipid accumulation activation of the protein should be observed as cells leave exponential growth and begin to enter stationary phase at approximately 10hrs.

Cells were resuspended in YNB media and growth monitored over time via optical density at 595nm. Cells were harvested at 30 min intervals as cells progressed through exponential phase, between 6 and 10 hours of growth. The resulting protein extracts were analysed via a western blot using a p38 antibody which detects dual phosphorylation of Hog1p at Thr174 and Ty176. Samples were also probed with a hog1 antibody to determine total Hog1p levels.

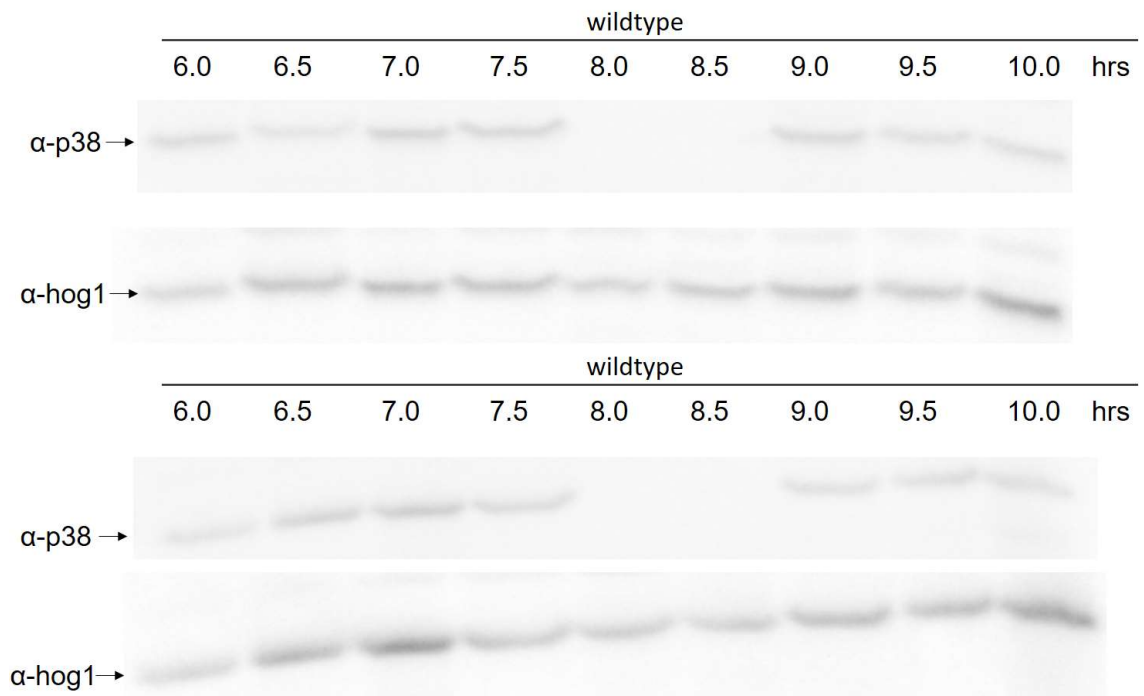


Figure 3.9. Duplicate Western blot of protein extractions from wild type *S. cerevisiae* cells over a time course of 6 to 10 hours of growth in YNB media and incubated with shaking, 180rpm, at 30°C. Membranes were first probed with a p38 antibody before being stripped and reprobed with a Hog1 antibody.

Westerns (Figure 3.9) show dual phosphorylation of Hog1p from 6 to 7.5 hours, followed by its loss at 8 and 8.5 hours, before dual phosphorylation is seen again from 9hrs onwards.

In the early exponential phase samples (6 – 7.5 hours) Hog1p is dually phosphorylated at Thr174 and Ty176 due to the transition from lag phase to exponential phase. In the mid exponential phase (8 – 8.5 hours), where the cells have adapted to the environment, there is no detectable phosphorylation at Thr174 and Ty176, indicating a lack of activation of Hog1p. In later exponential (9 – 10 hours) there is again phosphorylation at Thr174 and Ty176 indicating a reactivation of Hog1p. This data suggests an activation of Hog1p, possibly via phosphorylation, as cells approach stationary phase where they begin to accumulate neutral lipid.

3.3 Hog1p activation appears to be Pbs2p independent

Data has shown that neutral lipid accumulation is reduced in the absence of Hog1p (*hog1Δ* cells) (Figure 3.7) and that Hog1p is phosphorylated at Thr174 and Ty176 as cells enter stationary phase (Figure 3.8). Hog1p is a well-established target of the MAPKK Pbs2p (Maayan *et al.* 2012), however *pbs2Δ* mutants show wild type levels of neutral lipid (Figure 3.7).

To investigate the role of Pbs2p and its regulation of Hog1p in neutral lipid accumulation, a *hog1Δpbs2Δ* double deletion strain was made. A growth curve of the *hog1Δpbs2Δ* mutant strain was undertaken and determined that it had similar growth phenotype to wildtype cells (Figure 3.10). To determine its effect on neutral lipid accumulation, Nile red assay was then performed with wild type, *pbs2Δ*, *hog1Δ* and *hog1pbs2Δ* cells, to determine neutral lipid levels in stationary phase.

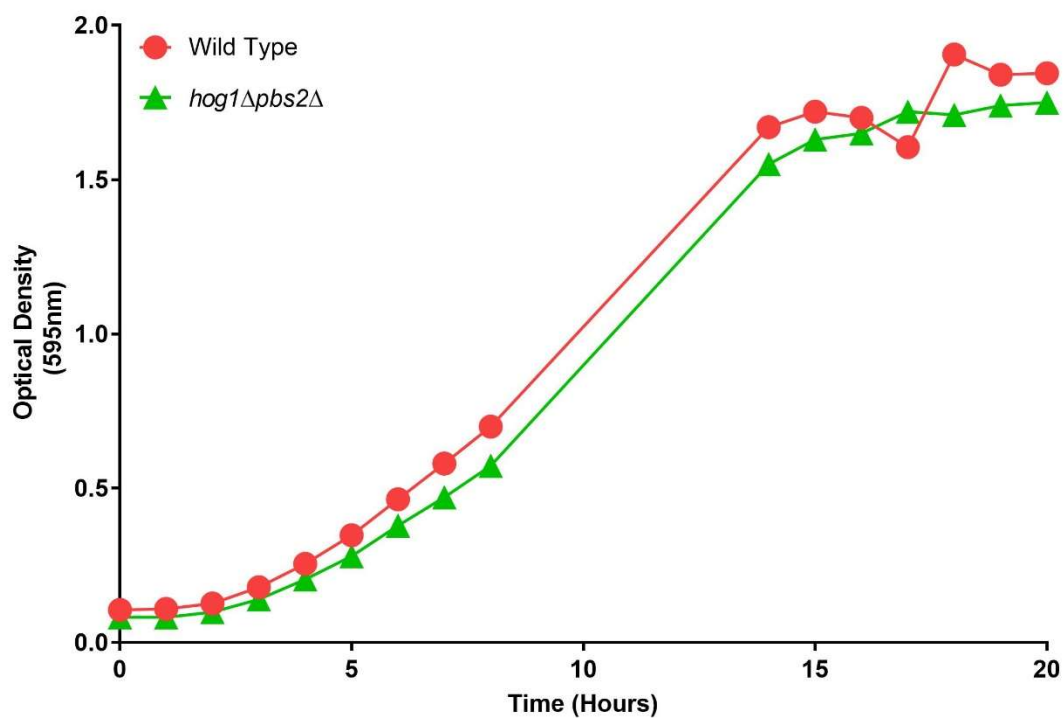


Figure 3.10. Growth curve of *S. cerevisiae* wild type and *hog1Δpbs2Δ* under normal conditions in yeast nitrogen base medium (YNB). Cultures were diluted to 2×10^6 cells ($OD_{595} \sim 0.1$) and incubated with shaking, 180rpm, at 30°C. Optical density readings at 595nm were taken hourly until mid to late stationary phase was reached.

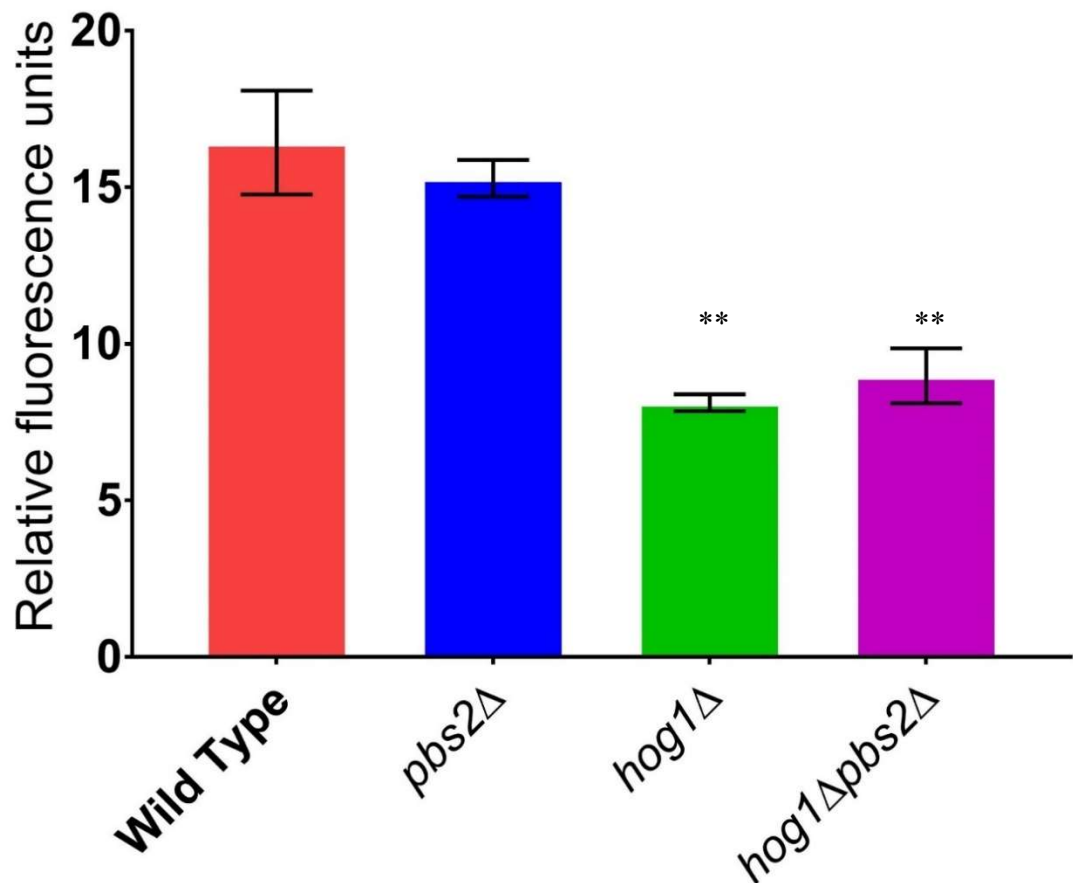


Figure 3.11. Neutral lipid fluorescence intensity of Nile Red stained *S. cerevisiae* wild type and *pbs2Δ*, *hog1Δ* and *hog1Δpbs2Δ* mutants. Cells were harvested 18 hrs post resuspension in YNB. Cells were washed twice in PBS before adjusting to a cell density of 2×10^7 cells/ml. 5×10^6 cells were transferred to the wells of black 96-well plates in triplicate. $25\mu\text{l}$ PBS/DMSO (1:1 v/v) and $5\mu\text{g/ml}$ Nile red were added to each sample. Plates were screened using the wavelengths: excitation 485nm, emission 535nm. Data shown as means of duplicates \pm SD. Significance indicated between wild type and the *hog1Δ* single and double delete mutants. ** $p \leq 0.01$. Data analysed by one way ANOVA with Tukey *post hoc* test.

Nile red data (Figure 3.11) showed similar levels of neutral lipid accumulation in both the wild type and *pbs2Δ* strain but a significant reduction in *hog1Δ* and *hog1Δpbs2Δ*, with levels being approximately half that of the wild type.

Data shows that there is no reduction in neutral lipid levels in a *pbs2Δ* single deletion and there was no additive effect for the *hog1Δpbs2Δ* double deletion mutant, suggesting that Pbs2p isn't required for cells to accumulate neutral lipids.

As data suggests that Hog1p activation is required for neutral lipid accumulation but Pbs2p is not, this indicates that Hog1p may be activated in a Pbs2p independent manner. As such, the phosphorylation state of Hog1p in late exponential phase was investigated in the presence and absence of Pbs2p.

Cells from wild type and *pbs2Δ S. cerevisiae* were grown in YNB and harvested at 8 to 10 hours of growth (the period that in Figure 3.8 showed a change in Hog1p phosphorylation at Thr174 and Ty176) and frozen in liquid nitrogen. Proteins were extracted, run on acrylamide gels and western blots performed.

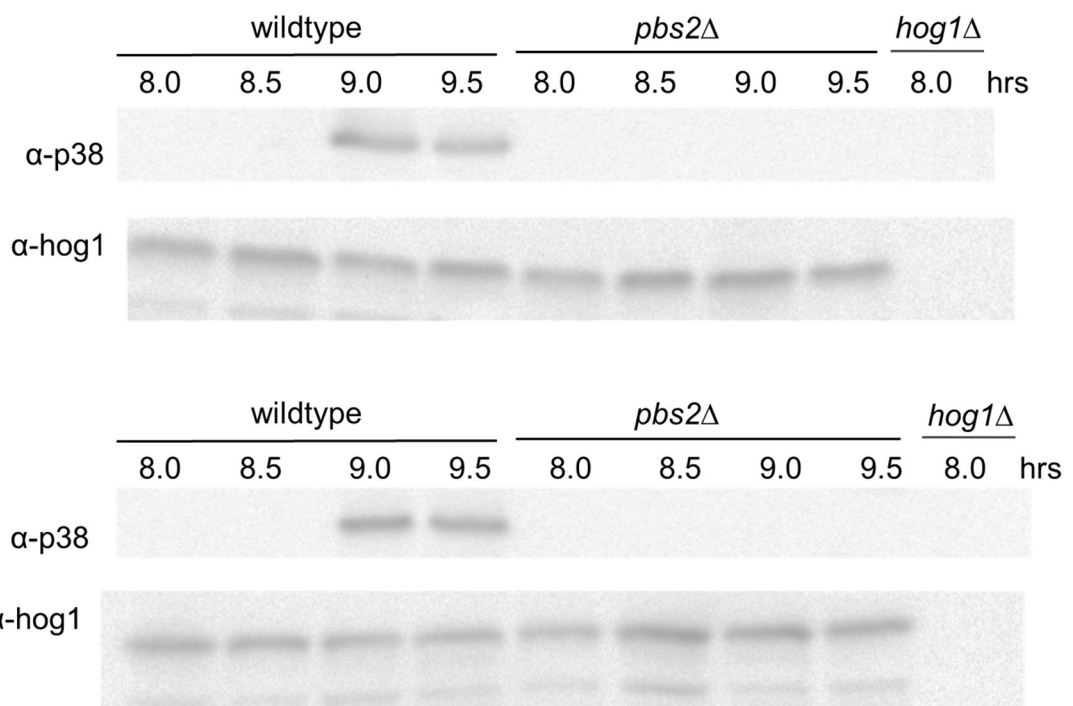


Figure 3.12. Duplicate Western blot of protein extractions from wild type and *pbs2Δ S. cerevisiae* cells over a time course of 8 to 10 hours of growth in YNB media and incubated with shaking, 180rpm, at 30°C. Membranes were first probed with α-p38 antibody before being stripped and reprobbed with Hog1p antibody.

Western blot data (Figure 3.12) shows a lack of dual phosphorylation at Thr174 and Ty176 across all time points investigated in the *pbs2Δ* cells, this differs from the wild type where dual phosphorylation is seen at 9 and 9.5 hours of growth; there is no dual phosphorylation at 8 or 8.5 hours as previously observed (Figure 3.11). The negative control of *hog1Δ* displayed no Hog1p in the cells as expected.

This data suggests that the dual phosphorylation at Thr174 and Ty176 observed during late exponential phase is as a result of Pbs2p. Dual phosphorylation doesn't appear to be essential for lipid accumulation as *pbs2Δ* lack dual phosphorylation at Thr174 and Ty176 neutral lipid accumulation still occurs (Figure 3.7).

As in *pbs2Δ* cells, Hog1 is not dually phosphorylated at Thr174 and Ty176 (Figure 3.12), it is possible that Hog1p is being phosphorylated and activated at alternative sites and/or only phosphorylated at one of these sites.

To determine whether Hog1p is being phosphorylated independently of Pbs2p as cells undergo the lipogenic switch, a Phos-tagTM was used to examine the phosphorylation state of Hog1p in a *pbs2Δ* strain. A Phos-tagTM gel was used to its ability to separate the proteins by their phosphorylation status, proteins with more sites phosphorylated will stay higher in the gel than those with less phosphorylation. As data shows a lack of phosphorylation at Thr174 and Ty176 in *pbs2Δ* cells we wanted to determine the number of phosphorylations (if any) on Hog1p in the *pbs2Δ* cells and compare them with the wild type. This would confirm whether Hog1p phosphorylation is needed for neutral lipid accumulation. To optimise the protein shift observed various concentrations of MnCl₂ (0.1mM to 0.2mM) were added to the protein gel. In addition, for the western blot analysis, due to reduced transfer efficiency the time was increased from 1 hour to 2.5 hours.

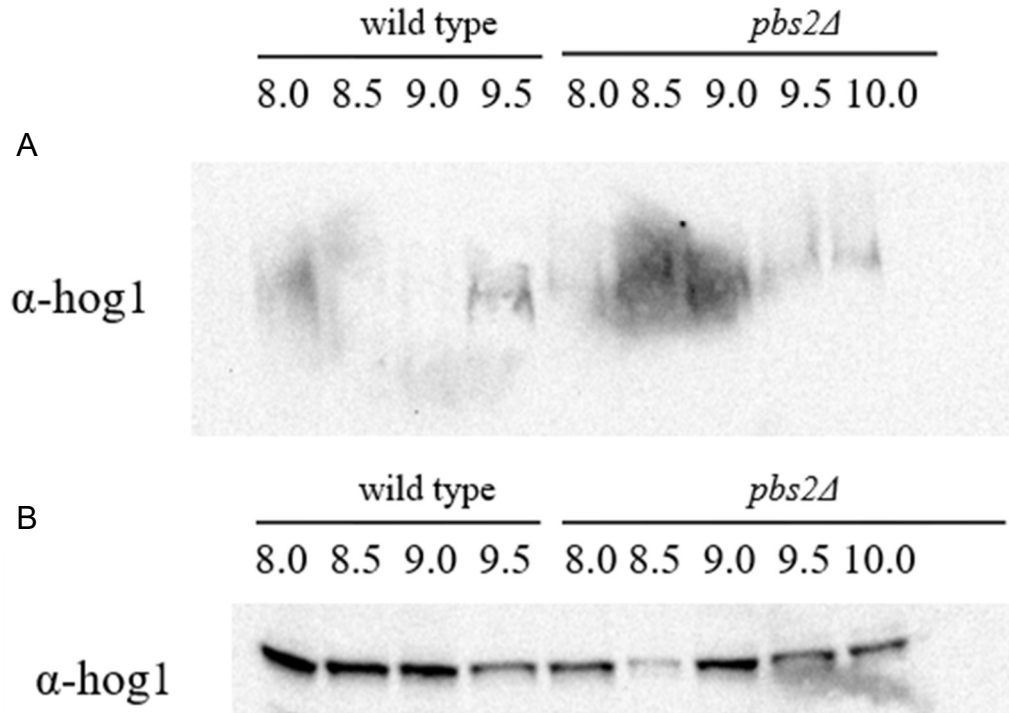


Figure 3.13.1 Western blot of Phos-tagTM gel (Gel A), Gel A did not transfer properly, and of a normal acrylamide gel (Gel B) of protein extractions from wild type and *pbs2Δ* *S. cerevisiae* cells over a time course of 8 to 10 hours of growth in YNB media and incubated with shaking, 180rpm, at 30°C. Phos-tagTM gel was run with 0.1mM MnCl₂ and transferred for 1 hour. Membranes were probed with hog1 antibody, an ECL secondary antibody was added to each primary to allow for visualisation on a BioradTM ChemiDocTM XRS+ machine.

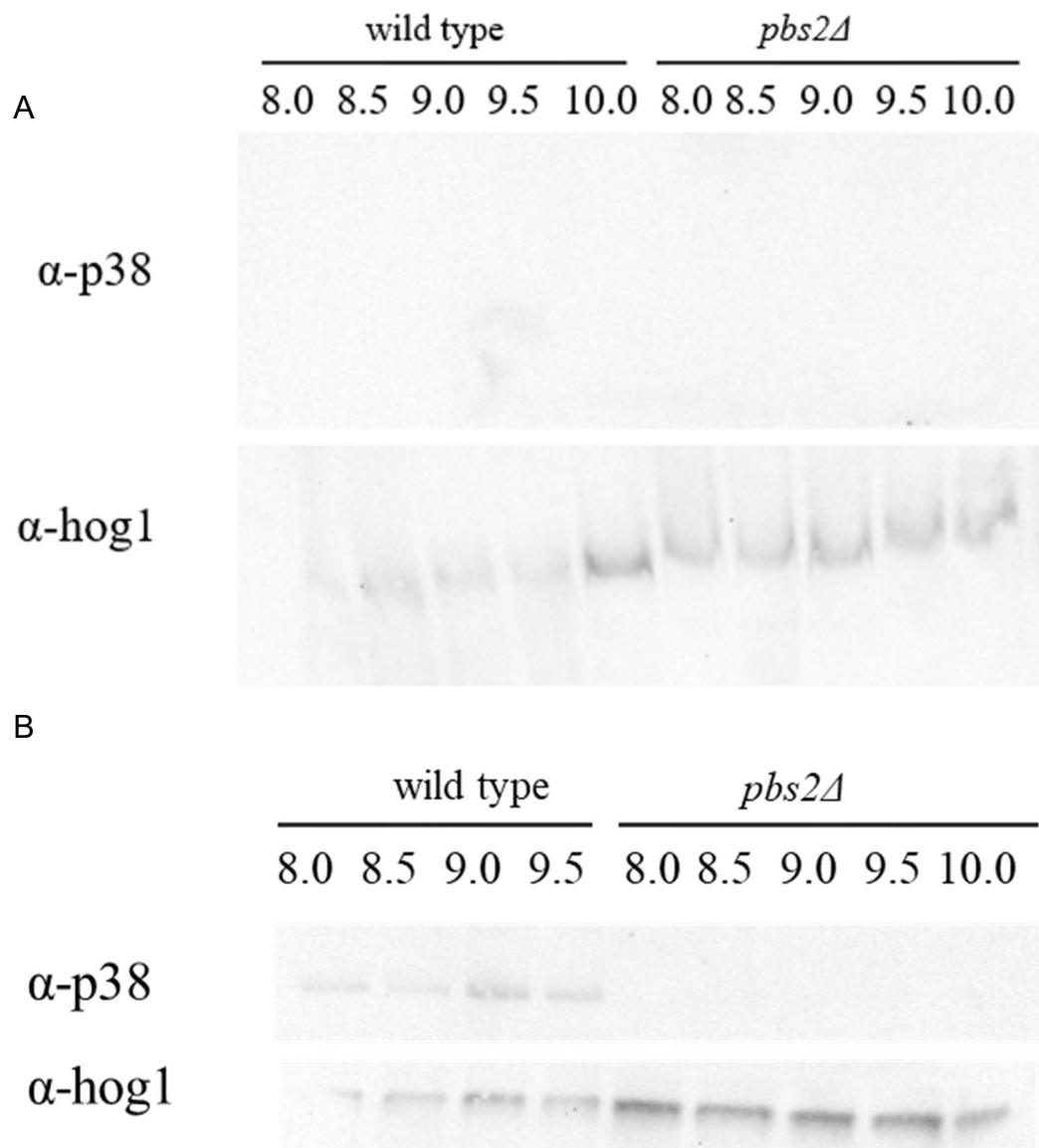


Figure 3.13.2. Western blot of Phos-tag™ gel (Gel A) and of a normal acrylamide gel (Gel B) of protein extractions from wild type and *pbs2Δ* *S. cerevisiae* cells over a time course of 8 to 10 hours of growth in YNB media and incubated with shaking, 180rpm, at 30°C. Phos-tag™ gel was run with 0.2mM MnCl₂ and transferred for 2.5 hours. Membranes were probed with p38 antibody first, then stripped and reprobbed with hog1 antibody, an ECL secondary antibody was added to each primary to allow for visualisation on a Biorad™ ChemiDoc™ XRS+ machine.

Wild type and *pbs2Δ* protein samples were initially run on a normal gel to confirm Hog1p and its dual phosphorylation state could be visualised and to ensure equal loading of the wells. Phospho-38 was not detected on the Phos-tag™ gel (Figure 3.13.2 A) but was detected on the regular gels (Figure 3.13.2 B). Gel A (Figure 3.13 A) did not transfer properly. On the Phos-tag™ gels (Figures 3.13.1 A and Figure 3.13.2 A) no shift is seen, this combined with the fact that the wild type 8 and 8.5 hours, which

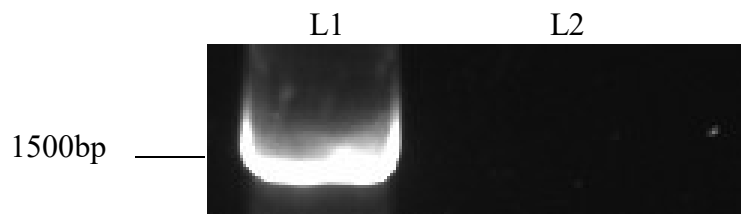
show no dual phosphorylation at Thr174 and Ty176 (Figure 3.12), have the same position in the gel as the 9, 9.5 and 10 hours, which are dually phosphorylated at Thr174 and Ty176 (Figure 3.9), suggests that the Phos-tag™ gel has not worked properly.

3.4 Sch9p is required for neutral lipid accumulation

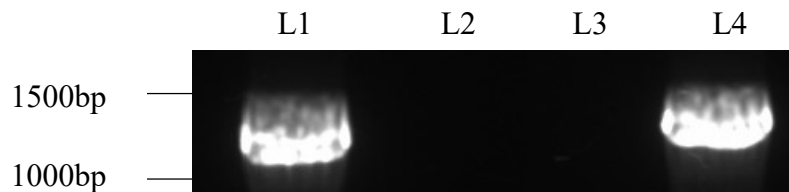
As Pbs2p appears not to be involved in Hog1p activation in neutral lipid accumulation, therefore phosphorylation by Pbs2p is not required for the activation of Hog1p in neutral lipid accumulation. A different kinase may be phosphorylating Hog1p at different sites, a potential candidate is Sch9p (a target of the Tor 1 complex) with evidence that it is potentially involved in the phosphorylation of Hog1p under conditions of osmotic stress (Pascual-Ahuir and Proft 2007).

sch9Δ cells were made via homologous recombination using an *SCH9* NAT deletion cassette. The *SCH9* deletion cassette was successfully amplified (Figure 3.14 A). Successful integration of the cassette into wild type *S. cerevisiae* was confirmed by PCR (Figure 3.14 B). Growth curves of the *sch9Δ* deletion strain (Figure 3.15 –3.16) showed no significant growth difference from the wild type. As no growth defects were observed, Nile Red assays were performed to determine levels of neutral lipids in the *sch9Δ*.

A.



B.



C.

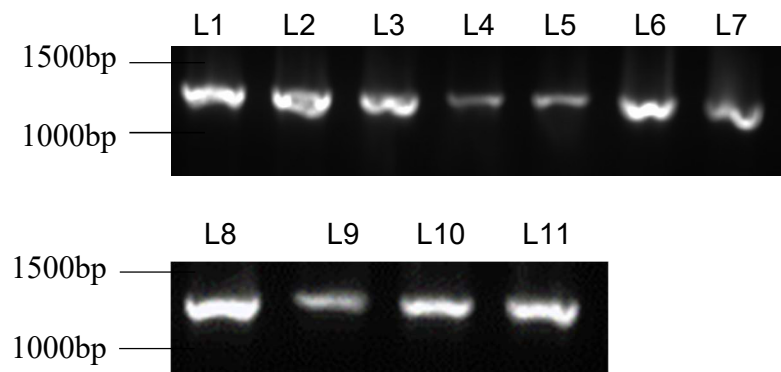


Figure 3.14. (A) Amplification of *SCH9* deletion cassettes. 1% agarose gel displaying amplification of a *sch9* deletion cassette utilising Sch9 S1 and S2 primers with a pFA6aNatMX6 template. Product was ~1.5kb in lane 1, lane 2 was a negative control.

(B) Testing of integration of cassette into wild type *S. cerevisiae*. 1% agarose displaying amplification from wild type *S. cerevisiae* gDNA with *SCH9* deletion cassette transformed in using Sch9 Up 100bp and Nat Rev primers using Taq polymerase. Products were of the expected size of ~1.3kb in lanes 1 and 4, these had successfully integrated the cassette, lanes 2 and 3 had not successfully integrated the cassette so no product was produced.

(C) Testing of integration of cassette into *hog1Δ* and *pbs2Δ* *S. cerevisiae*. 1% agarose displaying amplification from *hog1Δ* and *pbs2Δ* *S. cerevisiae* gDNA with *SCH9* deletion cassette transformed in using Sch9 Up 100bp and Nat Rev primers using Taq polymerase. Products were of the expected size of ~1.3kb in lanes 1 – 7 were *hog1Δ*, lanes 8-11 were *pbs2Δ*.

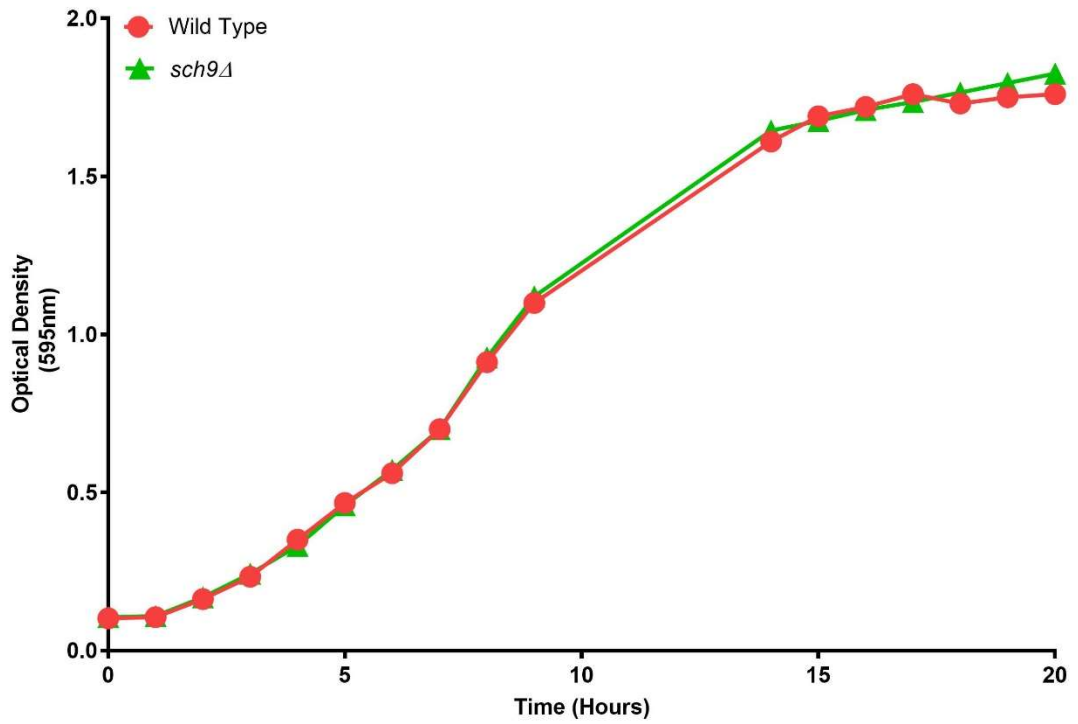


Figure 3.15. Growth curve of *S. cerevisiae* wild type and *sch9Δ* under normal conditions in yeast nitrogen base medium (YNB). Cultures were diluted to 2×10^6 cells ($OD_{595} \sim 0.1$) and incubated with shaking, 180rpm, at 30°C. Optical density readings at 595nm were taken hourly until mid to late stationary phase was reached.

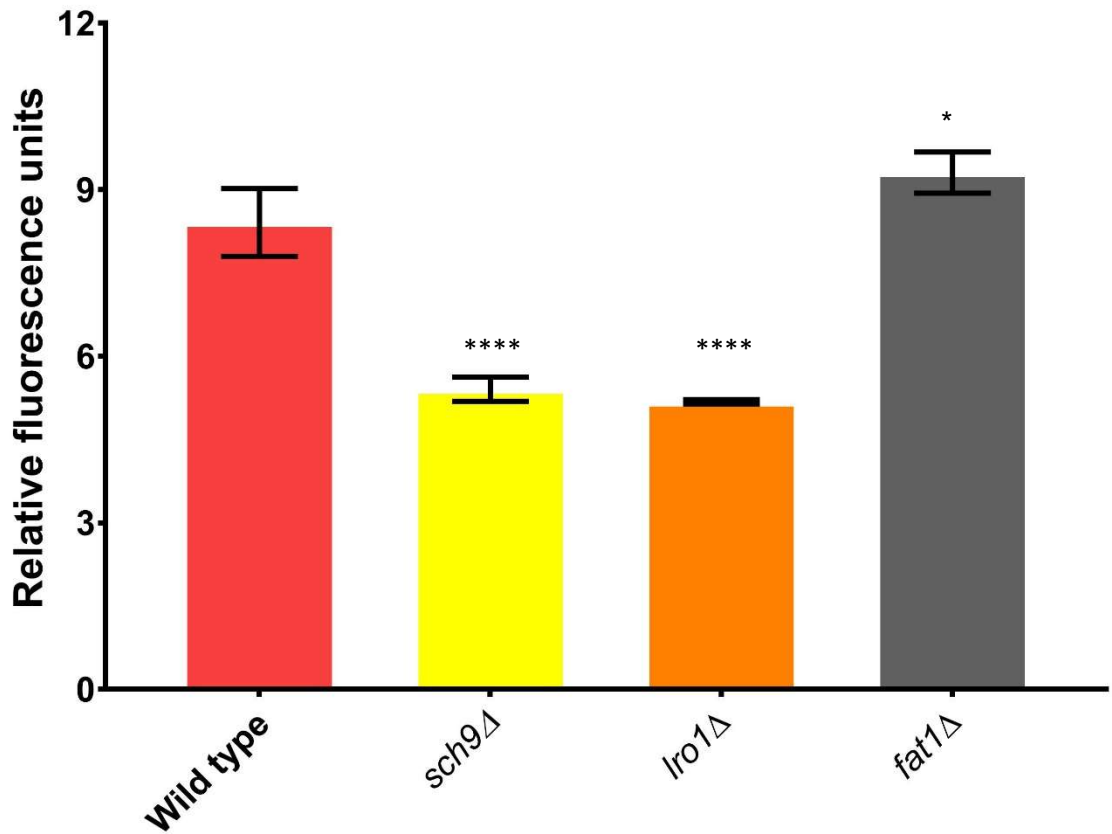


Figure 3.16. Neutral lipid fluorescence intensity of Nile Red stained *S. cerevisiae* wild type and *msn2/4Δ*, *sch9Δ*, *lro1Δ* and *fat1Δ* mutants. Cells were harvested 18 hrs post resuspension in YNB. Cells were washed twice in PBS before adjusting to a cell density of 2×10^7 cells/ml. 5×10^6 cells were transferred to the wells of black 96-well plates in triplicate. 25 μ l PBS/DMSO (1:1 v/v) and 5 μ g/ml Nile red were added to each sample. Plates were screened using the wavelengths: excitation 485nm, emission 535nm. Data shown as means of duplicates \pm SD. Significance indicated between wild type and *msn2/4Δ*, *lro1Δ* and *sch9Δ*. * $p \leq 0.1$ **** $p \leq 0.001$. Data analysed by one way ANOVA with Tukey *post hoc* test.

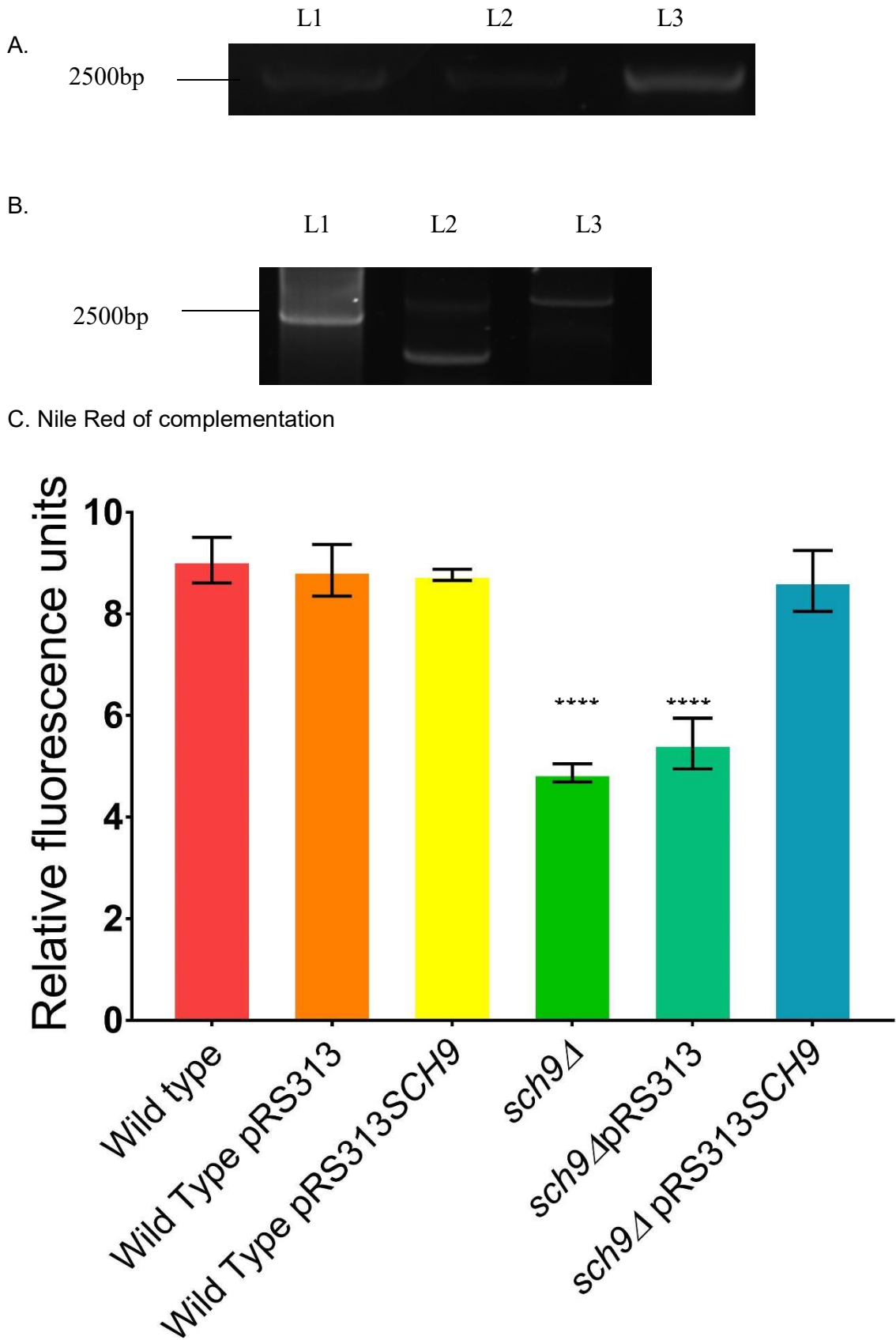


Figure 3.17. Complementation of *sch9*Δ phenotype (A) 1% agarose gel displaying amplification of *sch9* from gDNA with Sch9 ORF Forward and Reverse primers with banding occurring at 2.5kb in 3 cell samples (L1 – L3)

(B) 1% agarose gel displaying PCR results of minipreped pRS313 plasmid with *SCH9* ORF Forward and Reverse primers showing successful integration of *sch9* into the plasmid. Product size expected was ~ 2.5kb in 3 cell samples (L1 - L3)

(C) Neutral lipid fluorescence intensity of Nile Red stained *S. cerevisiae* wild type and *sch9Δ* transformed with the plasmid pRS313 and pRS313*SCH9*. Cells were harvested 18 hrs post resuspension in YNB. Cells were washed twice in PBS before adjusting to a cell density of 2×10^7 cells/ml. 5×10^6 cells were transferred to the wells of black 96-well plates in triplicate. 25μl PBS/DMSO (1:1 v/v) and 5μg/ml Nile red were added to each sample. Plates were screened using the wavelengths: excitation 485nm, emission 535nm. Data shown as means of duplicates ±SD. Significance indicated between wild type and *sch9Δ* and *sch9Δ*pRS313. **** $p \leq 0.0001$. Data analysed by one way ANOVA with Tukey *post hoc* test.

Nile Red results (Figure 3.16) show a significant decrease of 1.5-fold in neutral lipid accumulation in *sch9Δ*. The controls *lro1Δ* and *fat1Δ* behaved as previously described.

To confirm that deletion of *SCH9* was causing the observed neutral lipid phenotype, the strain was complemented with a wild type copy of *SCH9* expressed from a plasmid.

SCH9 was successfully amplified by PCR using wild type *S. cerevisiae* genomic DNA (Figure 3.17 A). The amplified *SCH9* was successfully cloned into the yeast vector pRS313 (Figure 3.17 B) and transformed into *sch9Δ* deletion cells. Nile Red data (Figure 3.17 C) showed no significant change in neutral lipid accumulation in between control wild type cells transformed with pRS313 and wild type cells containing pRS313*SCH9*. In *sch9Δ* cells containing the control vector, pRS313, a significant decrease in neutral lipid accumulation of 1.8-fold was observed. However, when *sch9Δ* cells contained pRS313*SCH9*, neutral lipid levels returned to those seen in the wild type. This data confirms that the neutral lipid phenotype observed in the *sch9Δ* strain is the result of loss of *SCH9*.

This data suggests that *SCH9* is required for neutral lipid accumulation as a deletion of this gene caused a significant decrease in neutral lipid accumulation, and its reintroduction caused a restoration of neutral lipid accumulation.

3.5 Hog1p is a potential target of the protein kinase, Sch9p

Both Sch9p and Hog1p are required for neutral lipid accumulation, therefore it is possible that Sch9p and of Hog1p are involved in the same pathway. To determine this a double, delete mutant was created using a *SCH9* NAT deletion cassette, resulting in *hog1Δsch9Δ* strain. In addition, to further investigate the upstream components of the HOG MAPK pathway, a *pbs2Δsch9Δ* strain was also produced. Both mutants were tested via PCR to ensure integration of the cassette (Figure 3.14 C). Growth curves (Figure 3.18 and Figure 3.19) showed no significant differences in growth between the double delete mutants and the wild type. A Nile Red assay was then performed to determine the neutral lipid phenotype of these mutants relative to the wild type.

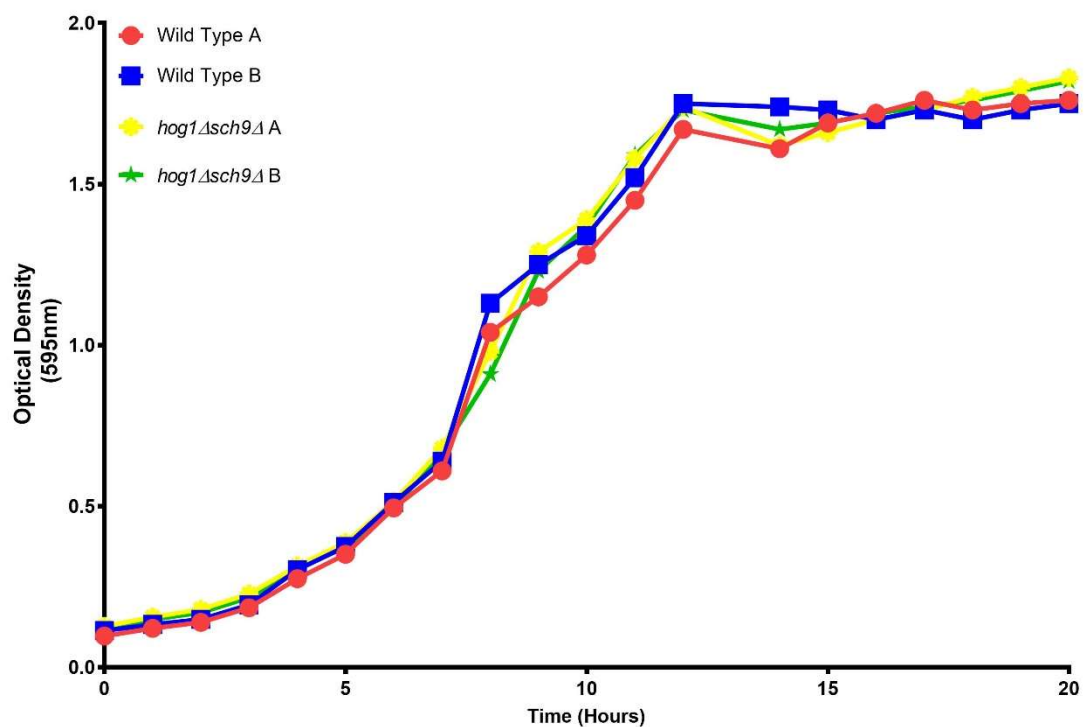


Figure 3.18. Growth curve of *S. cerevisiae* wild type and *hog1Δsch9Δ* under normal conditions in yeast nitrogen base medium (YNB). Cultures were diluted to 2×10^6 cells ($OD_{595} \sim 0.1$) and incubated with shaking, 180rpm, at 30°C. Optical density readings at 595nm were taken hourly until mid to late stationary phase was reached.

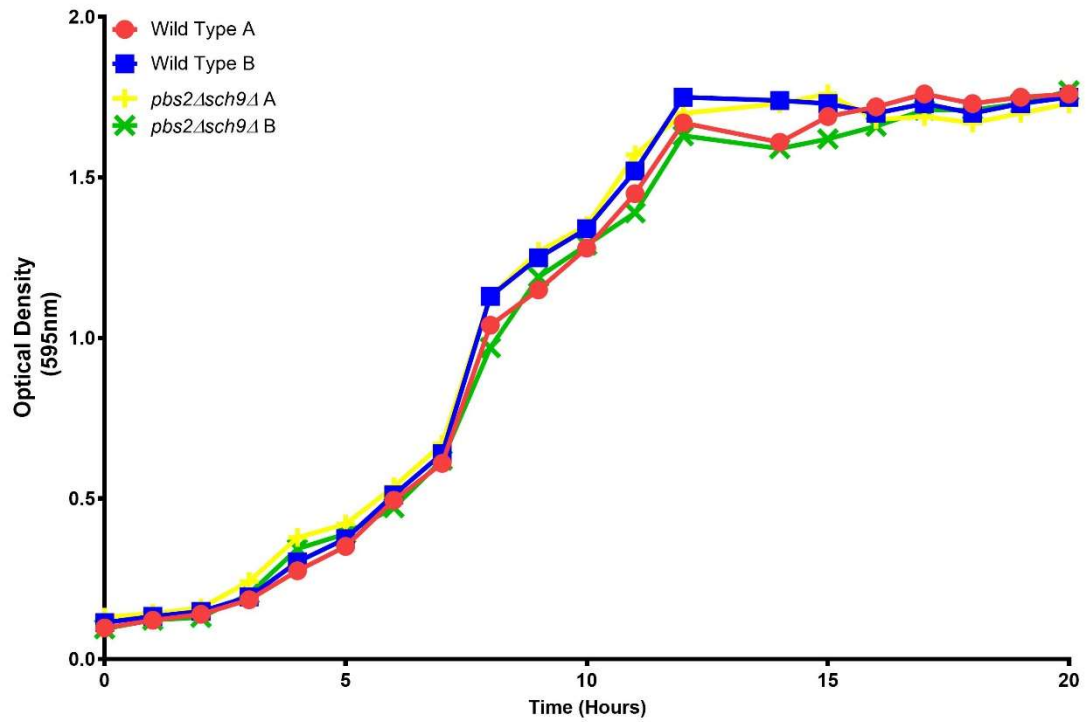


Figure 3.19. Growth curve of *S. cerevisiae* wild type and *pbs2Δsch9Δ* under normal conditions in yeast nitrogen base medium (YNB). Cultures were diluted to 2×10^6 cells ($OD_{595} \sim 0.1$) and incubated with shaking, 180rpm, at 30°C. Optical density readings at 595nm were taken hourly until mid to late stationary phase was reached.

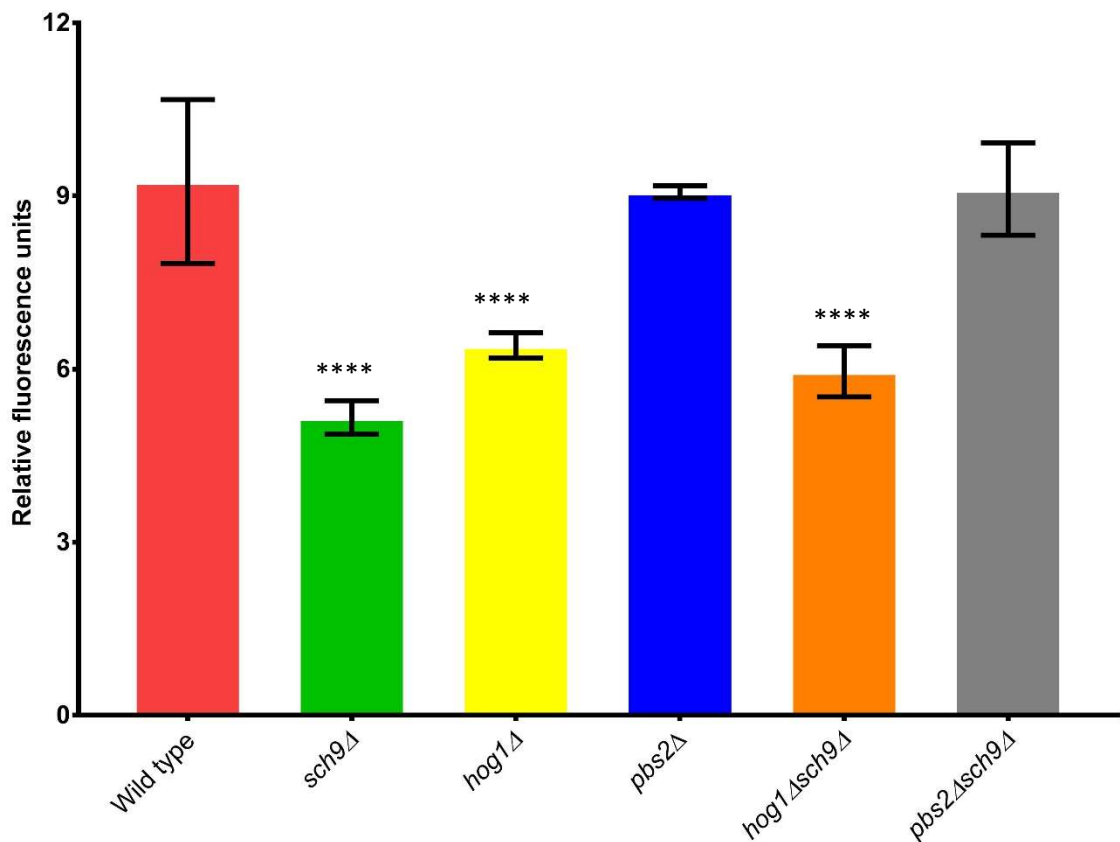


Figure 3.20. Neutral lipid fluorescence intensity of Nile Red stained *S. cerevisiae* wild type and *sch9Δ*, *hog1Δ* and *pbs2Δ* single and double delete mutants. Cells

were harvested 18 hrs post resuspension in YNB. Cells were washed twice in PBS before adjusting to a cell density of 2×10^7 cells/ml. 5×10^6 cells were transferred to the wells of black 96-well plates in triplicate. 25 μ l PBS/DMSO (1:1 v/v) and 5 μ g/ml Nile red were added to each sample. Plates were screened using the wavelengths: excitation 485nm, emission 535nm. Data shown as means of duplicates \pm SD. Significance indicated between wild type and *hog1 Δ* , *hog1 Δ sch9 Δ* and *sch9 Δ* . **** $p \leq 0.0001$. Data analysed by one way ANOVA with Tukey *post hoc* test.

Nile Red data (Figure 3.20) shows a significant decrease in *sch9 Δ* (1.8 fold) and *hog1 Δ* (1.4 fold) (shown previously; Figure 3.7 and Figure 3.17) and in *hog1 Δ sch9 Δ* (1.5fold). However, the *pbs2 Δ sch9 Δ* strain showed that *SCH9 Δ* neutral lipid phenotype is rescued by a *PBS2* delete.

These data suggest that Sch9p and Hog1p are involved in the same pathway that regulates neutral lipid accumulation, as no additive effect was observed. If these proteins had been involved in separate pathways, a further reduction in neutral lipid levels would be expected. If multiple pathways involved in lipid homeostasis are affected (e.g. lipid production and lipid degradation) then you would expect a different phenotype than if one is (e.g. if lipid production is reduced and degradation increased you'd expect less lipid accumulation than if just lipid production were reduced).

3.6 Deletion of *MSN2/4* and *DGA1* result in a reduction of neutral lipid levels

Hog1p is important for regulating neutral lipid accumulation but it is unknown if it acts directly or has downstream targets. Two potential targets are the transcription factors Msn2/4 and the diacylglycerol acyltransferase Dga1p. Msn2/4p are transcription factors that are known to be targets of Hog1p. Dga1p is a diacylglycerol acyltransferase and so is involved in neutral lipid synthesis and is involved in neutral lipid accumulation (Rostron *et al* 2015). It spans the ER membrane and is localised there (Liu *et al* 2011).

An *msn2/4 Δ* strain had been previously obtained from the NBRP. However, a genomic *dga1 Δ* strain was not available and had to be made via homologous recombination using a *DGA1* NAT deletion cassette. A *DGA1* deletion cassette was successfully

amplified (Figure 3.21 A) and integrated into wild type (Figure 3.21 B). A *dga1Δ* growth curve showed no significant difference of growth relative to the wild type (Figure 3.23). A *msn2/4Δ* growth curve showed comparable growth relative to the wild type (Figure 3.22). A Nile red assay was then performed to determine levels of neutral lipid in these single mutants compared to wildtype cells. The Nile red data (Figure 3.24) showed a significant decrease of 1.6-fold in neutral lipid accumulation in *dga1Δ* and in *msn2/4Δ* cells. The controls *lro1Δ* and *fat1Δ* accumulated lipid as expected.

To confirm that deletion of *DGA1* was responsible for the decrease in lipid accumulation, a wild type copy of *DGA1* was reintroduced on a pRS316 plasmid into the *dga1Δ* mutants.

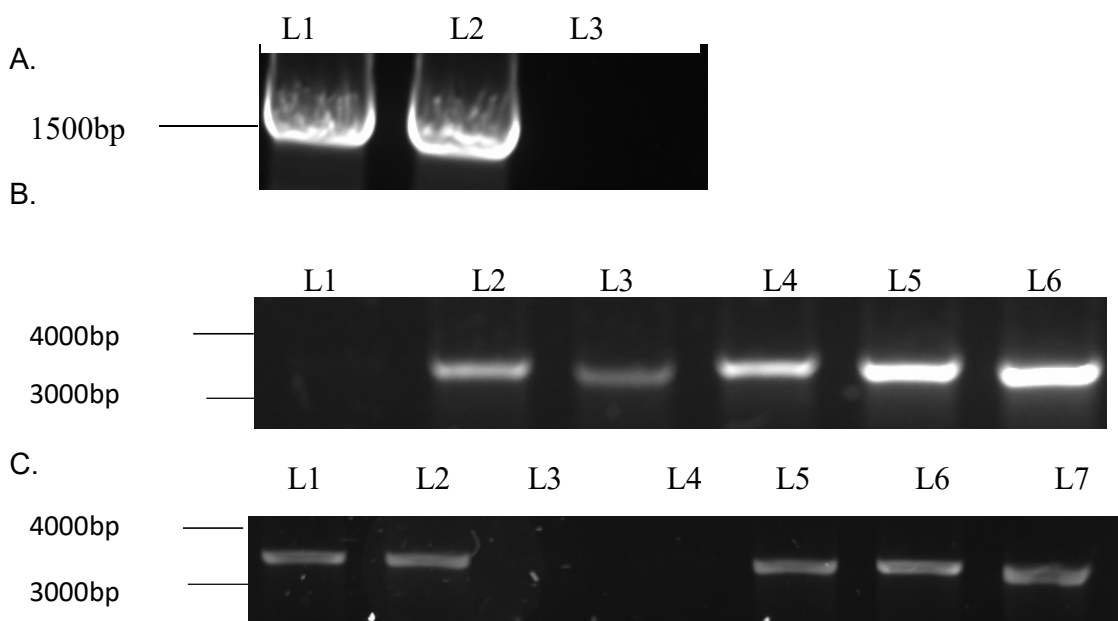


Figure 3.21. Deletion of genomic copy of *DGA1* (A) 1% agarose gel displaying amplification of a *dga1* deletion cassette utilising Dga1 S1 and S2 primers with a pFA6aNatMX6 template. Product was ~1.5kb in lanes 1 and 2, lane 3 was a negative control. (B) Confirmation of *DGA1* deletion in wildtype cells. 1% agarose gel displaying PCR results of gDNA amplification with Dga1 forward and NAT reverse primers showing successful integration of *dga1* deletion cassette into *wild type* cells (L2-6). Product size expected was ~3.5kb in lanes 2 – 6, negative control in lane 1. (C) Confirmation of *DGA1* deletion in *hog1Δ* and *pbs2Δ* cells. 1% agarose gel displaying PCR results of gDNA amplification with Dga1 forward and NAT reverse primers showing successful integration of *DGA1* deletion cassette into *hog1Δ* (lanes 1 – 2) and *pbs2Δ* cells (lanes 5 - 7). Product size expected was ~3.5kb.

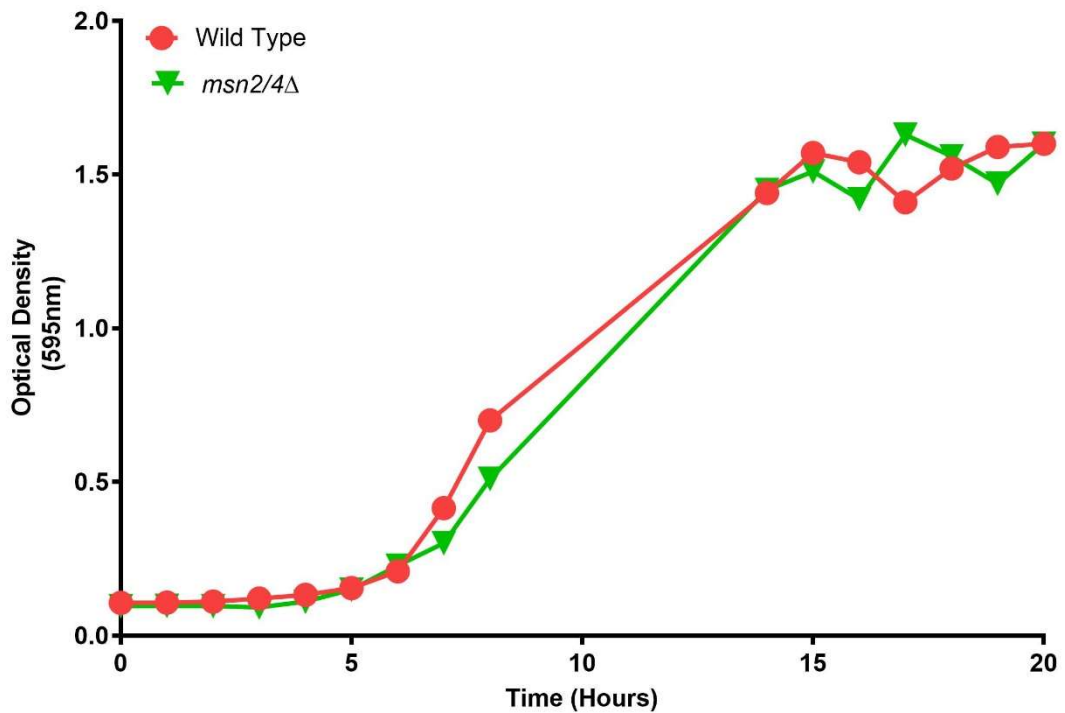


Figure 3.22. Growth curve of *S. cerevisiae* wild type and *msn2/4Δ* under normal conditions in yeast nitrogen base medium (YNB). Cultures were diluted to 2×10^6 cells ($OD_{595} \sim 0.1$) and incubated with shaking, 180rpm, at 30°C. Optical density readings at 595nm were taken hourly until mid to late stationary phase was reached.

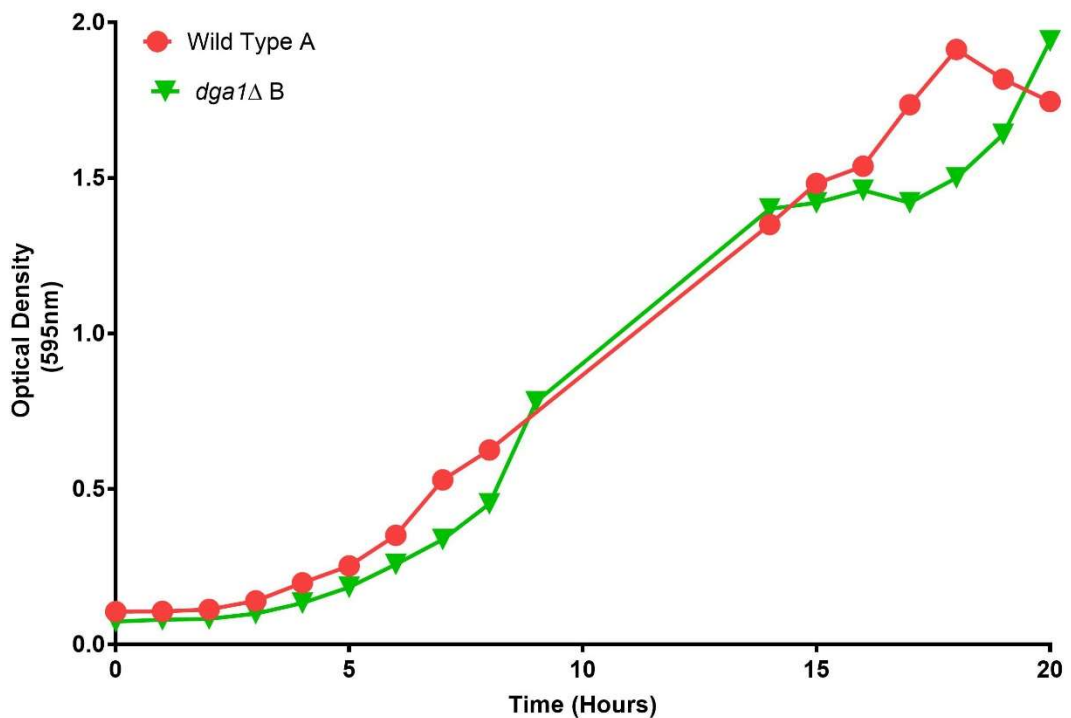


Figure 3.23. Growth curve of *S. cerevisiae* wild type and *dga1Δ* under normal conditions in yeast nitrogen base medium (YNB). Cultures were diluted to 2×10^6 cells ($OD_{595} \sim 0.1$) and incubated with shaking, 180rpm, at 30°C. Optical density readings at 595nm were taken hourly until mid to late stationary phase was reached.

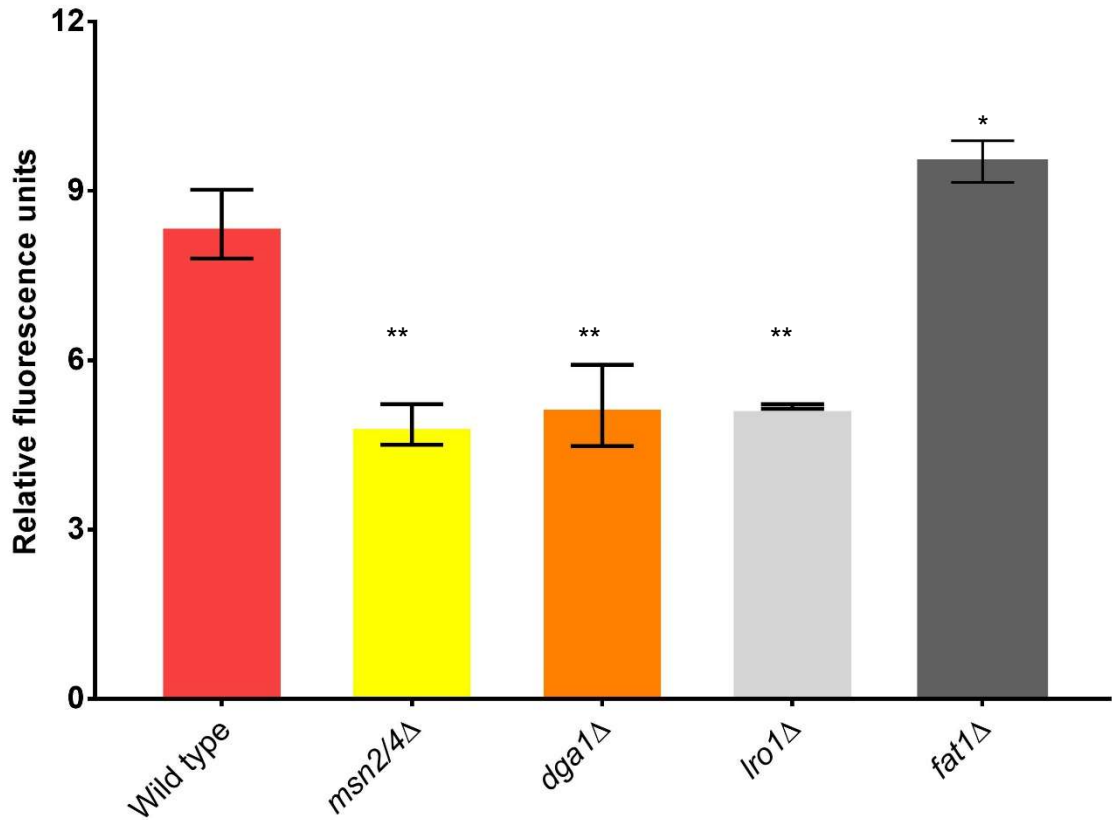


Figure 3.24. Neutral lipid fluorescence intensity of Nile Red stained *S. cerevisiae* wild type and HOG component mutants. Cells were harvested 18 hrs post resuspension in YNB. Cells were washed twice in PBS before adjusting to a cell density of 2×10^7 cells/ml. 5×10^6 cells were transferred to the wells of black 96-well plates in triplicate. 25 μ l PBS/DMSO (1:1 v/v) and 5 μ g/ml Nile red were added to each sample. Plates were screened using the wavelengths: excitation 485nm, emission 535nm. Data shown as means of duplicates \pm SD. Significance indicated between wild type and *dga1Δ* and *lro1Δ*. * $p \leq 0.1$, ** $p \leq 0.01$. Data analysed by one way ANOVA with Tukey *post hoc* test.

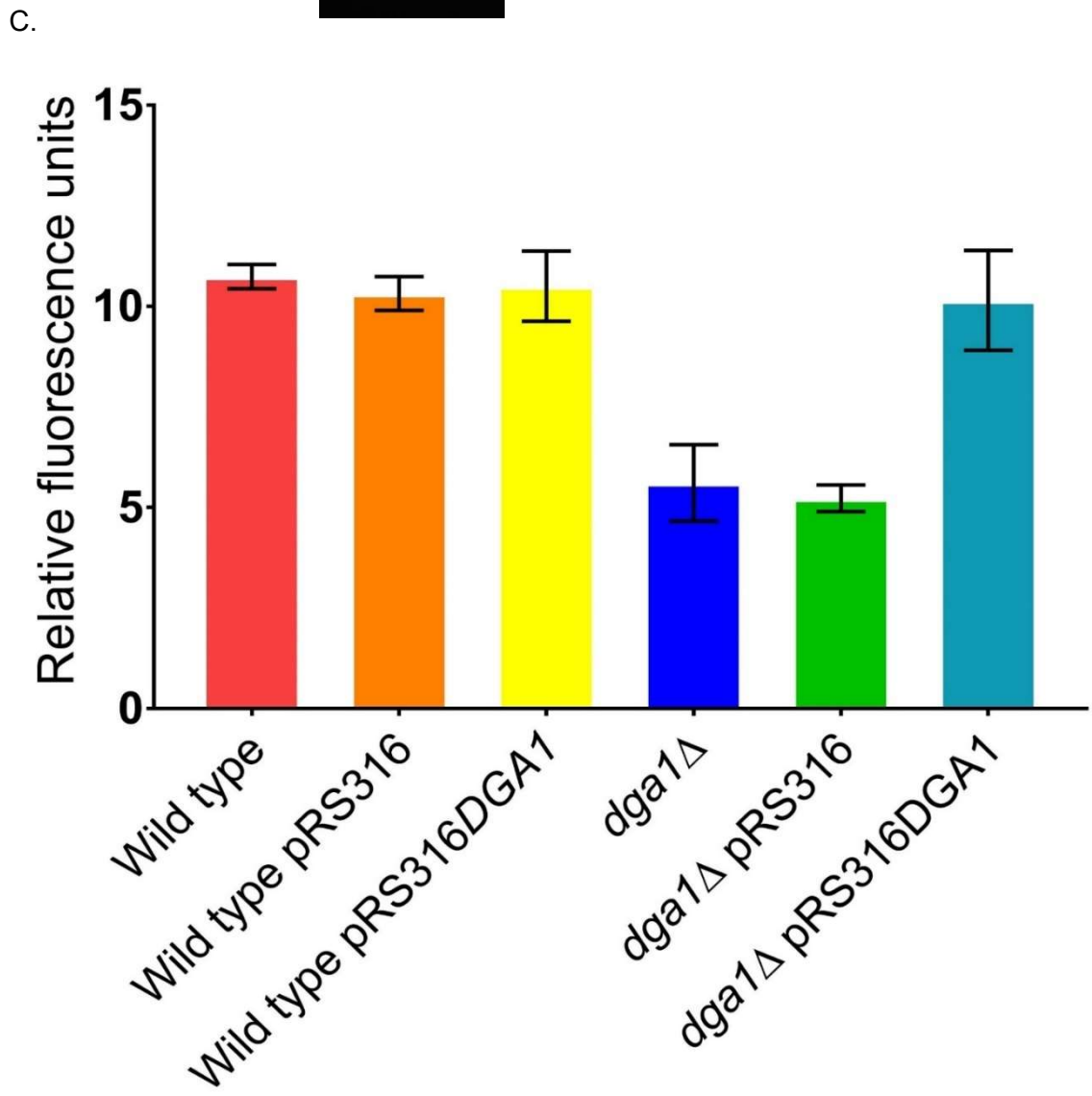
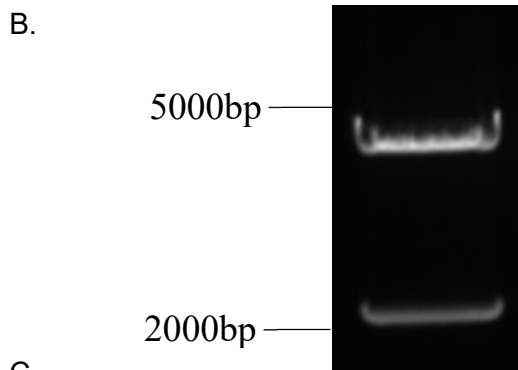
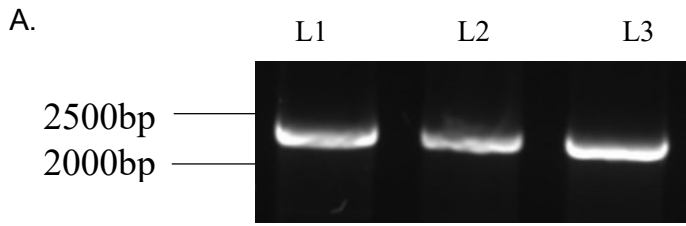


Figure 3.25. Cloning of *DGA1* (a) 1% agarose displaying gel extraction of amplification of *DGA1* from Wild Type *S. cerevisiae* gDNA using Dga1 For and Dga1 Rev primers using Phusion polymerase. Products were of the expected size of ~2.2kb. Lanes 1 through 3 contained the gel extracted *DGA1*. (b) 1% agarose gel displaying a restriction enzyme digest of pRS316dga1, with banding occurring at ~5kb and ~2 kb as is expected for pRS316 (4.8kb) and *dga1* (2.2kb). (C) Neutral lipid fluorescence intensity of Nile Red stained *S. cerevisiae* wild type and *dga1Δ* mutants which have had plasmids carrying the *dga1* gene added to assess if this restores wild type phenotype, a control of empty plasmid (p313) was used. Cells were harvested 18 hrs post resuspension in YNB. Cells were washed twice in PBS before adjusting to a cell density of 2×10^7 cells/ml. 5×10^6 cells were transferred to the wells of black 96-well plates in triplicate. 25μl PBS/DMSO (1:1 v/v) and 5μg/ml Nile red were added to each sample. Plates were screened using the wavelengths: excitation 485nm, emission 535nm. Data shown as means of duplicates ±SD. Significance indicated between wild type and *dga1Δ* and *dga1Δ*pRS316. **** $p \leq 0.001$. Data analysed by one way ANOVA with Tukey *post hoc* test.

DGA1 was successfully amplified by PCR using wild type *S. cerevisiae* genomic DNA (Figure 3.25 A). The amplified *DGA1* was successfully cloned into the yeast vector pRS316 (Figure 3.25 B) and transformed into *dga1Δ* deletion cells. This was then sequenced by Source BioScience to confirm insertion (Appendix 1). Nile Red data (Figure 3.25 C) showed no significant change in neutral lipid accumulation in between control wild type cells transformed with pRS316 and wild type cells containing pRS316*DGA1*. In *dga1Δ* cells containing the control vector, pRS316, a significant decrease in neutral lipid accumulation of ~2 fold was observed. However, when *dga1Δ* cells contained pRS316*DGA1*, neutral lipid levels returned to those seen in the wild type. This data confirms that the neutral lipid phenotype observed in the *dga1Δ* strain is the result of loss of *DGA1*.

These data suggest that both Msn2/4p and Dga1p are involved in neutral lipid accumulation.

3.7 Dga1p appears to be a downstream target of Hog1

As data suggests Dga1p is involved in neutral lipid accumulation it is possible that it could be a direct or indirect target of Hog1p.

Double delete mutants were created using a *DGA1* Nat deletion cassette, resulting in *hog1Δdga1Δ* and *pbs2Δdga1Δ* mutants. Cassette was amplified and transformed into cells (Figure 3.21 A) PCR confirmed integration of the deletion cassette into *hog1Δ* and *pbs2Δ* cells (Figure 3.21 C). A *pbs2* double delete mutant was created as neutral lipid accumulation seems to take place independently of Pbs2p (Figure 3.7), so it would be expected that there would be no additional effect to neutral lipid accumulation in the double delete. Growth Curves (Figure 3.26 and Figure 3.27) show no significant growth differences between the double delete mutants, and wild type cells. A Nile Red assay was performed after characterisation of the growth of the mutants relative to wild type.

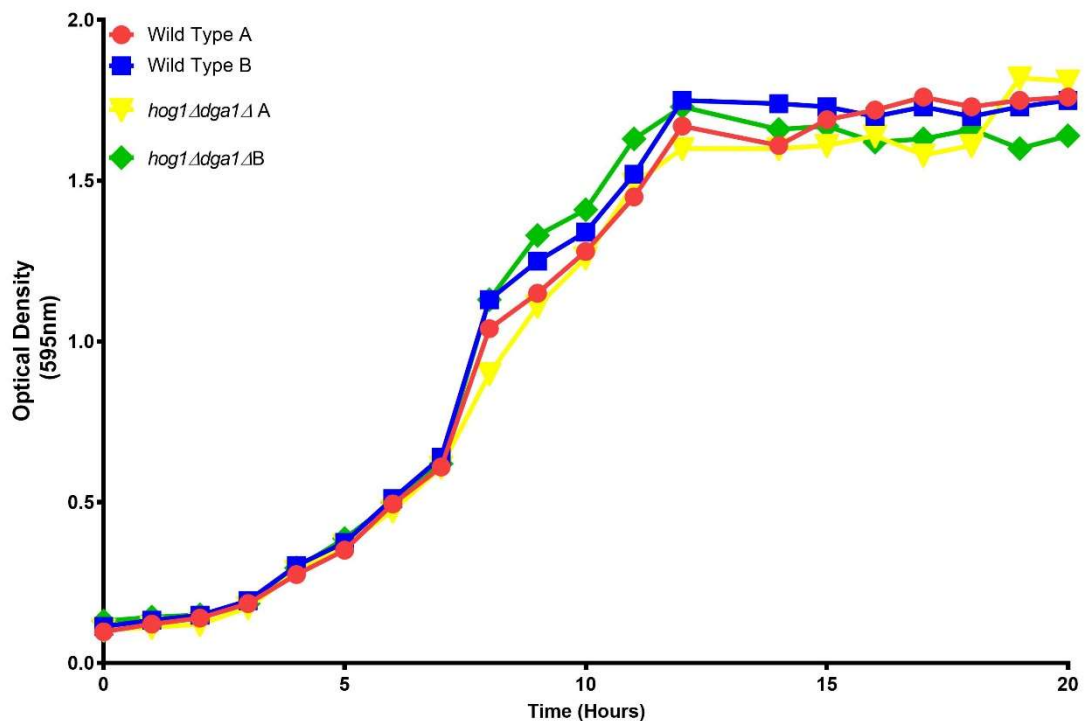


Figure 3.26. Growth curve of *S. cerevisiae* wild type and *hog1Δdga1Δ* under normal conditions in yeast nitrogen base medium (YNB). Cultures were diluted to 2×10^6 cells ($OD_{595} \sim 0.1$) and incubated with shaking, 180rpm, at 30°C. Optical density readings at 595nm were taken hourly until mid to late stationary phase was reached.

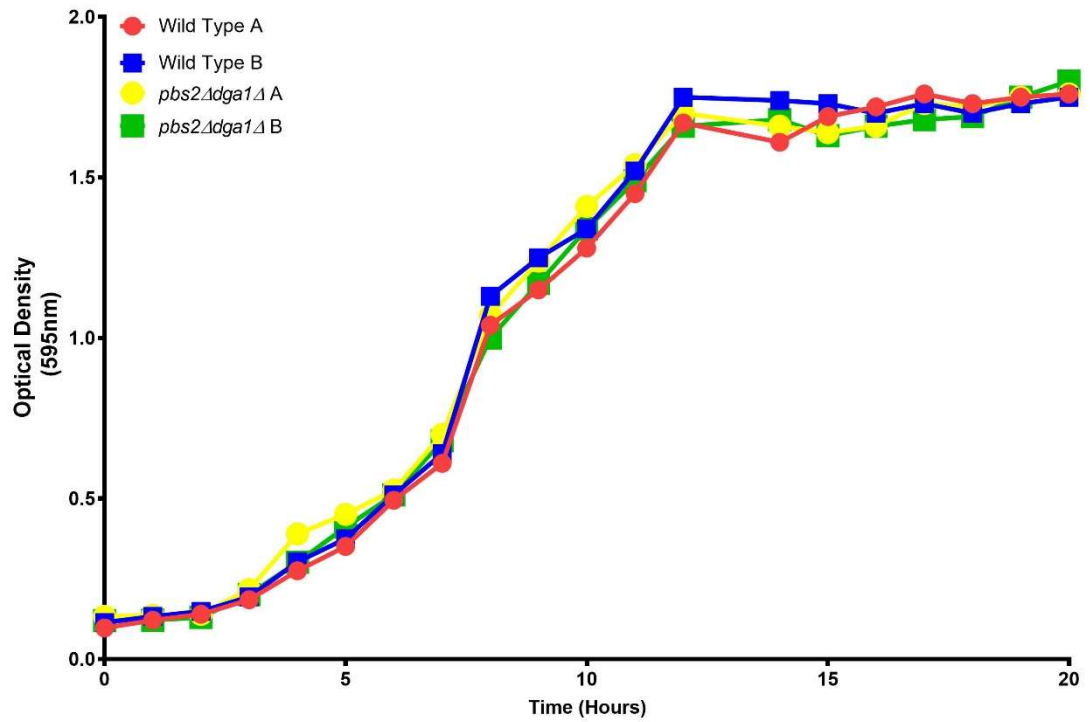


Figure 3.27. Growth curve of *S. cerevisiae* wild type and *pbs2Δdga1Δ* under normal conditions in yeast nitrogen base medium (YNB). Cultures were diluted to 2×10^6 cells ($OD_{595} \sim 0.1$) and incubated with shaking, 180rpm, at 30°C. Optical density readings at 595nm were taken hourly until mid to late stationary phase was reached.

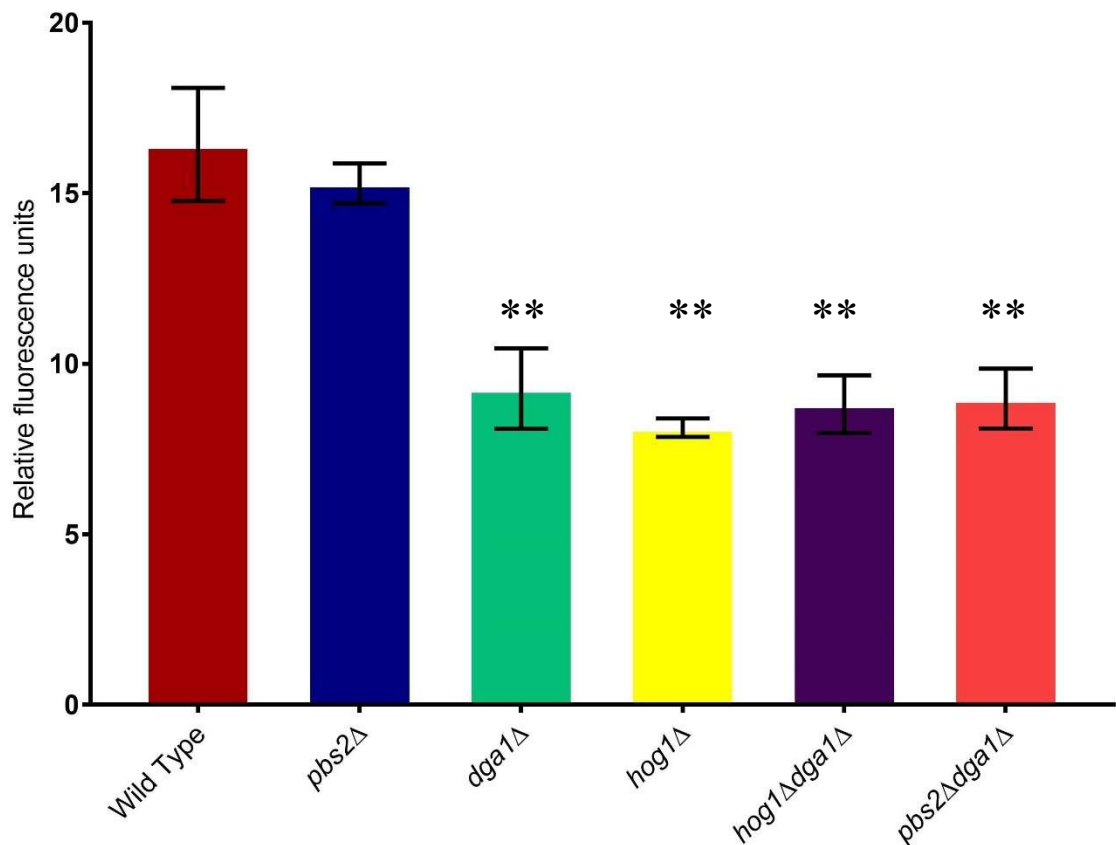


Figure 3.28. Neutral lipid fluorescence intensity of Nile Red stained *S. cerevisiae* wild type and HOG component mutants. Cells were harvested 18 hrs post resuspension in YNB. Cells were washed twice in PBS before adjusting to a cell density of 2×10^7 cells/ml. 5×10^6 cells were transferred to the wells of black 96-well plates in triplicate. 25 μ l PBS/DMSO (1:1 v/v) and 5 μ g/ml Nile red were added to each sample. Plates were screened using the wavelengths: excitation 485nm, emission 535nm. Data shown as means of duplicates \pm SD. Significance indicated between wild type and the *hog1Δ*, *pbs2Δ* single and double delete mutants. ** $p \leq 0.01$. Data analysed by one way ANOVA with Tukey *post hoc* test.

Nile red data (Figure 3.28) shows wild type levels of neutral lipid in the *pbs2Δ* strain, as previously described. Both the single (*dga1Δ* and *hog1Δ*) and double deletion (*hog1Δdga1Δ* and *pbs2Δdga1Δ*) strains, showed a significant neutral lipid decrease between 1.7 and 2-fold.

These data suggest that Dga1p is on the same pathway of Hog1p. Neutral lipid accumulation in the *hog1Δdga1Δ* mutant is similar to that of *dga1Δ* and *hog1Δ* mutants; no additive effect is seen as would be expected if Hog1p and Dga1p acted via separate pathways. *pbs2Δdga1Δ* neutral lipid accumulation is similar to that of *dga1Δ* and *hog1Δ* mutants, given that *pbs2Δ* did not accumulate less neutral lipid than wild

type it is likely that the decrease in the *pbs2Δdga1Δ* mutant is due to the deletion of *DGA1* and the deletion of *PBS2* has no effect on neutral lipid accumulation.

3.8 Dga1p contains 4 potential MAPK sites

As data suggests that Hog1p and Dga1p on the same pathway (Figure 3.28), Dga1p is a potential target of Hog1p. Hog1p activates proteins via phosphorylation at conserved sites (S/T P), Dga1p has four of these sites. These sites were mutated to try to identify which (if any) are required for neutral lipid accumulation. If these sites (or a site) are required then it may suggest that Hog1p is regulating neutral lipid accumulation via phosphorylation, this could be confirmed by immunoprecipitation which would show a direct interaction between the proteins.

Potential MAPK sites were identified by analysing protein sequence data curated by Uniprot and *Saccharomyces* genome database, specifically looking for S/T P sites in the amino acid sequence, four were identified. These sites were mutated to prevent phosphorylation by changing the serine or threonine to an alanine, which cannot be phosphorylated.

```

1  MSGTFNDIRR RKKEEGSPTA  GITERHENKS  LSSIDKREQT  LKPQLESCCP  LATPFERRLO
61  TLAVAWHTSS FVLFSIFTLF  AISTPALWVL  AIPYMIYFFF  DRSPATGEVV  NRYSLRFRSL
121 PIWKWYCDYF PISLIKTVNL  KPTFTLSKNK  RVNEKNYKIR  LWPTKYSINL  KSNSTIDYRN
181 QECTGPTYLF  GYHPHGIGAL  GAFGAFATEG  CNYSKIFPGI  PISLMTLVTQ  FHIPLYRDYL
241 LALGISSVSR  KNALRTLST  QSICIVVGGGA  RESLLSSTNG  TQLIILNKRKG  FIKLAIQTGN
301 INLVPVFAFG  EVDCYNVLST  KKDSVLGKMQ  LWFKENFGFT  IPIFYARGLF  NYDFGLLPFR
361 APINVVVGRP  IYVEKKITNP  PDDVVNHFD  LYIAELKRLY  YENREKYGVP  DAELKIVG

```

Figure 3.29. Potential MAPK phosphorylation sites (S/T P) in the N terminus of Dga1p indicated in bold, underlined and red. (Phosphorylation sites were determined from data curated by Uniprot and *Saccharomyces* genome database.)

The intent was to mutate each of these sites (S17, T53, T84 and S103) to get single point mutation variants of the protein. These single mutants would then be used to make multiple residue mutant variations (e.g. S17 + T53, or all 4 together). These mutated *DGA1* genes would then be cloned into a pRS316 plasmid and transformed

into a *dga1Δ* mutant. As reintroduction of wild type *DGA1* restores phenotype it would be expected that these mutants would also restore phenotype, unless the sites mutated are essential for lipid accumulation. Use of multi residue mutants would allow the identification of sites that may be phosphorylated together to allow for neutral lipid accumulation (e.g. an S17 mutant may accumulate lipid just fine, as may a T53 mutant, but an S17 T53 mutant may not). Deletion mutants with these mutated *DGA1*'s integrated via plasmid would then be assayed by the Nile Red method to determine neutral lipid levels. The QuikChange method and extended primer PCR methods were attempted to create these mutants. Mutation of *DGA1* was unsuccessful with both methods tested

3.9 Tagged *DGA1* is not detectable by Western Blotting

Dga1p is involved in neutral lipid accumulation, a potential point of interest was the amount of Dga1p in cells as the lipogenic switch occurred. We were interested in what happens to Dga1p during the lipogenic switch in terms of interaction with other proteins, the levels of protein and any posttranslational modifications that occur to the protein. Of particular interest is the potential interaction between Dga1p and Hog1p. This would require *DGA1* to be tagged to allow for detection, as such Dga1p was C terminally tagged with a HA tag. Tagged *DGA1* would be required to determine its phosphorylation state and to perform immunoprecipitation to assess Dga1p's interaction with Hog1p.

A *DGA1*-3HA tagging cassette was made via PCR as described in 2.3.1.2 and transformed into wild type, *hog1Δ* and *pbs2Δ* cells as described in 2.4.1.3. The *DGA1*-3HA tagging cassette was successfully amplified (Figure 3.30 A), a product of the appropriate size (~1500bp) was produced using the primers Dga1 S2 and S3 which amplify and 3' HA tag the *DGA1* from gDNA. PCR was performed with a and Nat REV primers, this would only amplify a product if *DGA1* had been tagged as the wild type S.

cerevisiae does not contain a site for the Nat REV primer to bind to. This PCR confirmed it had successfully integrated into wild type (Figure 3.30 B), *hog1Δ* and *pbs2Δ* cells (Figure 3.30 C) as amplification was seen in some colonies, these colonies were the ones used for further work. Protein extraction of cells were performed and run on a polyacrylamide protein gel to determine whether the tagged protein could be detected by western blot using a 3HA antibody and its associated secondary antibody, which allowed for visualisation using ECL reagents.

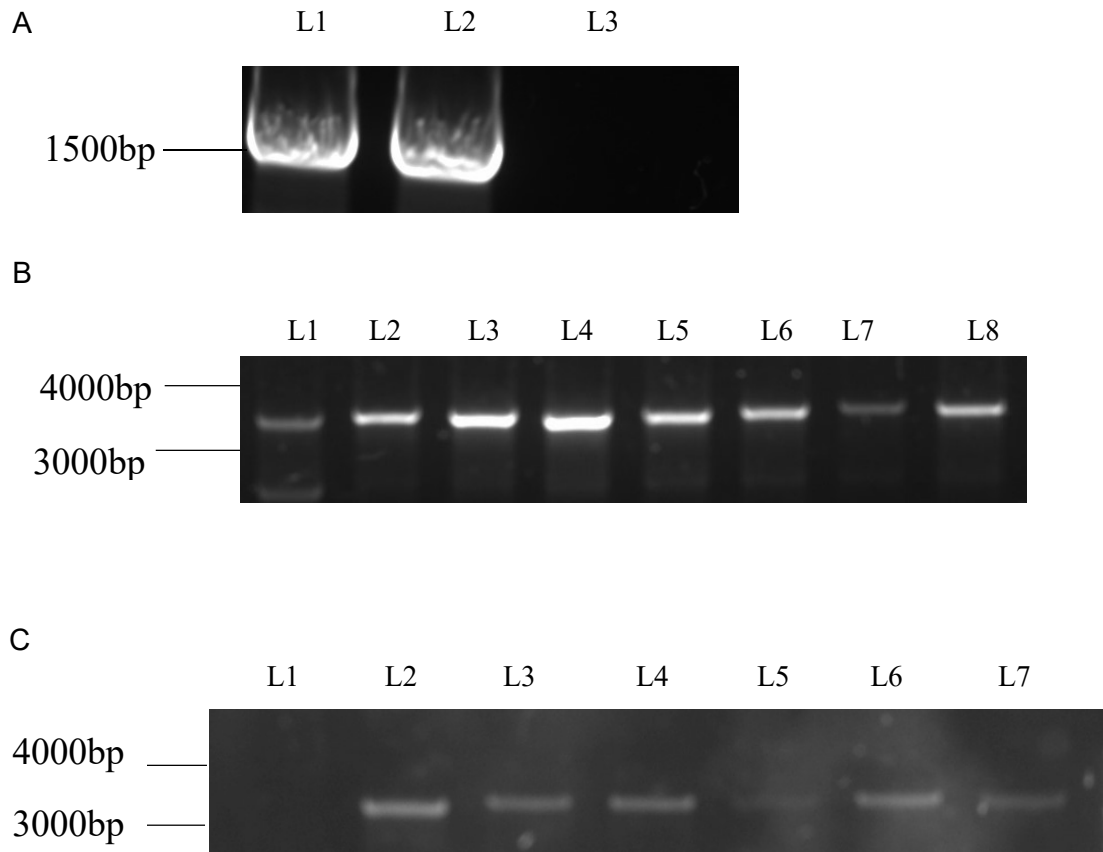


Figure 3.30. Genomic tagging of *DGA1*. (A) 1% agarose gel displaying amplification of a *DGA1* 3HA tagging cassette utilising Dga1 S2 and S2 primers with a pFA6aNatMX6 template, product was ~1.5kb. Lanes 1 and 2 are the cassette, lane 3 is a negative control. (B) 1% agarose gel displaying PCR results of gDNA amplification with Dga1 forward and NAT reverse primers showing successful integration of 3HA-dga1 tagging cassette into Wild Type *S. cerevisiae* cells (lanes 1-8). Product size expected was ~3.5kb. (C) 1% agarose gel displaying PCR results of gDNA amplification with Dga1 forward and NAT reverse primers showing successful integration of 3HA-dga1 tagging cassette into *hog1Δ* and *pbs2Δ* cells. Product size expected was ~3.5kb. Lane 1 is a negative control (wild type gDNA), lanes 2 – 4 are *hog1Δ* lanes 5 – 7 are *pbs2Δ*.

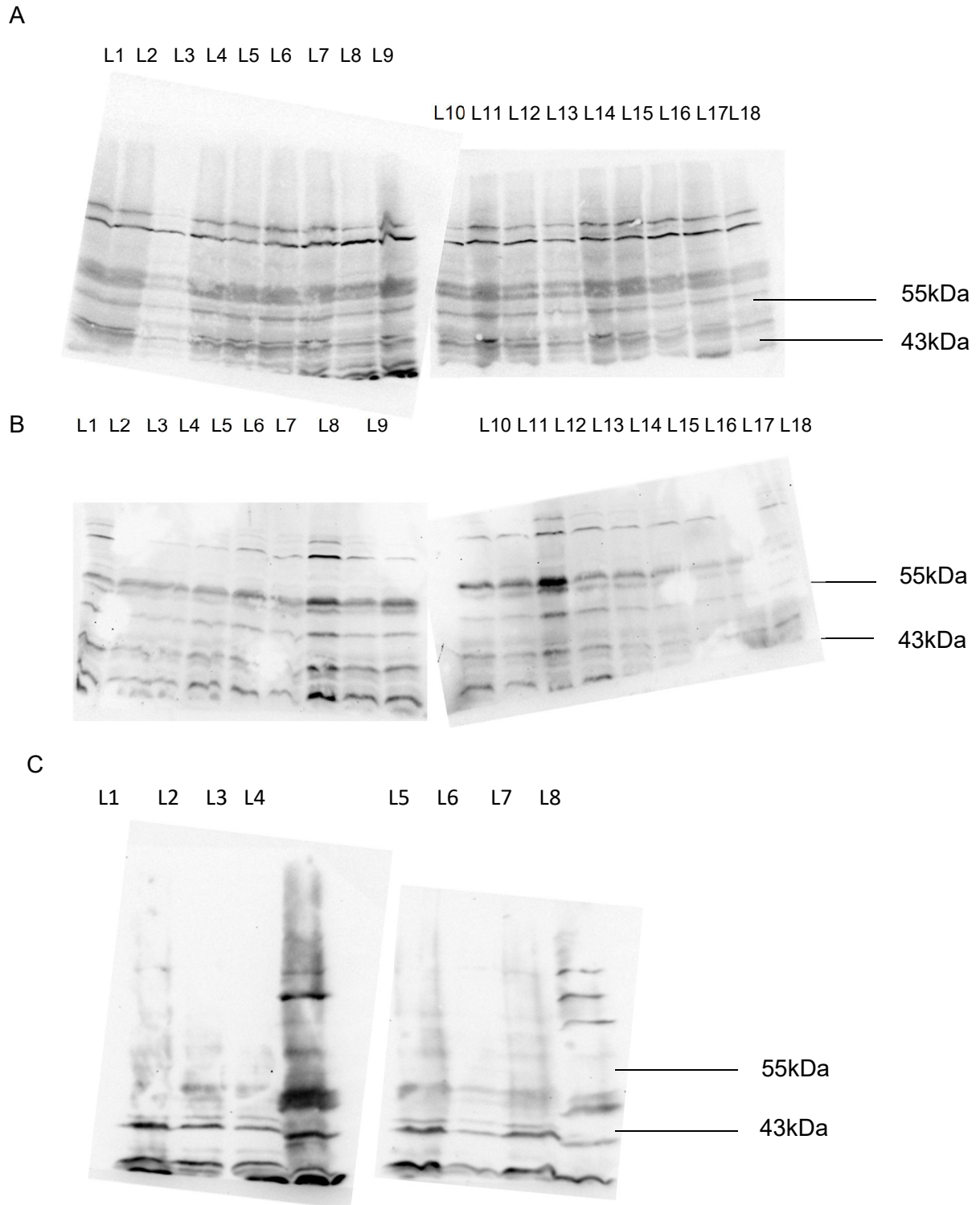


Figure 3.31. A) Western blot of protein extractions from *dga1-3HA* tagged *S. cerevisiae* (L1 – L18 [lanes 1 – 8 were protein extractions from a cell with an integrated tagging cassette, lane 9 was from wild type control; lanes 10 – 17 were protein extractions from a cell with an integrated tagging cassette, lane 18 was from wild type control]) at 8 hours of growth in YNB media and incubated with shaking, 180rpm, at 30°C. Membranes were probed with α -3HA, an ECL secondary antibody was added to the primary antibody to allow for visualisation on a Biorad™ ChemiDoc™ XRS+ machine. **B) Western blot of protein extractions from *dga1-3HA* tagged *S. cerevisiae*** (L1 – L18 [lanes 1 – 8 were protein extractions from a cell with an

integrated tagging cassette, lane 9 was from wild type control; lanes 10 – 17 were protein extractions from a cell with an integrated tagging cassette, lane 18 was from wild type control]) at 8 of growth in YNB media and incubated with shaking, 180rpm, at 30°C. Membranes were probed with α -3HA, an ECL secondary antibody was added to the primary antibody to allow for visualisation on a Biorad™ ChemiDoc™ XRS+ machine. **C) Western blot of protein extractions from *dga1*-3HA tagged *S. cerevisiae*** (L1 and L5), wild type *Schizosaccharomyces pombe* (L2, L3, L6 and L7) and *S. pombe* 429 atf21-3HA::kan pcr1::ura4 cells (L4 and L8) at 8 of growth in YNB media and incubated with shaking, 180rpm, at 30°C. Membranes were probed with α -3HA, an ECL secondary antibody was added to the primary antibody to allow for visualisation on a Biorad™ ChemiDoc™ XRS+ machine.

Figure 3.31 A – C shows that 3HA tagged Dga1p was not detectable by western, with no clear band being detected at 47kDa, the expected size of 3HA tagged Dga1p.

Control lanes were run in all gels (Figures 3.31 A – C). In the case of Figures 3.31 A and B wild type controls were used in the last lane, these did not show any difference compared to the tested samples. Controls of *Schizosaccharomyces pombe* (*S. pombe*) wildtype and atf21-3HA::kan pcr1::ura4 cells as well as untagged *S. cerevisiae* were used on Figure 3.31 C and did not show any difference to that of the tagged wild type cell; these were used due to the inability to detect 3HA tagged Dga1p from tagged cell protein extractions in Figures 3.31 A and B.

This western data suggested no detection of the 3HA tagged Dga1p. It is possible that there is an issue with either the primary HA antibody or the secondary antibody, with no detection with extractions of cells that contain the 3HA cassette or from *S. pombe* samples which has Atf21p genomically tagged with 3HA.

4.0 Discussion

The MAPK Hog1 is required for neutral lipid accumulation

Lipid accumulation occurs in cancer cells due to the change in cellular metabolism, predominantly through the Warburg effect (Warburg 1925; Warburg 1956), which is driven by a need for the cells to keep growing rapidly in a tumour environment (Esechie *et al* 2009). Understanding the regulation of lipogenesis is important as it allows for a better understanding of cancer progression and rate of growth (as the Warburg effect alters metabolism so cancer cells accumulate lipid). It also creates a potential target for therapy (Liu *et al* 2017) as lipogenesis is important to cancer cell function and for sustaining their rapid growth (Hanahan *et al* 2011). Suppression or cessation of lipogenesis may prove to be an effective treatment to either slow growth rate (and so allow for more effective surgical removal of the cancer) or cause cancer cell death (either by disrupting metabolism so much as to cause death or by making energy so limited as to prevent cancer cells from suppressing the immune system. Mammalian cells are expensive and difficult to work with so the use of a model organism with high homology is desirable. *S. cerevisiae* is a well-established model organism (Zhang *et al* 2003; Henry *et al* 2012) with many conserved pathways with that of mammalian cells; normal *S. cerevisiae* cells naturally accumulate lipid under conditions of nitrogen limitation (Natter *et al* 2013). (Siepel *et al* 2005; Hamza *et al* 2015). As such it was used in this study to investigate regulation of lipid accumulation by the homologue of p38 MAPK pathway, the HOG MAPK pathway (Hay *et al* 2004; Dann and Thomas 2006; Loewith *et al* 2011).

The data in Figure 3.1 suggest that Hog1p has a key role in neutral lipid accumulation. However, other HOG pathway components upstream of Hog1p (Ssk2p, Ste11p and Pbs2p) don't have an obvious role, with their deletion not affecting accumulation of neutral lipids.

The role of Hog1p in lipid accumulation has been supported by data from mammalian cells with p38, the homologue of Hog1p, playing an important role in the regulation of neutral lipids accumulation in macrophages (Mei *et al* 2012). p38 inhibits macroautophagy by suppression of the key macrophage autophagy gene, *ULK1*. Once p38 is activated the ratio of cholesterol esters over free cholesterol increased in favour of the cholesterol esters (Mei *et al* 2012). Due to the high homology between *S. cerevisiae* and mammalian lipid metabolism (Carman *et al* 2007; van Meer *et al* 2008; Nielsen 2009) and MAPK pathways (Waskiewicz *et al* 1995; Banuett 1998; Wagner *et al* 2009) it is possible that Hog1p dependent regulation of lipid metabolism is occurring in *S. cerevisiae*.

The Hog1p homologue in *S. pombe*, Sty1p, has been implicated in the storage of neutral lipid in lipid droplets and for controlling the levels of triacylglycerol (Grimard *et al* 2008), with evidence suggesting that MAPK regulation of lipid storage and that this is conserved in other eukaryotes (Grimard *et al* 2008). Grimard *et al* 2008 utilised an *sty1Δ* in combination with a lipase inhibitor (thus preventing lipid degradation) and it was concluded that Sty1p (and JNK2) play a role in lipid degradation regulation rather than biosynthesis. The use of a lipid inhibitor however is a significant departure from the methodology used in this study and may explain why no decrease in neutral lipid was observed in the deletion strains used in that study.

Given the high level of conservation of the MAPK pathway between mammalian, fission and budding yeast it is that the same is true for Hog1p as for Sty1p, that Hog1p is involved in the regulation of lipid degradation. Perhaps it directly or indirectly regulates lipase inhibition and so its deletion from a cell (and no inhibition of lipase activity) would increase the degradation of neutral lipid; if more lipids are being degraded then a cell will accumulate less of them.

Other MAPK pathways are known to regulate lipid homeostasis for example, the cell wall integrity MAPK pathway which regulates responses to cell membrane and cell wall stress (Nunez *et al* 2008). In certain environmental conditions levels of phospholipids, through regulation of their turnover and synthesis, are affected by this pathway (Nunez *et al* 2008). The cell wall integrity MAPK Slt2p (Mpk1p) has an essential role in the regulation of lipid homeostasis with *slt2Δ* (*mpk1Δ*) cells showing altered lipid metabolism, including the accumulation of neutral lipids, phosphatidylcholine, diacylglycerol and triacylglycerol (Nunez *et al* 2008). This suggests a negative regulatory role of lipid accumulation for Slt2p, in opposition to the data obtained for Hog1p. However, in their experimentation media was supplemented with inositol and choline. Inositol is a phospholipid precursor, and elicits a stress response from the cell (Henry *et al* 2014). When inositol is added to yeast media the synthesis of the phospholipid phosphatidylinositol increases significantly, and more of it is accumulated in the cell (Loewen *et al* 2004; Gaspar *et al* 2006; Gaspar *et al* 2011). This would result in phospholipid accumulation in significant excess even in wild type cells which may affect the neutral lipid phenotype. Choline was also added to the growth media, it has long been recognised as improving growth rates of cells (Nagle 1969) and is recognised as an essential nutrient for mammals (Zeisel *et al* 2009) and fungi (Markham *et al* 1993). Increased growth rates would result in less time needed to reach stationary phase. To determine if this research data is applicable experiments (all those done in this study) would have to be redone with inositol and choline added to growth media to eliminate them as contributing factors (which they are likely to be due to how they affect cellular metabolism). Slt2p has been found to interact with Hog1p in the process of mitophagy under heat and nitrogen starvation stress conditions and was determined experimentally via the use of fluorescently tagged proteins and fluorescence microscopy in various mutants including *hog1Δ* (Mao *et al* 2011; Córcoles-Sáez *et al* 2012), therefore it is possible that Hog1p may act via Slt2p or Slt2p may act via Hog1p. Experiments utilising GFP tagged variants of these proteins may allow for visualisation of co-localisation within the cell. The use of immunoprecipitation

may allow for the identification of this interaction if it is acting directly in this case (if indeed it is acting at all in lipid accumulation). Slt2p also interacts with other HOG pathway components such as Ssk2p, Ste11p and Pbs2p (Aronova *et al* 2007; Torres *et al* 2002; Chan *et al* 2000; Reinke *et al* 2004; Breitzkreutz *et al*, 2010; Soulard *et al* 2010; Wang *et al* 2011), and with some of Hog1p's target Msn2/4 (Sharifpoor *et al* 2012) Interactions between Slt2p and the upstream components of the HOG pathway may suggest Slt2p indirectly interacts with Hog1p, through its MAP2K, MAP3K or MAP4K. Double deletion *hog1Δslt2Δ* mutants could be created and their neutral lipid levels compared with the single deletion mutants to see if phenotype is rescued which is the expected phenotype if they do not interact as Hog1p positively regulates lipid accumulation and it would appear, though work in normal media would have to be performed to confirm, that Slt2p negatively regulates lipid accumulation.

Regulation of neutral lipid accumulation via Hog1p is Pbs2p independent.

If Hog1p is involved in neutral lipid accumulation we would expect to observe activation of the protein. Hog1p is typically activated by dual phosphorylation on Thr174 and Tyr176 (Maayan *et al* 2012), which can be detected via an α -P-p38 antibody via western blot analysis. This allows for the analysis of the phosphorylation state of Hog1p during different phases of growth.

Figure 3.9 shows that in the early exponential phase samples (6 – 7.5 hours) Hog1p is dually phosphorylated at Thr174 and Tyr176 before moving into mid exponential phase (8 – 8.5 hours) where phosphorylation is lost, indicating a lack of activation of Hog1p. In late exponential (9 – 10 hours) Hog1p is phosphorylated again as cells move towards stationary phase. This data suggests an activation of Hog1p, via phosphorylation, as cells approach stationary phase wherein they begin to accumulate neutral lipid due to nitrogen limitation in the growth media (Henry *et al* 1973; Behalova *et al* 1992; Natter *et al* 2013).

Hog1p is phosphorylated in early exponential phase due to its role in G1 and G2 cell cycle progression, cells are rapidly dividing. This phosphorylation is lost in late exponential phase due to it no longer being needed as excessive Hog1p activation is lethal to cells due to long term stresses arresting cell division and leading to apoptosis (Brewster *et al* 1993; Zhan *et al* 1999). Hog1p is rephosphorylated upon entry into stationary phase, likely as a result of nutrient limitation stress in stationary phase (Smith *et al* 2004). Therefore, could the activation of Hog1p by dual phosphorylation seen in late exponential phase be due to the lipogenic switch or due to the nutrient limitation stress occurring as nitrogen is depleted from the media.

Both nitrogen and carbon limitation exert stress on *S. cerevisiae* (Aoki *et al* 2011) and either one of these (most likely the nitrogen limitation) could explain the phosphorylation seen, in essence the dual phosphorylation of Hog1p observed could be as a result of nitrogen nutrient limitation. This is supported by Aoki *et al* 2011 who found Hog1p being dually phosphorylated in response to nitrogen limitation (Aoki *et al* 2011). This is further supported by Smith *et al* 2002 who describes that the Hog1p homologue, Sty1p, in *S. pombe* is dually phosphorylated by Wis1p (the *S. pombe* homologue of Pbs2p) in response to nutrient limitation. If the phosphorylation observed in Hog1p in late exponential is the result of nitrogen limitation, the question arises is this required for neutral lipid accumulation? To determine this, initial experiments were undertaken to measure neutral lipid levels in *pbs2Δ* cells.

Hog1p is classically activated by Pbs2p phosphorylation at Thr174 and Ty176 (Maayan *et al* 2012) in response to conditions of hyperosmotic stress and of nitrogen limitation (de Nadal *et al* 2002; Aoki *et al* 2011). However, accumulation of neutral lipids in a *pbs2Δ* mutant were shown to be similar to the wild type (Figure 3.7). This indicates that Pbs2p is not required for lipid accumulation, however, is this reflected in the phosphorylation pattern of Hog1. Western blot analysis of Hog1p phosphorylation in a

pbs2 Δ strain compared to wildtype, demonstrates that the dual phosphorylation of Hog1p at Thr174 and Tyr176 is completely lost during all growth phases (Figure 3.12).

Data also suggests that the dual phosphorylation at Thr174 and Ty176, observed during late exponential phase in wild type cells, is as a result of Pbs2p in conditions of nitrogen limitation (Maayan *et al* 2012). As such, this dual phosphorylation by Pbs2p in late exponential phase doesn't appear to be essential for lipid accumulation and suggests activation of Hog1p via an alternative mechanism.

There is evidence from the literature that Hog1p can be activated/phosphorylated via different mechanisms; e.g. via the kinase Pbs2p (Rodriguez-Pena *et al* 2010) or potentially via autophosphorylation (Maayan *et al* 2012).

Using a genetic screen, several hyperactive mutants of Hog1p were identified (Bell *et al* 2001). A number of these mutants were in the L16 domain, in Hog1p the region P309 to R358, which is highly conserved among Hog1p homologues. Some of these sites are Pbs2p independent such as sites F318L and F318S. The identification of these sites raised the question, if these sites allow Pbs2p independent Hog1p activation then which kinase is phosphorylating these Pbs2p independent sites? These sites could be phosphorylated by Hog1p, via autophosphorylation (Maayan *et al* 2012). Further work has been done with the sites Y68H, D170A, F318L, F318S, W320R, F322L, and W332R identified in Bell *et al* 2001; these sites have been shown to be activated in a Pbs2p independent manner (Bell *et al* 2001). The sites D170A, F318S and F318L have been shown autophosphorylated (Maayan *et al* 2012). The C-terminal regulatory region (between Y337 and F343) of Hog1p has been suggested to be responsible for autophosphorylation ability (Maayan *et al* 2012). This site overlaps with the Pbs2p interacting site, and is required for Pbs2p dependent activation of Hog1p (Maayan *et al* 2012). The site L341 seems to be essential to this autophosphorylation ability, truncation of the protein C-terminal region beyond L341 prevents Hog1p activity ion

pbs2Δ cells. However, the amino acid itself does not appear to matter as mutation of L341 to A341 did not affect the autophosphorylation ability of Hog1p in a *pbs2Δ* cell. This region appears to be evolutionary conserved in the mammalian orthologue of Hog1p, p38 α , a deletion of Y342 to F348 removes p38 α 's ability to autophosphorylate. This may explain the neutral lipid accumulation observed in the *pbs2Δ* cells.

Hog1p could be activated despite lacking the dual phosphorylation at Thr174 and Ty176 that Pbs2p dependent activation requires. Autophosphorylation at a previously uncharacterised site or at one of the two Pbs2p dependent sites (Thr174 and Ty176) may suffice; this would not be detectable by the α -P-p38 antibody and so would be in line with the results observed (Figure 3.9).

In addition, a large scale phosphoproteomic analysis of *S. cerevisiae*, from cells at grown in YPD media until an A_{600} of 0.7 was reached, then treated with 0.05% methyl methanesulfonate for 3 h, has identified two further phosphorylation sites in Hog1p, Ser178 and Thr179 (Albuquerque *et al* 2008). Either of these sites could be involved in activation of Hog1p during neutral lipid accumulation, however, it would need to be established if these sites are Pbs2p independent.

Having determined that dual phosphorylation of Hog1p at Thr174 and Ty176 was not required for neutral lipid accumulation and, based on previously published data, experiments were conducted to determine if other potential phosphorylation sites could be detected. Phos-tagTM has been utilised extensively and successfully by many researchers (Oh *et al* 2008; Yang *et al* 2010; Aokia *et al* 2011; Aguilar *et al* 2011; Hukkelhoven *et al* 2012; Ban *et al* 2013; Longoni *et al* 2015; Kinoshita *et al* 2017) to separate protein isoforms based on the number of phosphorylation sites (Kinoshita *et al* 2009). The Phos-tagTM nanomolecule acts by binding to anionic substituents as seen in phosphorylated proteins, with the phosphate groups holding the negative charge (Kinoshita *et al* 2009). This slows the progression of phosphorylated proteins through

an acrylamide gel, allowing a separation of proteins by phosphorylation states (more phosphorylated sites mean more places on a protein for Phos-tag™ to bind to). As such, a Phos-tag™ gel was used to determine whether any other phosphorylation of Hog1p could be observed in the absence of Pbs2p. In each case, wild type controls were included to ensure that the Pbs2p dependent dual phosphorylation of Hog1 could be observed. Further, all samples were run on protein gels without Phos-tag™ to confirm the presence of Hog1p.

In all cases, the protein gels without Phos-tag™, total Hog1p was detected in both the wildtype and *pbs2Δ* samples. Further, the dually phosphorylated form of Hog1p was observed in the wildtype, but not the *pbs2Δ* samples. However, following western blot analysis of, the Phos-tag™ gels, no signal was detected with the α-P-p38 antibody (Figure 3.13 A) with samples that had previously worked in the absence of Phos-tag™ (Figure 3.13 B). With the α-hog1 antibody, a faint signal was detected, although not to the extent seen with the non- Phos-tag™ gels. (Figure 3.13.2). Due to the lack of detection of Hog1p, both the total and phosphorylated form, using the Phos-tag™ gels no conclusions could be made about Pbs2p independent phosphorylation state of Hog1p during the lipogenic switch.

The α-P-p38 and α-hog1 antibodies had both worked well on regular gels so the antibodies themselves were not the issue. Given that the same protein samples that were used worked well in the absence of Phos-tag™, it is unlikely that these impacted on the result. Given that Phos-tag™ gels have been used extensively so it is likely that the preparation of these Phos-tag™ gels needed to be optimised for the epitopes for the Hog1p and α-P-p38 antibody were masked on Hog1p when it was run on the Phos-tag™ gel.

The manganese method (see 2.5.4 Phos-tag™) was the only one attempted during this study, however Kinoshita *et al* 2011 describes a zinc based method that can separate some phosphoprotein isoforms which the manganese method cannot. It is possible that Hog1p is one of these proteins whose isoforms cannot be separated using the manganese method, however a clear band should still be visible with all of the Hog1p isoforms together in one band.

Alternative methods for the detection of phosphorylation sites exist such as mass spectrometry. Chi *et al* 2007 used electron transfer dissociation mass spectrometry to identify phosphorylation sites on proteins from *S. cerevisiae*. They identified over 1200 phosphorylation sites on over 600 proteins, with a variable expression range of proteins from very low levels (<50 of that protein per cell) to very highly expressed proteins (>1,000,000 copies per cell). The use of protein immunoprecipitation, using the Hog1 antibody, would eliminate issues encountered with proteins recovered from crude cell extractions (Dephoure *et al* 2013), ensuring increased purity of the protein where it may otherwise be in low relative abundance in the cell. Ho *et al* 2002 purified *S. cerevisiae* proteins using immunoprecipitation before utilising mass spectrometry.

However, mass spectrometry is not inherently quantitative, and with standard methodologies gives qualitative results. There has however been much work in the development of quantitative mass spectrometry techniques. Keilhauer *et al* 2015 utilise an intensity-based label-free quantitative liquid chromatography–mass spectrometry analysis to investigate protein-protein interactions with GFP-tagged proteins and their interactors in budding yeast (Keilhauer *et al* 2015).

2D electrophoresis is another method that can be used to detect phosphorylated protein isoforms. 2D electrophoresis has been used to identify multiple phosphorylated isoforms of the transcription factor Atf1p in *Schizosaccharomyces pombe* under conditions of stress (Lawrence *et al* 2007). These phosphorylated isoforms were found

to be dependent on Sty1, the *S. pombe* homologue of Hog1p. As such, a similar experiment could be undertaken during the lipogenic switch, to determine the phosphorylated isoforms of Hog1p in a wild type and *pbs2Δ* mutant.

Sch9p is required for neutral lipid accumulation

With respect to neutral lipid accumulation, Hog1p seems to be activated in a Pbs2p independent manner. As Hog1p is classically activated by phosphorylation, it is possible that an alternative kinase is involved in lipid accumulation in response to nitrogen limitation in the environment. Utilising GFP tagged Hog1p would allow for the observation of the localisation of Hog1p during the activation of neutral lipid accumulation on live cells (Goodwin 1999; Haraguchi *et al* 2000; Ettinger *et al* 2014) and so to determine if Hog1p is actually being activated during the lipogenic switch. This will also indicate if nuclear localisation is required for neutral lipid accumulation.

The TOR pathway regulates cell growth in response to cellular stresses and nutrient availability and activates cellular responses such as protein synthesis and gene transcription (Hay *et al* 2004) (Loewith *et al* 2010). In conditions with plentiful nutrients, Tor1p inhibits transcriptional activators such as Msn2/4p by sequestering them within the cytoplasm (Crespo *et al* 2002). In conditions of nitrogen limitation Tor1p activity is inhibited, resulting in the release of transcription factors and activation of gene transcription (Rødskær *et al* 2014). It should be noted that TOR component deletion mutants have reduced neutral lipid levels indicating the TOR pathway's role in neutral lipid accumulation (Madeira *et al* 2015). This is highly conserved among eukaryotes, with mammalian (Laplante *et al* 2009b) and plant (Imamura *et al* 2016) cell orthologues of TOR being important for their lipid accumulation.

Sch9p is an AGC family protein kinase, a group of protein kinases whose catalytic domains are related to PK1 (Hanks *et al* 1995), that is a target of Tor1p (Urban *et al*

2007; Wei *et al* 2009). It is indirectly involved in, among other things, the regulation of oxidative and osmotic stresses through Sko1p (Pascual-Ahuir *et al* 2007). It is also involved in nitrogen limitation stress upon its dephosphorylation it acts to change the cell's nitrogen source from ammonium to urea (Urban *et al* 2007). Sch9 is functionally related to protein kinase A and shares phosphorylation targets, such as the MAPK Hog1 (Chen *et al* 2014), and shares a consensus sequence of R[R/K]x[S/T]; serine/threonine residues preceded by an arginine at the -3 position and arginine/lysine at -2 (Huber *et al* 2011). Msn2/4p is also a target of Sch9p (Madeira *et al* 2015).

Data (Figures 3.16 and 3.17) suggests that *SCH9* is required for neutral lipid accumulation, as a deletion of this gene caused a significant decrease in neutral lipid accumulation. The *sch9Δ* phenotype was rescued when the deletion was complemented with pRS313*SCH9* (Figure 3.17). This confirms previous data, where Nile Red staining was reduced in *sch9Δ* cells compared to wild type cells (Wei *et al* 2009). It is suggested that the decrease in neutral lipids may be due to an increase in the activity of the lipolytic enzyme, Tlg2p. Tlg2p has been shown to have lipolytic activity towards neutral lipids when expressed in *E. coli* and in yeast (Van Heusden *et al* 1998), it should be noted that it is localised in the mitochondria (Ham *et al* 2005), while Hog1p and Sch9p are primarily localised in the cytoplasm (Huh *et al*, 2003). GFP tagging of Hog1p and or Sch9p could allow for determining whether they co-localise or they localise with Tlg2p in the mitochondria. The *S. pombe* Hog1p homologue, Sty1p, has been found in the mitochondria (Di *et al* 2012) which indicates (due to the high level of homology between *S. cerevisiae* and *S. pombe*) that this may be occurring in *S. cerevisiae*.

S. pombe contains at least 3 Sch9p homologues, Sck1, Sck2 and Psk1 (Nakashima *et al* 2012), one of which, Sck1, interacts with Sty1 (Ryan *et al* 2012) supporting the idea of an interaction between Hog1p and Sch9p in *S. cerevisiae*.

There is however no evidence from this study to suggest that Hog1p is being phosphorylated at all, only that it is activated in a Pbs2p independent manner. While Hog1p is classically phosphorylated for activation, this may not be the mechanism of activation in the case of neutral lipid accumulation.

Hog1p is a potential target of the protein kinase, Sch9p

To determine if Hog1p is a target of Sch9 during the lipogenic switch, the neutral lipid levels in stationary phase were compared in both single and double deletion mutants of *HOG1* and *SCH9*. Both single deletions and double deletions of genes caused a similar reduction in accumulated neutral lipids when compared to the wild type (Figure 3.7, Figure 3.16 and Figure 3.20).

These data suggest that Sch9p and Hog1p are involved in the same pathway that regulates neutral lipid accumulation, as no additive effect was observed. If these proteins had been involved in separate pathways, a further reduction in neutral lipid levels would be expected. This technique has been used in a number of studies including Haber *et al* 2013 who used it to investigate partially redundant pairs of genes in *S. cerevisiae* and in *S. pombe* (Roguev *et al* 2007; Roguev *et al* 2008; Ryan *et al* 2012). This technique has been used to compare the phosphate signal transduction pathway in *S. cerevisiae* (which is well characterised) and *S. pombe* (which was not well characterised), with results suggesting that only the upper most genes share similar roles in both yeast species (Henry *et al*, 2011).

Sch9p has been shown to be involved in the osmostress-regulated transcriptional response, acting via the transcription factor Sko1p. Sko1p is also a target of Hog1p under osmostress conditions (Pascual-Ahuir *et al* 2007). Sch9p acts by forming a complex with Hog1p, which binds to and phosphorylates Sko1p. There is no evidence that Sch9p phosphorylates Hog1p, but it might regulate other proteins in complex with

Hog1p. As such without Hog1p, Sch9p can't bind and activate specific target proteins. However, this interaction between Sch9p and Hog1p has only been observed following osmotic stress response, so further work would need to be done to determine whether this mechanism exists during the accumulation of neutral lipid.

Sch9p also associates to genes in a Hog1p dependent manner, with a complete lack of Sch9p localisation to *GRE2* and *CTT1* in a *hog1Δ* mutant (Pascual-Ahuir *et al* 2007). This indicates multiple Hog1p dependent actions of Sch9p, of which some may be involved in lipid accumulation (Figure 3.7 and Figure 3.16). If Hog1p is absent, recruitment of Sch9p to the promoter could not occur, resulting in a similar phenotype of a strain lacking Sch9p (as in *sch9Δ*). Utilising GFP tagging of Hog1p and Sch9p could allow for determination of their localisation upon the lipogenic switch, once tagged these proteins can be observed by fluorescence microscopy of cell samples taken throughout the lipogenic switch (e.g. every 30 minutes from 6 to 12 hours). It may be possible to determine if it localises at certain promoters using chromatin immunoprecipitation (ChIP) could also be performed to determine if these proteins are bound to specific gene promoters. If Hog1p and Sch9p are forming a complex and localising at the same genes this should result in them precipitating together. The *hog1Δ* and *sch9Δ* mutants could be used in a ChIP looking to see if the proteins Hog1p and Sch9p bound to a promoter of a gene that is associated to in a Hog1p dependent manner. Key neutral lipid genes, such as *DGA1* and *LRO1* (Oelkers *et al* 2002), are potential targets of this complex. Utilising sequence data from *Saccharomyces* genome database the region 1kB upstream of the gene (predicted to contain the promoter) of *DGA1* and *LRO1* were compared using NCBI BLAST to try to identify shared consensus site for binding of these proteins. 4 alignments were found (see Figure 4.1). Hog1p has been shown to bind to genes with the STRE 5' CCCCT '3 (Varela *et al* 1995), this sequence does not occur anywhere 1Kb upstream from *DGA1*.

Dgal	1216	TGTACTCTTCT	1226
Lro1	2452	TGTACTCTTCT	2442
Dgal	1639	CTATTCCAAGA	1649
Lro1	2471	CTATTCCAAGA	2481
Dgal	1370	TGGAAGTGGTA	1380
Lro1	2552	TGGAAGTGGTA	2542
Dgal	2183	GCGGAGTTGAA	2193
Lro1	2874	GCGGAGTTGAA	2884

Figure 4.1 Sequence alignments between *DGA1* and *LRO1* + 1Kb. Sequence data from *Saccharomyces* genome database. Sequences compared using NCIB BLAST.

To test if Sch9p is interacting with Hog1p an immunoprecipitation (IP) experiment could be performed using cell lysates obtained as cells start to accumulate lipid. Sch9p would need to be tagged and the Hog1p antibody would be used to pull down proteins in the IP assay. The protein extractions would be run on a gel and probed for the tagged Sch9, if the proteins are interacting tagged Sch9 would be detected. The proteins could then be identified by utilising immunoprecipitation and their relevant antibodies.

Homologues of Sch9p and Hog1p in other organisms have been found to interact. In *Aspergillus fumigatus*, the SchAp (Sch9p) protein modulates SakAp (Hog1p) activity under conditions of osmotic stress (de Castro *et al*, 2016). An increase in SakAp phosphorylation in a *SchAΔ* mutant has been observed, with phosphorylation resulting in activation of the kinase. The implications from the data from *Aspergillus fumigatus* would suggest that there should be an equal or increased amount of Hog1p phosphorylation in a *sch9Δ* and equal amounts or increased levels of lipid accumulation, this is however not observed in *S. cerevisiae* (Figure 3.16), indicating that *A. fumigatus* may have significant differences in lipid metabolism regulation.

There is indication that the *S. pombe* Sch9p homologue, Sck1p, may be involved in response to nutrient availability through the Hog1p homologue Sty1p (Mudge *et al* 2014). A similar interaction between Sch9p and Hog1p in response to nutrient stress may be occurring in *S. cerevisiae* due to high level of homology between *S. pombe* and *S. cerevisiae*. Sck1p acts as an indirect regulator of PKA activity, via Gpa2p. It should be noted that Mudge *et al* 2014 focuses on glucose (carbon) limitation rather than nitrogen limitation, however both carbon and nitrogen limitation signals act through the Wis1-Spc1/Sty1 SAPK pathway in *S. pombe*.

If Sch9 isn't the activating kinase for Hog1p, alternative proteins could be detected using the following technique. Cell samples could be taken throughout the lipogenic switch (late exponential to early stationary phase) and lysed. Using a Hog1p antibody and coimmunoprecipitation the Hog1 protein and anything its binding will be isolated from the cell lysates. This purified protein sample could then be run on a protein gel, stained and protein bands analysed using mass spectroscopy (Link *et al* 1999).

It should be noted that the *pbs2Δsch9Δ* double delete restored the neutral lipid phenotype to wildtype levels (Figure 3.20). This deletion was tested by PCR using primers which would detect the *SCH9* deletion cassette (Sch9 Up 100 bp and Nat Rev) and was confirmed by gel electrophoresis that amplification had occurred indicating that the deletion cassette had integrated successfully. To ensure that the deletion cassettes were functioning cells grown on selection media for both deletions (First on G418 YPD and then NAT YPD), unless both cassettes were present and functional the cells would not be able to grow on the selection media (wild type and single deletion cells were used as controls and none of them grew). Growth with the *pbs2Δsch9Δ* double delete was observed on both G418 and NAT YPU selection plates indicating correct function of the cassette. This suggests that deletion of *PBS2* is able to rescue the levels of neutral lipids in the cell, suggesting Pbs2p might be a negative regulatory of neutral lipid accumulation. However, significantly increased levels of lipid

accumulation were not observed in a *pbs2Δ* mutant (Figure 3.7). The Nile Red method itself is able to detect deletion mutants with increased neutral lipid accumulation, as is observed with the *fat1Δ* mutant (Figure 3.7), this has also been demonstrated in the literature (Rostron *et al* 2015). While PCR has confirmed *SCH9* deletion the most obvious explanation is that *SCH9* hasn't been deleted. This could be confirmed by complementing the *pbs2Δ* by cloning *PBS2* in a plasmid and seeing if the neutral lipid levels return to *sch9Δ* levels. If the levels reduce (in what is now a *sch9Δ pbs2Δ* mutant with Pbs2p inserted on a vector) then this would not only confirm the deletion of *SCH9* it could indicate a possible interaction between Pbs2p and other downstream components of lipid metabolism which would need to be investigated further.

In neutral lipid accumulation, Msn2/4p and Dga1 are potential downstream targets of Hog1p

As Hog1p activation is required for neutral lipid accumulation, potential downstream targets need to be identified. Once activated, Hog1p can act either directly by phosphorylating targets (either in the cytoplasm or nucleus) or indirectly by translocating to the nucleus and recruiting RNA polymerase II to target gene promoters (Ferrigno *et al* 1998, Alepuz *et al.* 2001).

The Nile red assay indicates that neutral lipid levels are reduced in both *dga1Δ* and *msn2/4Δ* cells when compared to wildtype cells, suggesting a role for both Msn2/4p and Dga1p in neutral lipid accumulation (Figure 3.24). There is a clear role for Dga1 in lipogenesis, it is a diacylglycerol acyltransferase which is the catalyst for the terminal step in triacylglycerol synthesis (Dahlqvist *et al* 2000). A deletion *DGA1* results in a decrease in triacylglycerol synthesis and neutral lipid accumulation; this is not surprising given the enzymes role in the production of neutral lipid (Oelkers *et al* 2002, Mora *et al* 2012, Rostron *et al* 2015).

Msn2/4p are transcription factors involved in many pathways such as the oxidative stress response and nutrient limitation stress and are known targets of Hog1p (Hasan *et al* 2002, Hohmann 2002). They act by binding to the stress response element located in the promoter regions of genes involved in stress response (Martínez-Pastor *et al* 1996).

TOR regulates Msn2/4p in response to nutrient limitation by stimulating their binding to BMH2 (a cytoplasmic protein) sequestering them in the cytoplasm (Beck and Hall 1999). Hog1p is known to interact with Msn2/4p (Alepez *et al* 2001; Capaldi *et al* 2008) upon its nuclear localisation, Msn2/4p is a known target of Hog1p (Hohmann 2002).

Msn2/4 is required for lipid accumulation as a reduction in lipid levels is observed in an *msn2/4Δ* mutant (Figure 3.24). This result may also explain why a reduction is observed in a *hog1Δ* mutant as a lack of Hog1p would result in Msn2/4p not being able to activate gene transcription of lipid related genes, such as *DGA1*. If Msn4p isn't activated in a *hog1Δ* cells, then transcription of *DGA1* would reduce and the levels of the enzyme would reduce so reducing the amount of lipid accumulated (Oelkers *et al* 2002). Msn2/4 bind to a 5bp STRE, 5' CCCCT 3' (Marchler *et al* 1993; Rodrigues-Pousada *et al* 2004). The *DGA1* promoter lacks the STRE that Msn2/4 bind to therefore Msn2/4 cannot bind directly to *DGA1* (based upon sequence data from *Saccharomyces* genome database, Figure 4.2) to induce expression. However, there is evidence that Msn4p activates transcription of *SFP1* (Split Finger Protein 1), which encodes Sfp1, a protein required for transcription of *DGA1* (Hu *et al* 2007). Under cellular stress, such as nitrogen limitation, Msn4 activates transcription of *SFP1* (Hu *et al* 2007), which encodes Sfp1, which is required for the transcription of *DGA1*. Therefore, in *hog1Δ* cells, transcription of *DGA1* would reduce resulting in a reduction of Dga1p and neutral lipid levels (Oelkers *et al* 2002). Sfp1p interacts directly with TORC1 resulting in Sfp1p phosphorylation. This interaction also acts to negatively regulate TORC1 phosphorylation of Sch9p (Lempiaainen *et al* 2009). This indicates a

feedback loop which may act to prevent excess Sfp1 and so excess Dga1p. If *SCH9* is deleted then it cannot complex with Hog1p, this would reduce activation of Msn2/4, which would in turn decrease the transcription of *SPF1* finally resulting in less Dga1p and lipid accumulation. The role of Msn2/4 in lipid accumulation and the inability of Msn2/4 to bind to *DGA1*'s promoter is supported by the literature (Rajvanshi *et al* 2017).

```

1  GATGAGATTA  TTGCCTTTAC  TGCGCCATTG  TCGTGGCAGG  ATCATTTCCT  TGTCTTCGAT
61  AGGCCATCAT  CTAGAGTTCA  TGTACTGGAA  ACTGAGCAAG  ACGTGGGATT  ACAAACCTAA
121  TATGCTTTTC  ACATGGTTTA  GGTACGCGAT  GAGTAAAACC  GCGCTAATCC  AATGCACGAA
181  GATGTTGGCC  ATCAAATACC  CTGACGTTCT  TTGTCTCTCC  GTTCATCCGG  GTCTGGTGAT
241  GAACACAAAC  TTATTCAGTT  ATTGGACAAG  GTTACCCATC  GTCGGTATTT  TCTTTTGGCT
301  GTTGTTCCAG  GTCGTAGGGT  TCTTTTTCGG  CGTATCGAAC  GAACAAGGTT  CACTAGCTTC
361  TTTGAAGTGT  GCATTGGACC  CGAATTTATC  TGTCGAAAAA  GATAACGGGA  AGTACTTCAC
421  CACGGGGGGT  AAAGAATCTA  AATCGAGCTA  CGTTTCTAAC  AATGTCGACG  AAGCGGCATC
481  GACTTGGATC  TGGACCGTTC  ATCAACTAAG  AGACCGTGGT  TTCGATATAT  AACAAAGACGG
541  AAAGATTGAA  AGAGTAGATA  GATGTACATT  TTATTTAAAT  ATTAGTTAGT  CGTTATTGTA
601  ACTGGTAATC  AGAGCAAGAA  GTTTTTCTGT  ACTTTGTTCT  CTGCAGGCAA  CTAAGTTACG
661  GGCCGACAAA  GGCTTATGAT  GTGCGTTTTT  TATTCAATTG  ATAGATTTCAG  TCAGCATTGA
721  CGTAATGGGA  AGGCTAGAAA  AAGAGAAGAC  TGAATTTGGA  AACTTATTCC  TCAAAGCAGA
781  CCAGTACTTC  CACCGCATTT  CTGTACTTAA  CCAAGCACGA  CAGTGGTCTA  TCAGGCTTGG
841  ATCTTTCACT  ACACTTCCGC  CAAAGTTTTT  TTTTTTTCCT  GTTTATCCCA  GATCACGTTT
901  GTTCCATTAA  GGAGGTTTAC  TATCATCTCA  TTCCATTTA  CACATACACT  TACATATACA
961  TAAGGAAACG  CAGAGGCATA  CAGTTTGAAC  AGTCACATAA

```

Figure 4.2 *DGA1* + 1Kb sequence. The sequence of the stream 1kb before *DGA1* gene based upon sequence data from *Saccharomyces* genome database. There are no points within this sequence which Msn2/4p can bind to meaning that Msn2/4p cannot act upon Dga1 transcription directly, but instead (if it is indeed acting upon it at all) must act indirectly (likely via Spf1).

Dga1p acts as a catalyst for the Acyl-CoA dependent acylation of diacylglycerol (Athenstaedt 2011; Sorger *et al* 2002) and is responsible for (along with Lro1p) most TAG synthesis within the cell (Oelkers *et al* 2002). Therefore, Dga1p is an essential enzyme in lipogenesis, with its deletion causing a significant reduction in neutral lipid levels in stationary phase (Figure 3.24) (Athenstaedt, 2011). Upon complementation of the *dga1Δ* strain with pRS316-*DGA1*, the neutral lipid phenotype was rescued when compared to the control. In the wildtype strain, transformed with pRS316-*DGA1*, neutral lipid levels were similar to the control wildtype strain, containing pRS316 alone. Overexpression of *DGA1* has been shown to significantly increase neutral lipid

accumulation resulting in *S. cerevisiae* becoming an oleaginous yeast and accumulating lipid up to 45% of cellular mass (Kamisaka *et al*, 2007), but this was not observed in these experiments. This is likely due to the fact that pRS316 is not an over expression plasmid (Sikorski *et al* 1989) and, as *DGA1* is under the control of its own promoter, limited overexpression would be observed. The expression profile could be confirmed using real-time quantitative PCR to determine transcriptional levels (Ponchel *et al* 2003) and, if the protein was tagged, using western blot analysis to determine protein levels in the cell (Ghaemmaghani *et al* 2003).

To determine if Hog1p and Dga1p are on the same pathway, as done with Sch9p, neutral lipid levels were measured in single and double delete mutants. Neutral lipid accumulation is reduced to a similar level in the *hog1Δdga1Δ* mutant to that of *dga1Δ* and *hog1Δ* mutants, when compared to wild type (Figure 3.28). As there is no additive effect on neutral lipid levels, this data suggests that Hog1p and Dga1p are on the same pathway therefore suggesting Dga1p is a potential downstream target of Hog1p. When *DGA1* was deleted in combination with *pbs2Δ*, a reduction in neutral lipid levels was observed compared to the wild type. These levels were comparable to the reduction seen in the single *dga1Δ* cells. As the *pbs2Δ* cells show wildtype levels of neutral lipids, this reduction must be the result of loss of Dga1p. This could be tested by reintroducing *DGA1*, on a plasmid, into *pbs2Δ dga1Δ* cells and confirming the rescue of the neutral lipid phenotype.

If Dga1p is a target of Hog1, its regulation may be direct, or indirect. If interaction is direct, then it could be via phosphorylation. Hog1p phosphorylates proteins on a conserved sequence, serine or threonine residues followed by a proline residue (S/T P) (Roux *et al* 2004). Therefore, if Dga1p is phosphorylated directly by Hog1p, it should contain this amino acid sequence. Figure 3.29 shows four potential MAPK sites identified in Dga1. To determine which of these sites are the most likely targets of Hog1p, one needs to consider the structure of Dga1 and the position of the potential

Of the four MAPK sites identified, S17 and T53 sites are both on the cytoplasmic side of the protein, thus it is possible for them to be phosphorylated by Hog1p. However, T84 and S103 are not, with T84 spanning the ER luminal membrane and S103 on the inside of the ER. There is no evidence that Hog1p is present in the ER, therefore it is unlikely that these sites are phosphorylated by Hog1p. In addition, both S17 and T53 are in N terminal region of Dga1 that is vital for neutral lipid accumulation, further indicating they may be a target for Hog1p (Liu *et al* 2011).

To determine whether phosphorylation of S17 and T53 was important for activity of the Dga1 protein, a mutagenesis strategy was designed to convert these two residues to alanine. Mutagenesis of S17 and T53 was attempted using two methods, the QuikChange and extended primer method. The QuikChange method copies the entire template plasmid and its insert, the primers determining the number of residues to be mutated (in this case a point mutation was performed). The wildtype parental plasmid is removed by digest with *DpnI*, a restriction enzyme which digests methylated DNA. Old DNA (i.e. parental) will be methylated by *E. coli*. Newly synthesised DNA via PCR will not and therefore will not be digested and so will be the only DNA transformed into *E. coli*. Although successful amplification of the plasmid was determined by agarose gel electrophoresis, no *E. coli* transformants were observed following the *DpnI* digest, to remove the parental plasmid. As the QuikChange method failed the troubleshooting guide was consulted. It was possible that although amplification was suggested by gel electrophoresis that the desired plasmid could have been lost following digestion by *DpnI*. It is possible that too little of the intact product was transformed into DH5α *E. coli*, the QuikChange method does not amplify as significantly as regular PCR so following *DpnI* digestion the concentration of plasmid may have been too low to allow for successful transformation. This same effect could be due to too low a concentration of template, the mutagenesis could be redone with increased concentrations of plasmid template as suggested in the troubleshooting guide (e.g. 200ng or 500ng) as the

concentration used was ~50ng. The in-house chemically competent *E. coli* cells may not have been sufficiently competent to transform the QuikChange product. Although successful with a previous purified plasmid (pRS316*DGA1*), this is extremely concentrated in comparison. The use of highly competent electrocompetent cells may have resolved this issue as they are significantly more efficient than chemically competent cells (Tu *et al* 2016). It is also possible that further work was needed to better optimise the PCR conditions, the conditions used were that included in the manual; 1 minute ignition denaturation at 95°C followed by 30 cycles of 1 minute of denaturation at 95°C, 1 minute of annealing at 55°C and 2 minutes of extension time per Kb of plasmid at 65°C. Optimisation of the annealing and extension conditions (length and temperature) may improve the success of the PCR (Lorenz 2012). The extended primer method consisted of 3 reactions (R1 – 3). R1 and R2 utilised a TOPO*DGA1* template using a *DGA1* mutagenesis primer (e.g. S17 For) and it's opposing normal *DGA1* primer (e.g Dga1 Rev), R1 and R2 utilising the opposite set to each other (e.g. R1; S17 For + Dga1 Rev, R2; S17 Rev + Dga1 For). After confirming R1 and R2 had worked a gel extraction was performed to purify and concentrate the products. R3 utilised normal *DGA1* primers (Dga1 For + Dga1 Rev) and used the products from R1 and R2 as templates, once amplified this product would be gel extracted and transformed into a vector (TOPO and pRS316 were to be attempted). R3 generated a product for S17 however said product did not successfully clone into a TOPO vector, this may be due to the product being of too low a concentration, ideally multiple reactions would be combined and gel extracted, however R3 proved to be unreliable resulting in little specific R3 product and so a low concentration for cloning. A TOPO vector was used as it allows for the easy integration of a gene into a plasmid, which then can be transformed into DH5- α *E. coli*. The TOPO vector had been used successfully in this project, with successful insertion of *DGA1* into the vector and successful transformation into DH5- α *E. coli*. The first two reactions for the extended primer method for S17, T53, T84 and S103 all worked successfully, issues arose with the third reaction. It is possible that the PCR reaction for R3 needed to be optimised,

however it is also possible that the issue was with the templates used. As the method relies upon two templates linking to form product (Heckman *et al* 2007) it relies even more on Brownian motion than a standard PCR. Thus, if the concentration of templates was too low then the chances of proper interaction are also lower (Bian *et al* 2016), which may explain the failures seen. The concentration of Mg²⁺ is also important, the standard HF buffer for Phusion used contained 1.5 mM MgCl₂, likely each of these mutagenesis reactions each needed individual optimisation with regards to Mg²⁺.

To determine if there is a direct interaction between Hog1p and Dga1, an immunoprecipitation (IP) could be performed. Using protein lysates from cells undergoing neutral lipid accumulation, Hog1p can be pulled down using a specific antibody and tagged Dga1p could then be detected by western blot analysis. This method is dependent on obtaining a genomically tagged copy of *DGA1* as there are currently no antibodies directly against Dga1p. A genomically tagged *DGA1* was made with a HA tag at the C terminal of the protein, selected with a NAT cassette. This was confirmed by PCR using genomic DNA from the yeast clones (Figure 3.30 A - C). However, when the PCR positive clones were tested by western blot analysis for presence of the C terminal tag, (Figure 3.31) no 3HA tagged Dga1p was observed. To determine whether the HA antibody was able to recognise the tag, a positive control was included from *S.pombe*, where *atf21* had been genomically tagged with HA. Unfortunately, no signal was detected from these samples suggesting that either the primary or secondary antibody were not working.

It is also possible that the *DGA1* gene, in the phase of growth used for the protein extractions, is not transcribed at a high enough level for detection. Alternatively, the protein could be rapidly degraded. The samples used were harvested in exponential phase, as Dga1p is involved in lipid accumulation and as lipid accumulation occurs in stationary phase better results may be seen with stationary phase samples.

Introduction of a tagged *DGA1* on a normal expression or over expression plasmid could be done in a *dga1Δ* to ensure all expressed *DGA1* is tagged.

To test the degradation of Dga1p the proteasome could be inhibited but utilisation of CRISPR interference which would utilise an only partially functional Cas9 which would bind to the selected gene (which would be selected by the use of a guideRNA) and prevent its transcription (Collins *et al* 2010; Martinez *et al* 2017). As most proteins are degraded in the proteasome, if this is true for Dga1, inhibiting its function would result in an increase in Dga1p levels in the cell (Collins *et al* 2010).

To test the levels of *DGA1* transcription a RT-PCR with Syber Green could be used to determine mRNA levels (Ponchel *et al* 2003). If done using cell extractions from multiple time points (e.g. 0 – 10 hours with 30-minute time points) one could not only see how *DGA1* transcription changed as cells begin to accumulate lipid but also with the use of an overexpression one could compare levels of transcription between it and the wild type. A northern blot could be performed to assess the levels of *DGA1* mRNA in the cell. This can be done using a radioactive label or a non-radioactive label (e.g. biotin, fluorescein, or digoxigenin), with digoxigenin labelled probes having largely replaced the others due to having high stability and not having the safety or disposal concerns that radioactive labels do (Wu *et al* 2013). Alternatively, a reverse transcription (RT) PCR could also be performed to assess expression levels. RT-PCR detects gene expression through creation of cDNA transcripts from mRNA (Shiao 2003). The method of RT-PCR described in Shiao 2003, that being, allows for quantitative assessment of protein expression. RT-PCR with Syber Green could also be used to determine mRNA levels (Ponchel *et al* 2003).

To determine if Hog1p is involved with the transcription of *DGA1*, either directly or indirectly though Msn2/4p, ChIP can be used. This method has been used to determine

the presence of Hog1p at specific gene promoters under a number of conditions (Pascual-Ahuir *et al* 2006 and Ahuir *et al* 2006). As such, whether Hog1 is localised to the promoter of *DGA1* can be determined. Work done previously has utilised a HA tagged Hog1p, crosslinked and harvested cells within 5 minutes of stress conditions (Pascual-Ahuir *et al* 2006). Previous work utilised salt stress rather than nutrient limitation, so the methodology would require adjustment and optimisation, perhaps taking samples over a time course of 30 minute intervals (from mid exponential to stationary phase). The methodology using HA tagged Dga1p and Hog1p could be attempted and the results compared, it is expected that an interaction with both proteins in both experiments would be observed if the two proteins interact directly. Observation of *DGA1* transcription and protein levels in a *hog1Δ* mutant would indicate an interaction, the methodologies for which have been discussed previously. It would be expected that if Hog1p is involved in Dga1p levels that a *HOG1* deletion strain would transcribe less *DGA1* and have less Dga1p in its cells.

If a direct interaction between Hog1p and Dga1p is confirmed, then the mutagenesis study of Dga1p determine the role of Hog1p phosphorylation in lipid accumulation. Dga1p could be tagged to allow for observation of protein levels and post translational modification throughout the lipogenic switch. By extracting and purifying Dga1p its phosphorylation state can be determined as was discussed previously for Hog1p

If interaction is indirect then Hog1p could be involved in the transcription of *DGA1*, either by Hog1p itself entering the nucleus and binding the *DGA1* promoter, or by with Hog1p activating another protein, such as Msn2/4p in the osmotic stress response (Hohmann 2002) as discussed previously. Msn4p is involved in the regulation of *DGA1* transcription through the activation of transcription of Spf1p (Hu *et al* 2007) as discussed previously.

This work has demonstrated that Hog1p is required for neutral lipid accumulation, whereas the upstream elements of the HOG MAPK pathway (Pbs2p, Ste11p and Ssk2p) are not. The role of Hog1p appears to be Pbs2p independent, suggesting that other proteins may be involved with evidence presented for a role of Sch9p, a kinase. Hog1p regulates many cellular processes via downstream targets. In the case of neutral lipid accumulation, data has been presented to suggest both Dga1p and Msn2/4p are targets of Hog1p, either by direct or indirect mechanism. As such, this thesis has presented a novel role of Hog1p in neutral lipid accumulation, which may impact on the future development of treatments for cancer lipogenesis. It is possible that treatments could be developed that target components of the lipogenesis regulatory pathways which go awry in cases of cancer, perhaps utilising technologies such as aptamers.

There is also another potential impact, that being biofuel production, generating oleaginous yeast from *S. cerevisiae* has been demonstrated in the literature, by genetically modifying *S. cerevisiae* (with the intent of altering the lipogenic nature of the cell through the Hog1 MAPK and its interacting pathways) it may be possible to generate a mutant *S. cerevisiae* strain that is ideal for biofuel production. *S. cerevisiae*'s well characterised nature combined with its already extensive use by industry would likely allow for a much easier start-up of a *S. cerevisiae* based biofuel industry (what with all the fermentation work done with its involvement in alcohol production) relative to that of some other oleaginous yeast such as *Lipomyces starkeyi*.

5.0 Appendix

5.1 Appendix 1 – Sequencing data from Source Bioscience

To determine if *DGA1* was successfully integrated into its vector it was sequenced. To determine if the sequence was as expected *DGA1* was located within the sequence data and compared via NCBI blast to a known sequence of *DGA1* (in this case from the

saccharomyces genome database).

NCBI BLAST – DGA1 SEQ

```
Query 1 ATGTCAGGAACATTCAATGATATAaagaagaaggaagaaggaagaaggaagCCCTACAGCC 60
      |
Sbjct 1 ATGTCAGGAACATTCAATGATATAAGAAGAAGGAAGAAGGAAGAAGGAAGCCCTACAGCC 60

Query 61 GGTATTACCGAAAGGCATGAGAATAAGTCTTTGTCAAGCATCGATAAAAGAGAACAGACT 120
      |
Sbjct 61 GGTATTACCGAAAGGCATGAGAATAAGTCTTTGTCAAGCATCGATAAAAGAGAACAGACT 120

Query 121 CTCAAACCACAAC TAGAGTCATGCTGTCCATTGGCGACCCCTTTTGAAAGAAGGTTACAA 180
      |
Sbjct 121 CTCAAACCACAAC TAGAGTCATGCTGTCCATTGGCGACCCCTTTTGAAAGAAGGTTACAA 180

Query 181 ACTCTGGCTGTAGCATGGCACACTTCTTCATTTGTACTCTTCTCCATATTTACGTTATTT 240
      |
Sbjct 181 ACTCTGGCTGTAGCATGGCACACTTCTTCATTTGTACTCTTCTCCATATTTACGTTATTT 240

Query 241 GCAATCTCGACACCAGCACTGTGGGTCTTGCTATTCCATATATGATTTA ttttttttttC 300
      |
Sbjct 241 GCAATCTCGACACCAGCACTGTGGGTCTTGCTATTCCATATATGATTTA -TTTTTTTTTC 299

Query 301 GATAGGTCTCCTGCAACTGGCGAAGTGGTAAATCGATACTCTCTTCGATTTTCGTTTCATTG 360
      |
Sbjct 300 GATAGGTCTCCTGCAACTGGCGAAGTGGTAAATCGATACTCTCTTCGATTTTCGTTTCATTG 359

Query 361 CCCATTTGGAAGTGGTATTGTGATTATTTCCCTATAAGTTTGATTA AAACTGTCAATTTA 420
      |
Sbjct 360 CCCATTTGGAAGTGGTATTGTGATTATTTCCCTATAAGTTTGATTA AAACTGTCAATTTA 419

Query 421 AAACCAACTTTTACGCTTTCAAAAAATAAGAGAGTTAACG aaaaaaTTACAAGATTAGA 480
      |
Sbjct 420 AAACCAACTTTTACGCTTTCAAAAAATAAGAGAGTTAACG AAAAAAATTACAAGATTAGA 479

Query 481 TTGTGGCCAAC TAAGTATTCCATTAATCTCAAAGCAACTCTACTATTGACTATCGCAAC 540
      |
Sbjct 480 TTGTGGCCAAC TAAGTATTCCATTAATCTCAAAGCAACTCTACTATTGACTATCGCAAC 539

Query 541 CAGGAATGTACAGGGCCAACGTACTTATTTGGTTACCATCCACACGGCATAGGAGCACTT 600
      |
Sbjct 540 CAGGAATGTACAGGGCCAACGTACTTATTTGGTTACCATCCACACGGCATAGGAGCACTT 599
```

```

Query 601 GGTGCGTTTGGAGCGTTTGCAACAGAAGGTTGTAACATTTCCAAGATTTTCCCAGGTATT 660
          |||
Sbjct 600 GGTGCGTTTGGAGCGTTTGCAACAGAAGGTTGTAACATTTCCAAGATTTTCCCAGGTATT 659

Query 661 CCTATTTCTCTGATGACACTGGTCACACAATTTTCATATCCCATTGTATAGAGACTACTTA 720
          |||
Sbjct 660 CCTATTTCTCTGATGACACTGGTCACACAATTTTCATATCCCATTGTATAGAGACTACTTA 719

Query 721 TTGGCGTTAGGTATTTCTTCAGTATCTCGGAAAAACGCTTTAAGGACTCTAAGCAAAAAT 780
          |||
Sbjct 720 TTGGCGTTAGGTATTTCTTCAGTATCTCGGAAAAACGCTTTAAGGACTCTAAGCAAAAAT 779

Query 781 CAGTCGATCTGCATTGTTGTTGGTGGCGCTAGGGAATCTTTATTAAGTTCAACAAATGGT 840
          |||
Sbjct 780 CAGTCGATCTGCATTGTTGTTGGTGGCGCTAGGGAATCTTTATTAAGTTCAACAAATGGT 839

Query 841 ACACAACCTGATTTTAAACAAAAGAAAGGGTTTTATTAAACTGGCCATTCAAACGGGGAAAT 900
          |||
Sbjct 840 ACACAACCTGATTTTAAACAAAAGAAAGGGTTTTATTAAACTGGCCATTCAAACGGGGAAAT 899

Query 901 ATTAACCTAGTGCCTGTGTTTGCATTTGGAGAGGTGGACTGTTATAATGTTCTGAGCACa 960
          |||
Sbjct 900 ATTAACCTAGTGCCTGTGTTTGCATTTGGANNGTGGACTGTTATAATGTTCTGAGCACA 959

Query 961 aaaaaaGATTCAGTCCTGGGTAAAATGCAACTATGGTTCAAAGAAAACCTTTGGTTTTACC 1020
          |||
Sbjct 960 AAAAAAGATTCAGTCCTGGGTAAAATGCAACTATGGTTCAAAGAAAACCTTTGGTTTTACC 1019

Query 1021 ATTCCCATTTTCTACGCAAGAGGATTATTCAATTACGATTTTCGGTTTGTGGCCATTTAGA 1080
          |||
Sbjct 1020 ATTCCCATTTTCTACGCAAGAGGATTATTCAATTACGATTTTCGGTTTGTGGCCATTNAGA 1079

Query 1081 GCGCCTATCAATGTTGTTGTTGGAAGGCCTATATACGTTGAAAAGAAAATAACAAATCCG 1140
          |||
Sbjct 1080 NNGCCTATCAATGTTGTTGTTGGAAGGCCTATATACNTTAAAAGAAAATAACAAATCCN 1139

Query 1141 CCAGA-TGATGTTGTTAATCATTTCATGA-TTT 1172
          || |
Sbjct 1140 CCNAANTGATGTTGTTAATCATTTCATGAATTT 1173

```

6.0 References

- AGUILAR, H.N., TRACEY, C.N., TSANG, S.C.F., MCGINNIS, J.M. and MITCHELL, B.F., 2011. Phos-Tag-Based Analysis of Myosin Regulatory Light Chain Phosphorylation in Human Uterine Myocytes. *Plos One*, 6(6), pp. e20903.
- ALBUQUERQUE, C.P., SMOLKA, M.B., PAYNE, S.H., BAFNA, V., ENG, J. and ZHOU, H., 2008. A multidimensional chromatography technology for in-depth phosphoproteome analysis. *Molecular & Cellular Proteomics*, 7(7), pp. 1389-1396.
- ALEPUZ, P., JOVANOVIC, A., REISER, V. and AMMERER, G., 2001. Stress-induced MAP kinase Hog1 is part of transcription activation complexes. *Molecular cell*, 7(4), pp. 767-777.
- AMEER, F., SCANDIUZZI, L., HASNAIN, S., KALBACHER, H. and ZAIDI, N., 2014. De novo lipogenesis in health and disease. *Metabolism*, 63(7), pp. 895-902.
- AOKI, Y., KANKI, T., HIROTA, Y., KURIHARA, Y., SAIGUSA, T., UCHIUMI, T. and KANG, D., 2011. Phosphorylation of Serine 114 on Atg32 mediates mitophagy. *Molecular biology of the cell*, 22(17), pp. 3206-3217.
- AOKIA, K., YAMADA, M., KUNIDA, K., YASUDA, S. and MATSUDA, M., 2011. Processive phosphorylation of ERK MAP kinase in mammalian cells. *Proceedings of the National Academy of Sciences of the United States of America*, 108(31), pp. 12675-12680.
- ARLIA-CIOMMO, A., SVISTKOVA, V., MOHTASHAMI, S. and TITORENKO, V.I., 2016. A novel approach to the discovery of anti-tumor pharmaceuticals: searching for activators of liponecrosis. *Oncotarget*, 7(5), pp. 5204-5225.

ARONOVA, S., WEDAMAN, K., ANDERSON, S., YATES, JOHN, III and POWERS, T., 2007. Probing the membrane environment of the TOR kinases reveals functional interactions between TORC1, actin, and membrane trafficking in *Saccharomyces cerevisiae*. *Molecular biology of the cell*, 18(8), pp. 2779-2794.

ATHENSTAEDT, K. and DAUM, G., 2006. The life cycle of neutral lipids: synthesis, storage and degradation. *Cellular and Molecular Life Sciences*, 63(12), pp. 1355-1369.

ATHENSTAEDT, K., 2011. YALI0E32769g (DGA1) and YALI0E16797g (LRO1) encode major triacylglycerol synthases of the oleaginous yeast *Yarrowia lipolytica*. *Biochimica Et Biophysica Acta-Molecular and Cell Biology of Lipids*, 1811(10), pp. 587-596.

BAENKE, F., PECK, B., MIESS, H. and SCHULZE, A., 2013. Hooked on fat: the role of lipid synthesis in cancer metabolism and tumour development. *Disease Models & Mechanisms*, 6(6), pp. 1353-1363.

BAN, Y., KOBAYASHI, Y., HARA, T., HAMADA, T., HASHIMOTO, T., TAKEDA, S. and HATTORI, T., 2013. alpha-Tubulin is Rapidly Phosphorylated in Response to Hyperosmotic Stress in Rice and Arabidopsis. *Plant and Cell Physiology*, 54(6), pp. 848-858.

BANUETT, F., 1998. Signalling in the yeasts: An informational cascade with links to the filamentous fungi. *Microbiology and Molecular Biology Reviews*, 62(2), pp. 249-+.

BARANWAL, S., AZAD, G.K., SINGH, V. and TOMAR, R.S., 2014. Signaling of Chloroquine-Induced Stress in the Yeast *Saccharomyces cerevisiae* Requires the Hog1 and Slr2 Mitogen-Activated Protein Kinase Pathways. *Antimicrobial Agents and Chemotherapy*, 58(9), pp. 5552-5566.

BECK, T. and HALL, M., 1999. The TOR signalling pathway controls nuclear localization of nutrient-regulated transcription factors. *Nature*, 402(6762), pp. 689-692.

BEHALOVA, B., HOZAK, P., BLAHOVA, M. and SILLINGER, V., 1992. Effect of Nitrogen Limitation and Sporulation on Sterol and Lipid Formation in *Saccharomyces-Cerevisiae*. *Folia microbiologica*, 37(6), pp. 442-449.

BELL, M., CAPONE, R., PASHTAN, I., LEVITZKI, A. and ENGELBERG, D., 2001. Isolation of hyperactive mutants of the MAPK p38/Hog1 that are independent of MAPK kinase activation. *Journal of Biological Chemistry*, 276(27), pp. 25351-25358.

BELLER, M., THIEL, K., THUL, P.J. and JAECKLE, H., 2010. Lipid droplets: A dynamic organelle moves into focus. *FEBS letters*, 584(11), pp. 2176-2182.

BESSOULE, J., LESSIRE, R., RIGOULET, M., GUERIN, B. and CASSAGNE, C., 1987. Fatty-Acid Synthesis in Mitochondria from *Saccharomyces-Cerevisiae*. *FEBS letters*, 214(1), pp. 158-162.

BIAN, X., KIM, C. and KARNIADAKIS, G.E., 2016. 111 years of Brownian motion. *Soft Matter*, 12(30), pp. 6331-6346.

BOTSTEIN, D. and FINK, G.R., 2011. Yeast: An Experimental Organism for 21st Century Biology. *Genetics*, 189(3), pp. 695-704.

BRACHMANN, C., DAVIES, A., COST, G., CAPUTO, E., LI, J., HIETER, P. and BOEKE, J., 1998. Designer deletion strains derived from *Saccharomyces cerevisiae* S288C: a useful set of strains and plasmids for PCR-mediated gene disruption and other applications. *Yeast*, 14(2), pp. 115-132.

BREITKREUTZ, A., CHOI, H., SHAROM, J.R., BOUCHER, L., NEDUVA, V., LARSEN, B., LIN, Z., BREITKREUTZ, B., STARK, C., LIU, G., AHN, J., DEWAR-DARCH, D., REGULY, T., TANG, X., ALMEIDA, R., QIN, Z.S., PAWSON, T., GINGRAS, A., NESVIZHSKII, A.I. and TYERS, M., 2010. A Global Protein Kinase and Phosphatase Interaction Network in Yeast. *Science*, 328(5981), pp. 1043-1046.

BREWSTER, J.L. and GUSTIN, M.C., 2014. Hog1: 20 years of discovery and impact. *Science Signaling*, 7(343), pp. re7.

CAPALDI, A.P., KAPLAN, T., LIU, Y., HABIB, N., REGEV, A., FRIEDMAN, N. and O'SHEA, E.K., 2008. Structure and function of a transcriptional network activated by the MAPK Hog1. *Nature genetics*, 40(11), pp. 1300-1306.

CARMAN, G.M. and HENRY, S.A., 2007. Phosphatidic acid plays a central role in the transcriptional regulation of glycerophospholipid synthesis in *Saccharomyces cerevisiae*. *Journal of Biological Chemistry*, 282(52), pp. 37293-37297.

CHAN, T., CARVALHO, J., RILES, L. and ZHENG, X., 2000. A chemical genomics approach toward understanding the global functions of the target of rapamycin protein (TOR). *Proceedings of the National Academy of Sciences of the United States of America*, 97(24), pp. 13227-13232.

CHEN, C., WANDURAGALA, S., BECKER, D. and DICKMAN, M., 2006. Tomato QM-Like protein protects *Saccharomyces cerevisiae* cells against oxidative stress by regulating intracellular proline levels. *Applied and Environmental Microbiology*, 72(6), pp. 4001-4006.

CHEN, D., WANG, Y., ZHOU, X., WANG, Y. and XU, J., 2014. The Sch9 Kinase Regulates Conidium Size, Stress Responses, and Pathogenesis in *Fusarium graminearum*. *Plos One*, 9(8), pp. e105811.

CHEN, R.E. and THORNER, J., 2007. Function and regulation in MAPK signaling pathways: Lessons learned from the yeast *Saccharomyces cerevisiae*. *Biochimica Et Biophysica Acta-Molecular Cell Research*, 1773(8), pp. 1311-1340.

CHI, A., HUTTENHOWER, C., GEER, L.Y., COON, J.J., SYKA, J.E.P., BAI, D.L., SHABANOWITZ, J., BURKE, D.J., TROYANSKAYA, O.G. and HUNT, D.F., 2007. Analysis of phosphorylation sites on proteins from *Saccharomyces cerevisiae* by electron transfer dissociation (ETD) mass spectrometry. *Proceedings of the National Academy of Sciences of the United States of America*, 104(7), pp. 2193-2198.

COLLINS, G.A., GOMEZ, T.A., DESHAIES, R.J. and TANSEY, W.P., 2010. Combined chemical and genetic approach to inhibit proteolysis by the proteasome. *Yeast* (Chichester, England), 27(11), pp. 965-974.

CORCOLES-SAEZ, I., BALLESTER-TOMAS, L., DE LA TORRE-RUIZ, M.A., PRIETO, J.A. and RANDEZ-GIL, F., 2012. Low temperature highlights the functional role of the cell wall integrity pathway in the regulation of growth in *Saccharomyces cerevisiae*. *Biochemical Journal*, 446, pp. 477-488.

CRESPO, J., POWERS, T., FOWLER, B. and HALL, M., 2002. The TOR-controlled transcription activators GLN3, RTG1, and RTG3 are regulated in response to intracellular levels of glutamine. *Proceedings of the National Academy of Sciences of the United States of America*, 99(10), pp. 6784-6789.

CZABANY, T., ATHENSTAEDT, K. and DAUM, G., 2007. Synthesis, storage and degradation of neutral lipids in yeast. *Biochimica Et Biophysica Acta-Molecular and Cell Biology of Lipids*, 1771(3), pp. 299-309.

DAHLQVIST, A., STAHL, U., LENMAN, M., BANAS, A., LEE, M., SANDAGER, L., RONNE, H. and STYMNE, H., 2000. Phospholipid : diacylglycerol acyltransferase: An enzyme that catalyzes the acyl-CoA-independent formation of triacylglycerol in yeast and plants. *Proceedings of the National Academy of Sciences of the United States of America*, 97(12), pp. 6487-6492.

DE CASTRO, P.A., DOS REIS, T.F., DOLAN, S.K., MANFIOLLI, A.O., BROWN, N.A., JONES, G.W., DOYLE, S., RIANO-PACHON, D.M., SQUINA, F.M., CALDANA, C., SINGH, A., DEL POETA, M., HAGIWARA, D., SILVA-ROCHA, R. and GOLDMAN, G.H., 2016. The *Aspergillus fumigatus* SchA(SCH9) kinase modulates SakA(HOG1) MAP kinase activity and it is essential for virulence. *Molecular microbiology*, 102(4), pp. 642-671.

DE NADAL, E., ALEPUZ, P. and POSAS, F., 2002. Dealing with osmostress through MAP kinase activation. *EMBO reports*, 3(8), pp. 735-740.

DE NADAL, E. and POSAS, F., 2010. Multilayered control of gene expression by stress-activated protein kinases. *Embo Journal*, 29(1), pp. 4-13.

DEPHOURE, N., GOULD, K.L., GYGI, S.P. and KELLOGG, D.R., 2013. Mapping and analysis of phosphorylation sites: a quick guide for cell biologists. *Molecular biology of the cell*, 24(5), pp. 535-542.

DHILLON, A.S., HAGAN, S., RATH, O. and KOLCH, W., 2007. MAP kinase signalling pathways in cancer. *Oncogene*, 26(22), pp. 3279-3290.

DI, Y., HOLMES, E.J., BUTT, A., DAWSON, K., MIRONOV, A., KOTIADIS, V.N., GOURLAY, C.W., JONES, N. and WILKINSON, C.R.M., 2012. H₂O₂ stress-specific regulation of *S. pombe* MAPK Sty1 by mitochondrial protein phosphatase Ptc4. *Embo Journal*, 31(3), pp. 563-575.

DIAZ-RUIZ, R., RIGOLET, M. and DEVIN, A., 2011. The Warburg and Crabtree effects: On the origin of cancer cell energy metabolism and of yeast glucose repression. *Biochimica Et Biophysica Acta-Bioenergetics*, 1807(6), pp. 568-576.

DOWNWARD, J., 2003. Targeting ras signalling pathways in cancer therapy. *Nature Reviews Cancer*, 3(1), pp. 11-22.

ESECHIE, A. and DU, G., 2009. Increased lipogenesis in cancer. *Communicative & Integrative Biology*, 2(6), pp. 545-548.

ETTINGER, A. and WITTMANN, T., 2014. Fluorescence live cell imaging. *Quantitative Imaging in Cell Biology*, 123, pp. 77-94.

FAUBERT, B., BOILY, G., IZREIG, S., GRISS, T., SAMBORSKA, B., DONG, Z., DUPUY, F., CHAMBERS, C., FUERTH, B.J., VIOLLET, B., MAMER, O.A., AVIZONIS, D., DEBERARDINIS, R.J., SIEGEL, P.M. and JONES, R.G., 2013. AMPK Is a Negative Regulator of the Warburg Effect and Suppresses Tumor Growth In Vivo. *Cell Metabolism*, 17(1), pp. 113-124.

FERRIGNO, P., POSAS, F., KOEPP, D., SAITO, H. and SILVER, P., 1998. Regulated nucleo/cytoplasmic exchange of HOG1 MAPK requires the importin beta homologs NMD5 and XPO1. *Embo Journal*, 17(19), pp. 5606-5614.

GASPAR, M.L., AREGULLIN, M.A., JESCH, S.A. and HENRY, S.A., 2006. Inositol induces a profound alteration in the pattern and rate of synthesis and turnover of membrane lipids in *Saccharomyces cerevisiae*. *Journal of Biological Chemistry*, 281(32), pp. 22773-22785.

GASPAR, M.L., HOFBAUER, H.F., KOHLWEIN, S.D. and HENRY, S.A., 2011. Coordination of Storage Lipid Synthesis and Membrane Biogenesis EVIDENCE FOR CROSS-TALK BETWEEN TRIACYLGLYCEROL METABOLISM AND PHOSPHATIDYLINOSITOL SYNTHESIS. *Journal of Biological Chemistry*, 286(3), pp. 1696-1708.

GHAEMMAGHAMI, S., HUH, W., BOWER, K., HOWSON, R., BELLE, A., DEPHOURE, N., O'SHEA, E. and WEISSMAN, J., 2003. Global analysis of protein expression in yeast. *Nature*, 425(6959), pp. 737-741.

GOODWIN, P., 1999. GFP biofluorescence: Imaging gene expression and protein dynamics in living cells - Design considerations for a fluorescence imaging laboratory. *Methods in Cell Biology*, Vol 58, 58, pp. 343-+.

GRIMARD, V., MASSIER, J., RICHTER, D., SCHWUDKE, D., KALAIIDZIDIS, Y., FAVA, E., HERMETTER, A. and THIELE, C., 2008. siRNA screening reveals JNK2 as an evolutionary conserved regulator of triglyceride homeostasis. *Journal of lipid research*, 49(11), pp. 2427-2440.

GUIJAS, C., PÉREZ-CHACÓN, G., ASTUDILLO, A.M., RUBIO, J.M., GIL-DE-GÓMEZ, L., BALBOA, M.A. and BALSINDE, J., 2012. Simultaneous activation of p38 and JNK by arachidonic acid stimulates the cytosolic phospholipase A(2)-dependent synthesis of lipid droplets in human monocytes. *Journal of lipid research*, 53(11), pp. 2343-2354.

HABER, J.E., BRABERG, H., WU, Q., ALEXANDER, R., HAASE, J., RYAN, C., LIPKIN-MOORE, Z., FRANKS-SKIBA, K.E., JOHNSON, T., SHALES, M., LENSTRA, T.L., HOLSTEGE, F.C.P., JOHNSON, J.R., BLOOM, K. and KROGAN, N.J., 2013. Systematic Triple-Mutant Analysis Uncovers Functional Connectivity between Pathways Involved in Chromosome Regulation. *Cell Reports*, 3(6), pp. 2168-2178.

HAM, H.J., RHO, H.J., SHIN, S.K. and YOON, H., 2010. The TGL2 Gene of *Saccharomyces cerevisiae* Encodes an Active Acylglycerol Lipase Located in the Mitochondria. *Journal of Biological Chemistry*, 285(5), pp. 3005.

HAMZA, A., TAMMPERE, E., KOFOED, M., KEONG, C., CHIANG, J., GIAEVER, G., NISLOW, C. and HIETER, P., 2015. Complementation of Yeast Genes with Human Genes as an Experimental Platform for Functional Testing of Human Genetic Variants. *Genetics*, 201(3), pp. 1263-U860.

HAN, G., GABLE, K., KOHLWEIN, S., BEAUDOIN, F., NAPIER, J. and DUNN, T., 2002. The *Saccharomyces cerevisiae* YBR159w gene encodes the 3-ketoreductase of the microsomal fatty acid elongase. *Journal of Biological Chemistry*, 277(38), pp. 35440-35449.

HANAHAH, D. and WEINBERG, R.A., 2011. Hallmarks of Cancer: The Next Generation. *Cell*, 144(5), pp. 646-674.

HANKS, S. and HUNTER, T., 1995. Protein Kinases .6. the Eukaryotic Protein-Kinase Superfamily - Kinase (Catalytic) Domain-Structure and Classification. *Faseb Journal*, 9(8), pp. 576-596.

HARAGUCHI, T., KOUJIN, T. and HIRAOKA, Y., 2000. Application of GFP: Time-lapse multi-wavelength fluorescence imaging of living mammalian cells. *Acta Histochemica et Cytochemica*, 33(3), pp. 169-175.

HASAN, R., LEROY, C., ISNARD, A., LABARRE, J., BOY-MARCOTTE, E. and TOLEDANO, M., 2002. The control of the yeast H₂O₂ response by the Msn2/4 transcription factors. *Molecular microbiology*, 45(1), pp. 233-241.

HAWLEY, S., DAVISON, M., WOODS, A., DAVIES, S., BERI, R., CARLING, D. and HARDIE, D., 1996. Characterization of the AMP-activated protein kinase kinase from rat liver and identification of threonine 172 as the major site at which it phosphorylates AMP-activated protein kinase. *Journal of Biological Chemistry*, 271(44), pp. 27879-27887.

HAY, N. and SONENBERG, N., 2004. Upstream and downstream of mTOR. *Genes & development*, 18(16), pp. 1926-1945.

HECKMAN, K.L. and PEASE, L.R., 2007. Gene splicing and mutagenesis by PCR-driven overlap extension. *Nature Protocols*, 2(4), pp. 924-932.

HEIDEN, M.G.V., CANTLEY, L.C. and THOMPSON, C.B., 2009. Understanding the Warburg Effect: The Metabolic Requirements of Cell Proliferation. *Science*, 324(5930), pp. 1029-1033.

HENRY, S. and HALVORSON, H., 1973. Lipid-Synthesis during Sporulation of *Saccharomyces-Cerevisiae*. *Journal of Bacteriology*, 114(3), pp. 1158-1163.

HENRY, S.A., GASPAR, M.L. and JESCH, S.A., 2014. The response to inositol: Regulation of glycerolipid metabolism and stress response signaling in yeast. *Chemistry and physics of lipids*, 180, pp. 23-43.

HENRY, S.A., KOHLWEIN, S.D. and CARMAN, G.M., 2012. Metabolism and Regulation of Glycerolipids in the Yeast *Saccharomyces cerevisiae*. *Genetics*, 190(2), pp. 317-349.

HENRY, T.C., POWER, J.E., KERWIN, C.L., MOHAMMED, A., WEISSMAN, J.S., CAMERON, D.M. and WYKOFF, D.D., 2011. Systematic Screen of *Schizosaccharomyces pombe* Deletion Collection Uncovers Parallel Evolution of the Phosphate Signal Transduction Pathway in Yeasts. *Eukaryotic Cell*, 10(2), pp. 198-206.

HO, Y., GRUHLER, A., HEILBUT, A., BADER, G., MOORE, L., ADAMS, S., MILLAR, A., TAYLOR, P., BENNETT, K., BOUTILIER, K., YANG, L., WOLTING, C., DONALDSON, I., SCHANDORFF, S., SHEWNARANE, J., VO, M., TAGGART, J., GOUDREAU, M., MUSKAT, B., ALFARANO, C., DEWAR, D., LIN, Z., MICHALICKOVA, K., WILLEMS, A., SASSI, H., NIELSEN, P., RASMUSSEN, K., ANDERSEN, J., JOHANSEN, L., HANSEN, L., JESPERSEN, H., PODTELEJNIKOV, A., NIELSEN, E., CRAWFORD, J., POULSEN, V., SORENSEN, B., MATTHIESEN, J., HENDRICKSON, R., GLEESON, F., PAWSON, T., MORAN, M., DUROCHER, D., MANN, M., HOGUE, C., FIGEYS, D. and TYERS, M., 2002. Systematic identification of protein complexes in *Saccharomyces cerevisiae* by mass spectrometry. *Nature*, 415(6868), pp. 180-183.

HOHMANN, S., 2002. Osmotic stress signaling and osmoadaptation in Yeasts. *Microbiology and Molecular Biology Reviews*, 66(2), pp. 300-+.

HSU, P.P., KANG, S.A., RAMESEDER, J., ZHANG, Y., OTTINA, K.A., LIM, D., PETERSON, T.R., CHOI, Y., GRAY, N.S., YAFFE, M.B., MARTO, J.A. and SABATINI, D.M., 2011. The mTOR-Regulated Phosphoproteome Reveals a Mechanism of mTORC1-Mediated Inhibition of Growth Factor Signaling. *Science*, 332(6035), pp. 1317-1322.

HU, Z., KILLION, P.J. and IYER, V.R., 2007. Genetic reconstruction of a functional transcriptional regulatory network. *Nature genetics*, 39(5), pp. 683-687.

HUBER, A., FRENCH, S.L., TEKOTTE, H., YERLIKAYA, S., STAHL, M., PEREPELKINA, M.P., TYERS, M., ROUGEMONT, J., BEYER, A.L. and LOEWITH, R., 2011. Sch9 regulates ribosome biogenesis via Stb3, Dot6 and Tod6 and the histone deacetylase complex RPD3L. *Embo Journal*, 30(15), pp. 3052-3064.

HUH, W., FALVO, J., GERKE, L., CARROLL, A., HOWSON, R., WEISSMAN, J. and O'SHEA, E., 2003. Global analysis of protein localization in budding yeast. *Nature*, 425(6959), pp. 686-691.

HUKKELHOVEN, E., LIU, Y., YEH, N., CIZNADIJA, D., BLAIN, S.W. and KOFF, A., 2012. Tyrosine Phosphorylation of the p21 Cyclin-dependent Kinase Inhibitor Facilitates the Development of Proneural Glioma. *Journal of Biological Chemistry*, 287(46), pp. 38523-38530.

HURLEY, R.L., BARRE, L.K., WOOD, S.D., ANDERSON, K.A., KEMP, B.E., MEANS, A.R. and WITTERS, L.A., 2006. Regulation of AMP-activated protein kinase by multisite phosphorylation in response to agents that elevate cellular cAMP. *Journal of Biological Chemistry*, 281(48), pp. 36662-36672.

IMAMURA, S., KAWASE, Y., KOBAYASHI, I., SHIMOJIMA, M., OHTA, H. and TANAKA, K., 2016. TOR (target of rapamycin) is a key regulator of triacylglycerol accumulation in microalgae. *Plant Signaling & Behavior*, 11(3), pp. e1149285.

JANKE, C., MAGIERA, M., RATHFELDER, N., TAXIS, C., REBER, S., MAEKAWA, H., MORENO-BORCHART, A., DOENGES, G., SCHWOB, E., SCHIEBEL, E. and KNOP, M., 2004. A versatile toolbox for PCR-based tagging of yeast genes: new fluorescent proteins, more markers and promoter substitution cassettes. *Yeast*, 21(11), pp. 947-962.

JEON, T. and OSBORNE, T.F., 2012. SREBPs: metabolic integrators in physiology and metabolism. *Trends in Endocrinology and Metabolism*, 23(2), pp. 65-72.

KAMISAKA, Y., KIMURA, K., UEMURA, H. and YAMAOKA, M., 2013. Overexpression of the active diacylglycerol acyltransferase variant transforms *Saccharomyces cerevisiae* into an oleaginous yeast. *Applied Microbiology and Biotechnology*, 97(16), pp. 7345-7355.

KAMISAKA, Y., TOMITA, N., KIMURA, K., KAINOU, K. and UEMURA, H., 2007. DGA1(diacylglycerol acyltransferase gene) overexpression and leucine biosynthesis significantly increase lipid accumulation in the Delta *snf2* disruptant of *Saccharomyces cerevisiae*. *Biochemical Journal*, 408, pp. 61-68.

KAPTEYN, J., TER RIET, B., VINK, E., BLAD, S., DE NOBEL, H., VAN DEN ENDE, H. and KLIS, F., 2001. Low external pH induces HOG1-dependent changes in the organization of the *Saccharomyces cerevisiae* cell wall. *Molecular microbiology*, 39(2), pp. 469-479.

KEILHAUER, E.C., HEIN, M.Y. and MANN, M., 2015. Accurate Protein Complex Retrieval by Affinity Enrichment Mass Spectrometry (AE-MS) Rather than Affinity Purification Mass Spectrometry (AP-MS). *Molecular & Cellular Proteomics*, 14(1), pp. 120-135.

KINOSHITA, E. and KINOSHITA-KIKUTA, E., 2011. Improved Phos-tag SDS-PAGE under neutral pH conditions for advanced protein phosphorylation profiling. *Proteomics*, 11(2), pp. 319-323.

KINOSHITA, E., KINOSHITA-KIKUTA, E., KARATA, K., KAWANO, T., NISHIYAMA, A., YAMATO, M. and KOIKE, T., 2017. Specific glutamic acid residues in targeted proteins induce exaggerated retardations in Phos-tag SDS-PAGE migration. *Electrophoresis*, 38(8), pp. 1139-1146.

KINOSHITA, E., KINOSHITA-KIKUTA, E. and KOIKE, T., 2009. Phosphate-Affinity Gel Electrophoresis Using a Phos-Tag Molecule for Phosphoproteome Study. *Current Proteomics*, 6(2), pp. 104-121.

KOCH, B., SCHMIDT, C. and DAUM, G., 2014. Storage lipids of yeasts: a survey of nonpolar lipid metabolism in *Saccharomyces cerevisiae*, *Pichia pastoris*, and *Yarrowia lipolytica*. *FEMS microbiology reviews*, 38(5), pp. 892-915.

KOLOUCHOVA, I., MAT'ATKOVA, O., SIGLER, K., MASAK, J. and REZANKA, T., 2016. Lipid accumulation by oleaginous and non-oleaginous yeast strains in nitrogen and phosphate limitation. *Folia microbiologica*, 61(5), pp. 431-438.

KREBS, E. and BEAVO, J., 1979. Phosphorylation-Dephosphorylation of Enzymes. Annual Review of Biochemistry, 48, pp. 923-959.

KRYCER, J.R., SHARPE, L.J., LUU, W. and BROWN, A.J., 2010. The Akt-SREBP nexus: cell signaling meets lipid metabolism. Trends in Endocrinology and Metabolism, 21(5), pp. 268-276.

LAPLANTE, M. and SABATINI, D.M., 2012. mTOR Signaling in Growth Control and Disease. Cell, 149(2), pp. 274-293.

LAPLANTE, M. and SABATINI, D.M., 2009a. An Emerging Role of mTOR in Lipid Biosynthesis. Current Biology, 19(22), pp. R1046-R1052.

LAPLANTE, M. and SABATINI, D.M., 2009b. mTOR signaling at a glance. Journal of cell science, 122(20), pp. 3589-3594.

LAWRENCE, C.L., MAEKAWA, H., WORTHINGTON, J.L., REITER, W., WILKINSON, C.R. and JONES, N., 2007. Regulation of Schizosaccharomyces pombe Atf1 protein levels by Sty1-mediated phosphorylation and heterodimerization with Pcr1. The Journal of biological chemistry, 282(8), pp. 5160-5170.

LAWRENCE, C., BOTTING, C., ANTROBUS, R. and COOTE, P., 2004. Evidence of a new role for the high-osmolarity glycerol mitogen-activated protein kinase pathway in yeast: Regulating adaptation to citric acid stress. Molecular and cellular biology, 24(8), pp. 3307-3323.

LEELAHAVANICHKUL, K., AMORNPHIMOLTHAM, P., MOLINOLO, A.A., BASILE, J.R., KOONTONGKAEW, S. and GUTKIND, J.S., 2014. A role for p38 MAPK in head

and neck cancer cell growth and tumor-induced angiogenesis and lymphangiogenesis. *Molecular Oncology*, 8(1), pp. 105-118.

LEMPIAEINEN, H., UOTILA, A., URBAN, J., DOHNAL, I., AMMERER, G., LOEWITH, R. and SHORE, D., 2009. Sfp1 Interaction with TORC1 and Mrs6 Reveals Feedback Regulation on TOR Signaling. *Molecular cell*, 33(6), pp. 704-716.

LIANG, G., YANG, J., HORTON, J., HAMMER, R., GOLDSTEIN, J. and BROWN, M., 2002. Diminished hepatic response to fasting/refeeding and liver X receptor agonists in mice with selective deficiency of sterol regulatory element-binding protein-1c. *Journal of Biological Chemistry*, 277(11), pp. 9520-9528.

LIANG, J. and MILLS, G.B., 2013. AMPK: A Contextual Oncogene or Tumor Suppressor? *Cancer research*, 73(10), pp. 2929-2935.

LIBERTI, M.V. and LOCASALE, J.W., 2016. The Warburg Effect: How Does it Benefit Cancer Cells? *Trends in biochemical sciences*, 41(3), pp. 211-218.

LINK, A., ENG, J., SCHIELTZ, D., CARMACK, E., MIZE, G., MORRIS, D., GARVIK, B. and YATES, J., 1999. Direct analysis of protein complexes using mass spectrometry. *Nature biotechnology*, 17(7), pp. 676-682.

LIU, Q., SILOTO, R.M.P., SNYDER, C.L. and WESELAKE, R.J., 2011. Functional and Topological Analysis of Yeast Acyl-CoA:Diacylglycerol Acyltransferase 2, an Endoplasmic Reticulum Enzyme Essential for Triacylglycerol Biosynthesis. *Journal of Biological Chemistry*, 286(15), pp. 13115-13126.

LIU, Q., LUO, Q., HALIM, A. and SONG, G., 2017. Targeting lipid metabolism of cancer cells: A promising therapeutic strategy for cancer. *Cancer letters*, 401, pp. 39-45.

LIU, Y., LIU, N., WU, D., BI, Q. and MENG, S., 2015. The longevity of tor1 Delta, sch9 Delta, and ras2 Delta mutants depends on actin dynamics in *Saccharomyces cerevisiae*. *Cell and Bioscience*, 5, pp. 18.

LOEWEN, C., GASPAR, M., JESCH, S., DELON, C., KTISTAKIS, N., HENRY, S. and LEVINE, T., 2004. Phospholipid metabolism regulated by a transcription factor sensing phosphatidic acid. *Science*, 304(5677), pp. 1644-1647.

LOEWITH, R., 2011. A brief history of TOR. *Biochemical Society transactions*, 39, pp. 437-442.

LOEWITH, R. and HALL, M.N., 2011. Target of Rapamycin (TOR) in Nutrient Signaling and Growth Control. *Genetics*, 189(4), pp. 1177-1201.

LOMAKIN, I.B., XIONG, Y. and STEITZ, T.A., 2007. The crystal structure of yeast fatty acid synthase, a cellular machine with eight active sites working together. *Cell*, 129(2), pp. 319-332.

LONGONI, P., DOUCHI, D., CARITI, F., FUCILE, G. and GOLDSCHMIDT-CLERMONT, M., 2015. Phosphorylation of the Light-Harvesting Complex II Isoform Lhcb2 Is Central to State Transitions. *Plant Physiology*, 169(4), pp. 2874-2883.

LOOKE, M., KRISTJUHAN, K. and KRISTJUHAN, A., 2011. Extraction of genomic DNA from yeasts for PCR-based applications. *BioTechniques*, 50(5), pp. 325-+.

MAAYAN, I., BEENSTOCK, J., MARBACH, I., TABACHNICK, S., LIVNAH, O., ENGELBERG, D. and GALLYAS, F., 2012. Osmostress Induces Autophosphorylation of Hog1 via a C-Terminal Regulatory Region That Is Conserved in p38 α . PLoS ONE, 7(9), pp. 1-12.

MADEIRA, J.B., MASUDA, C.A., MAYA-MONTEIRO, C.M., MATOS, G.S., MONTERO-LOMELI, M. and BOZAQUEL-MORAIS, B.L., 2015. TORC1 Inhibition Induces Lipid Droplet Replenishment in Yeast. *Molecular and cellular biology*, 35(4), pp. 737-746.

MAGER, W. and WINDERICKX, J., 2005. Yeast as a model for medical and medicinal research. *Trends in pharmacological sciences*, 26(5), pp. 265-273.

M., RODRIGUEZ-PENA, J., GARCIA, R., NOMBELA, C. and ARROYO, J., 2010. The high-osmolarity glycerol (HOG) and cell wall integrity (CWI) signalling pathways interplay: a yeast dialogue between MAPK routes. *Yeast*, 27(8), pp. 495-502.

MAO, K., WANG, K., ZHAO, M., XU, T. and KLIONSKY, D.J., 2011. Two MAPK-signaling pathways are required for mitophagy in *Saccharomyces cerevisiae*. *Journal of Cell Biology*, 193(4), pp. 755-767.

MAO, L., YUAN, L., SLAKEY, L.M., JONES, F.E., BUROW, M.E. and HILL, S.M., 2010. Inhibition of breast cancer cell invasion by melatonin is mediated through regulation of the p38 mitogen-activated protein kinase signaling pathway. *Breast Cancer Research*, 12(6), pp. R107.

MARCHLER, G., SCHULLER, C., ADAM, G. and RUIS, H., 1993. A *Saccharomyces Cerevisiae* Uas Element Controlled by Protein Kinase-a Activates Transcription in Response to a Variety of Stress Conditions. *Embo Journal*, 12(5), pp. 1997-2003.

MARKHAM, P., ROBSON, G., BAINBRIDGE, B. and TRINCI, A., 1993. Choline - its Role in the Growth of Filamentous Fungi and the Regulation of Mycelial Morphology. *FEMS microbiology letters*, 104(3-4), pp. 287-300.

MARQUES, J.M., RODRIGUES, R.J., DE MAGALHAES-SANT'ANA, A.C. and GONCALVES, T., 2006. *Saccharomyces cerevisiae* Hog1 protein phosphorylation upon exposure to bacterial endotoxin. *Journal of Biological Chemistry*, 281(34), pp. 24687-24694.

MARSHALL, C.J., 1994. MAP kinase kinase kinase, MAP kinase kinase and MAP kinase. *Current opinion in genetics & development*, 4(1), pp. 82-89.

MARTIN, S. and PARTON, R., 2006. Lipid droplets: a unified view of a dynamic organelle. *Nature Reviews Molecular Cell Biology*, 7(5), pp. 373-378.

MARTINEZ-PASTOR, M., MARCHLER, G., SCHULLER, C., MARCHLERBAUER, A., RUIS, H. and ESTRUCH, F., 1996. The *Saccharomyces cerevisiae* zinc finger proteins Msn2p and Msn4p are required for transcriptional induction through the stress-response element (STRE). *Embo Journal*, 15(9), pp. 2227-2235.

MARTINEZ, V., LAURITSEN, I., HOBEL, T., LI, S., NIELSEN, A.T. and NORHOLM, M.H.H., 2017. CRISPR/Cas9-based genome editing for simultaneous interference with gene expression and protein stability. *Nucleic acids research*, 45(20), pp. e171.

MASUI, K., CLOUGHESY, T.F. and MISCHEL, P.S., 2012. Molecular pathology in adult high-grade gliomas: from molecular diagnostics to target therapies. *Neuropathology and applied neurobiology*, 38(3), pp. 271-291.

MCCUBREY, J.A., STEELMAN, L.S., CHAPPELL, W.H., ABRAMS, S.L., WONG, E.W.T., CHANG, F., LEHMANN, B., TERRIAN, D.M., MILELLA, M., TAFURI, A., STIVALA, F., LIBRA, M., BASECKE, J., EVANGELISTI, C., MARTELLI, A.M. and FRANKLIN, R.A., 2006. ROLES OF THE RAF/MEK/ERK PATHWAY IN CELL GROWTH, MALIGNANT TRANSFORMATION AND DRUG RESISTANCE. *Biochimica et biophysica acta*, 1773(8), pp. 1263-1284.

MEI, S., GU, H., WARD, A., YANG, X., GUO, H., HE, K., LIU, Z. and CAO, W., 2012. p38 Mitogen-activated Protein Kinase (MAPK) Promotes Cholesterol Ester Accumulation in Macrophages through Inhibition of Macroautophagy. *Journal of Biological Chemistry*, 287(15), pp. 11761-11768.

MENENDEZ, J.A. and LUPU, R., 2007. Fatty acid synthase and the lipogenic phenotype in cancer pathogenesis. *Nature Reviews Cancer*, 7(10), pp. 763-777.

MORA, G., SCHARNEWSKI, M. and FULDA, M., 2012. Neutral Lipid Metabolism Influences Phospholipid Synthesis and Deacylation in *Saccharomyces cerevisiae*. *Plos One*, 7(11), pp. e49269.

MOUNIER, C., BOURAOUI, L. and RASSART, E., 2014. Lipogenesis in cancer progression (Review). *International journal of oncology*, 45(2), pp. 485-492.

MUDGE, D.K., YANG, F., CURRIE, B.M., KIM, J.M., YEDA, K., BASHYAKARLA, V.K., IVEY, F.D. and HOFFMAN, C.S., 2014. Sck1 Negatively Regulates Gpa2-Mediated Glucose Signaling in *Schizosaccharomyces pombe*. *Eukaryotic Cell*, 13(2), pp. 202-208.

MULLEN, P.J., YU, R., LONGO, J., ARCHER, M.C. and PENN, L.Z., 2016. The interplay between cell signalling and the mevalonate pathway in cancer. *Nat Rev Cancer*, 16(11), pp. 718-731.

NAGLE, S.C., 1969. Improved growth of mammalian and insect cells in media containing increased levels of choline. *Applied Microbiology*, 17(2), pp. 318-319.

NAKASHIMA, A., OTSUBO, Y., YAMASHITA, A., SATO, T., YAMAMOTO, M. and TAMANOI, F., 2012. Psk1, an AGC kinase family member in fission yeast, is directly phosphorylated and controlled by TORC1 and functions as S6 kinase. *Journal of cell science*, 125(23), pp. 5840-5849.

NATTER, K. and KOHLWEIN, S.D., 2013. Yeast and cancer cells - common principles in lipid metabolism. *Biochimica Et Biophysica Acta-Molecular and Cell Biology of Lipids*, 1831(2), pp. 314-326.

NIELSEN, J., 2009. Systems biology of lipid metabolism: From yeast to human. *FEBS letters*, 583(24), pp. 3905-3913.

NUNEZ, L.R., JESCH, S.A., GASPAR, M.L., ALMAGUER, C., VILLA-GARCIA, M., RUIZ-NORIEGA, M., PATTON-VOGT, J. and HENRY, S.A., 2008. Cell Wall Integrity MAPK Pathway Is Essential for Lipid Homeostasis. *Journal of Biological Chemistry*, 283(49), pp. 34204-34217.

OELKERS, P., CROMLEY, D., PADAMSEE, M., BILLHEIMER, J. and STURLEY, S., 2002. The DGA1 gene determines a second triglyceride synthetic pathway in yeast. *Journal of Biological Chemistry*, 277(11), pp. 8877-8881.

OH, H. and IRVINE, K.D., 2008. In vivo regulation of Yorkie phosphorylation and localization. *Development*, 135(6), pp. 1081-1088.

O'ROURKE, S., HERSKOWITZ, I. and O'SHEA, E., 2002. Yeast go the whole HOG for the hyperosmotic response. *Trends in Genetics*, 18(8), pp. 405-412.

PASCUAL-AHUIR, A. and PROFT, M., 2007. The Sch9 kinase is a chromatin-associated transcriptional activator of osmostress-responsive genes. *Embo Journal*, 26(13), pp. 3098-3108.

PASCUAL-AHUIR, A., STRUHL, K. and PROFT, M., 2006. Genome-wide location analysis of the stress-activated MAP kinase Hog1 in yeast. *Methods*, 40(3), pp. 272-278.

PLOEGH, H.L., 2007. A lipid-based model for the creation of an escape hatch from the endoplasmic reticulum. *Nature*, 448(7152), pp. 435-438.

PONCHEL, F., TOOMES, C., BRANSFIELD, K., LEONG, F., DOUGLAS, S., FIELD, S., BELL, S., COMBARET, V., PUISIEUX, A., MIGHELL, A., ROBINSON, P., INGLEHEARN, C., ISAACS, J. and MARKHAM, A., 2003. Real-time PCR based on SYBR-Green I fluorescence: An alternative to the TaqMan assay for a relative quantification of gene rearrangements, gene amplifications and micro gene deletions. *Bmc Biotechnology*, 3, pp. 18.

PORSTMANN, T., SANTOS, C.R., GRIFFITHS, B., CULLY, M., WU, M., LEEVERS, S., GRIFFITHS, J.R., CHUNG, Y. and SCHULZE, A., 2008. SREBP activity is regulated by mTORC1 and contributes to Akt-dependent cell growth. *Cell Metabolism*, 8(3), pp. 224-236.

QI, M. and ELION, E., 2005. MAP kinase pathways. *Journal of cell science*, 118(16), pp. 3569-3572.

RAJVANSHI, P.K., ARYA, M. and RAJASEKHARAN, R., 2017. The stress-regulatory transcription factors Msn2 and Msn4 regulate fatty acid oxidation in budding yeast. *The Journal of biological chemistry*, .

REINKE, A., ANDERSON, S., MCCAFFERY, J., YATES, J., ARONOVA, S., CHU, S., FAIRCLOUGH, S., IVERSON, C., WEDAMAN, K. and POWERS, T., 2004. TOR complex 1 includes a novel component, Tco89p (YPL180w), and cooperates with Ssd1p to maintain cellular integrity in *Saccharomyces cerevisiae*. *Journal of Biological Chemistry*, 279(15), pp. 14752-14762.

RODKAER, S.V. and FAERGEMAN, N.J., 2014. Glucose- and nitrogen sensing and regulatory mechanisms in *Saccharomyces cerevisiae*. *Fems Yeast Research*, 14(5), pp. 683-696.

RODRIGUES-POUSADA, C., NEVITT, T., MENEZES, R., AZEVEDO, D., PEREIRA, J. and AMARAL, C., 2004. Yeast activator proteins and stress response: an overview. *FEBS letters*, 567(1), pp. 80-85.

ROGUEV, A., BANDYOPADHYAY, S., ZOFALL, M., ZHANG, K., FISCHER, T., COLLINS, S.R., QU, H., SHALES, M., PARK, H., HAYLES, J., HOE, K., KIM, D., IDEKER, T., GREWAL, S.I., WEISSMAN, J.S. and KROGAN, N.J., 2008. Conservation and rewiring of functional modules revealed by an epistasis map in fission yeast. *Science*, 322(5900), pp. 405-410.

ROGUEV, A., WIREN, M., WEISSMAN, J.S. and KROGAN, N.J., 2007. High-throughput genetic interaction mapping in the fission yeast *Schizosaccharomyces pombe*. *Nature Methods*, 4(10), pp. 861-866.

ROSKOSKI, R., JR., 2012. ERK1/2 MAP kinases: Structure, function, and regulation. *Pharmacological Research*, 66(2), pp. 105-143.

ROSSLER, H., RIECK, C., DELONG, T., HOJA, U. and SCHWEIZER, E., 2003. Functional differentiation and selective inactivation of multiple *Saccharomyces cerevisiae* genes involved in very-long-chain fatty acid synthesis. *Molecular Genetics and Genomics*, 269(2), pp. 290-298.

ROSTRON, K.A., 2015. Utilising Yeast as a Model Organism to Deconstruct the Regulation of Tumour Associated Lipogenesis. PhD thesis(University of Central Lancashire), pp. Available at <http://clock.uclan.ac.uk/12710/>.

ROSTRON, K.A., ROLPH, C.E. and LAWRENCE, C.L., 2015. Nile red fluorescence screening facilitating neutral lipid phenotype determination in budding yeast, *Saccharomyces cerevisiae*, and the fission yeast *Schizosaccharomyces pombe*. *Antonie Van Leeuwenhoek International Journal of General and Molecular Microbiology*, 108(1), pp. 97-106.

ROUX, P. and BLENIS, J., 2004. ERK and p38 MAPK-activated protein kinases: a family of protein kinases with diverse biological functions. *Microbiology and Molecular Biology Reviews*, 68(2), pp. 320-+.

RYAN, C.J., ROGUEV, A., PATRICK, K., XU, J., JAHARI, H., TONG, Z., BELTRAO, P., SHALES, M., QU, H., COLLINS, S.R., KLIEGMAN, J.I., JIANG, L., KUO, D., TOSTI, E., KIM, H., EDELMANN, W., KEOGH, M., GREENE, D., TANG, C., CUNNINGHAM,

P., SHOKAT, K.M., CAGNEY, G., SVENSSON, J.P., GUTHRIE, C., ESPENSHADE, P.J., IDEKER, T. and KROGAN, N.J., 2012. Hierarchical Modularity and the Evolution of Genetic Interactomes across Species. *Molecular cell*, 46(5), pp. 691-704.

SAITO, H. and POSAS, F., 2012. Response to Hyperosmotic Stress. *Genetics*, 192(2), pp. 289-318.

SCHMIDT, C., ATHENSTAEDT, K., KOCH, B., PLOIER, B. and DAUM, G., 2013. Regulation of the Yeast Triacylglycerol Lipase Tgl3p by Formation of Nonpolar Lipids. *Journal of Biological Chemistry*, 288(27), pp. 19939-19948.

SEVER, R. and BRUGGE, J.S., 2015. Signal Transduction in Cancer. *Cold Spring Harbor Perspectives in Medicine*, 5(4), pp. a006098.

SHARIFPOOR, S., VAN DYK, D., COSTANZO, M., BARYSHNIKOVA, A., FRIESEN, H., DOUGLAS, A.C., YOUN, J., VANDERSLUIJ, B., MYERS, C.L., BALAZS PAPP, BOONE, C. and ANDREWS, B.J., 2012. Functional wiring of the yeast kinome revealed by global analysis of genetic network motifs. *Genome research*, 22(4), pp. 791-801.

SHAUL, Y.D. and SEGER, R., 2007. The MEK/ERK cascade: From signaling specificity to diverse functions. *Biochimica Et Biophysica Acta-Molecular Cell Research*, 1773(8), pp. 1213-1226.

SHIAO, Y., 2003. A new reverse transcription-polymerase chain reaction method for accurate quantification. *Bmc Biotechnology*, 3, pp. 22.

SIEPEL, A., BEJERANO, G., PEDERSEN, J., HINRICHS, A., HOU, M., ROSENBLOOM, K., CLAWSON, H., SPIETH, J., HILLIER, L., RICHARDS, S.,

WEINSTOCK, G., WILSON, R., GIBBS, R., KENT, W., MILLER, W. and HAUSSLER, D., 2005. Evolutionarily conserved elements in vertebrate, insect, worm, and yeast genomes. *Genome research*, 15(8), pp. 1034-1050.

SIKORSKI, R. and HIETER, P., 1989. A System of Shuttle Vectors and Yeast Host Strains Designed for Efficient Manipulation of Dna in *Saccharomyces-Cerevisiae*. *Genetics*, 122(1), pp. 19-27.

SMITH, D., NICHOLLS, S., MORGAN, B., BROWN, A. and QUINN, J., 2004. A conserved stress-activated protein kinase regulates a core stress response in the human pathogen *Candida albicans*. *Molecular biology of the cell*, 15(9), pp. 4179-4190.

SMITH, D., TOONE, W., CHEN, D., BAHLER, J., JONES, N., MORGAN, B. and QUINN, J., 2002. The *Srk1* protein kinase is a target for the *Sty1* stress-activated MAPK in fission yeast. *Journal of Biological Chemistry*, 277(36), pp. 33411-33421.

SORGER, D. and DAUM, G., 2002. Synthesis of triacylglycerols by the acyl-coenzyme A: Diacyl-glycerol acyltransferase *Dga1p* in lipid particles of the yeast *Saccharomyces cerevisiae*. *Journal of Bacteriology*, 184(2), pp. 519-524.

SOULARD, A., CREMONESI, A., MOES, S., SCHUETZ, F., JENOE, P. and HALL, M.N., 2010. The Rapamycin-sensitive Phosphoproteome Reveals That TOR Controls Protein Kinase A Toward Some But Not All Substrates. *Molecular biology of the cell*, 21(19), pp. 3475-3486.

SG. DANN, G. THOMAS, 2006. The amino acid sensitive TOR pathway from yeast to mammals. *FEBS Letters*, 580(12), pp. 2821-2829.

SUN, H., ZHU, X., LU, P.Y., ROSATO, R.R., TAN, W. and ZU, Y., 2014.

Oligonucleotide Aptamers: New Tools for Targeted Cancer Therapy. *Molecular Therapy-Nucleic Acids*, 3, pp. e182.

TORRES, J., DI COMO, C., HERRERO, E. and DE LA TORRE-RUIZ, M., 2002.

Regulation of the cell integrity pathway by rapamycin-sensitive TOR function in budding yeast. *Journal of Biological Chemistry*, 277(45), pp. 43495-43504.

TU, Q., YIN, J., FU, J., HERRMANN, J., LI, Y., YIN, Y., STEWART, A.F., MUELLER, R. and ZHANG, Y., 2016. Room temperature electrocompetent bacterial cells improve DNA transformation and recombineering efficiency. *Scientific Reports*, 6, pp. 24648.

URBAN, J., SOULARD, A., HUBER, A., LIPPMAN, S., MUKHOPADHYAY, D., DELOCHE, O., WANKE, V., ANRATHER, D., AMMERER, G., RIEZMAN, H., BROACH, J.R., DE VIRGILIO, C., HALL, M.N. and LOEWITH, R., 2007. Sch9 is a major target of TORC1 in *Saccharomyces cerevisiae*. *Molecular cell*, 26(5), pp. 663-674.

VAN HEUSDEN, G., NEBOHACOVA, M., OVERBEEKE, T. and STEENSMA, H., 1998. The *Saccharomyces cerevisiae* TGL2 gene encodes a protein with lipolytic activity and can complement an *Escherichia coli* diacylglycerol kinase disruptant. *Yeast*, 14(3), pp. 225-232.

VAN MEER, G., VOELKER, D.R. and FEIGENSON, G.W., 2008. Membrane lipids: where they are and how they behave. *Nature Reviews Molecular Cell Biology*, 9(2), pp. 112-124.

VANDER HEIDEN, M.G., 2011. Targeting cancer metabolism: a therapeutic window opens. *Nature Reviews Drug Discovery*, 10(9), pp. 671-684.

VARELA, J., PRAEKELT, U., MEACOCK, P., PLANTA, R. and MAGER, W., 1995. The *Saccharomyces-Cerevisiae* Hsp12 Gene is Activated by the High-Osmolarity Glycerol Pathway and Negatively Regulated by Protein-Kinase-a. *Molecular and cellular biology*, 15(11), pp. 6232-6245.

WAGNER, E.F. and NEBREDA, A.R., 2009. Signal integration by JNK and p38 MAPK pathways in cancer development. *Nature Reviews Cancer*, 9(8), pp. 537-549.

WALTHER, T.C. and FARESE, R.V., JR., 2012. Lipid Droplets and Cellular Lipid Metabolism. *Annual Review of Biochemistry*, Vol 81, 81, pp. 687-714.

WALTHER, T.C. and FARESE, R.V., JR., 2009. The life of lipid droplets. *Biochimica Et Biophysica Acta-Molecular and Cell Biology of Lipids*, 1791(6), pp. 459-466.

WANG, X., SHEFF, M.A., SIMPSON, D.M. and ELION, E.A., 2011. Ste11p MEKK signals through HOG, mating, calcineurin and PKC pathways to regulate the FKS2 gene. *Bmc Molecular Biology*, 12, pp. 51.

WARBURG, O., 1925. *Über den Stoffwechsel der Carcinomzelle (About the metabolism of the carcinoma cell)*. *Klin Wochenschr Berl*(4), pp. 534-536.

WARBURG, O., 1956. *On the origin of cancer cells*. *Science (New York, N.Y.)*, 123(3191), pp. 309-314.

WASKIEWICZ, A. and COOPER, J., 1995. Mitogen and Stress-Response Pathways - Map Kinase Cascades and Phosphatase Regulation in Mammals and Yeast. *Current opinion in cell biology*, 7(6), pp. 798-805.

WEI M, FABRIZIO P, HU J, GE H, CHENG C, LI L and LONGO VD, 2008. Life span extension by calorie restriction depends on Rim15 and transcription factors downstream of Ras/PKA, Tor, and Sch9. - *Curator Triage*; - Sgd, (1553-7390),.

WEI, M., FABRIZIO, P., MADIA, F., HU, J., GE, H., LI, L.M. and LONGO, V.D., 2009. Tor1/Sch9-Regulated Carbon Source Substitution Is as Effective as Calorie Restriction in Life Span Extension. *Plos Genetics*, 5(5), pp. e1000467.

WILFLING, F., WANG, H., HAAS, J.T., KRAHMER, N., GOULD, T.J., UCHIDA, A., CHENG, J., GRAHAM, M., CHRISTIANO, R., FROEHLICH, F., LIU, X., BUHMAN, K.K., COLEMAN, R.A., BEWERSDORF, J., FARESE, R.V., JR. and WALTHER, T.C., 2013. Triacylglycerol Synthesis Enzymes Mediate Lipid Droplet Growth by Relocalizing from the ER to Lipid Droplets. *Developmental Cell*, 24(4), pp. 384-399.

WU, J., HUANG, H.Y. and HOPPER, A.K., 2013. A rapid and sensitive nonradioactive method applicable for genome-wide analysis of *Saccharomyces cerevisiae* genes involved in small RNA biology. *Yeast (Chichester, England)*, 30(4), pp. 119-128.

YANG, L., XUE, Z., HE, Y., SUN, S., CHEN, H. and QI, L., 2010. A Phos-Tag-Based Approach Reveals the Extent of Physiological Endoplasmic Reticulum Stress. *Plos One*, 5(7), pp. e11621.

YANG, P., WANG, Y., PENG, X., YOU, G., ZHANG, W., YAN, W., BAO, Z., WANG, Y., QIU, X. and JIANG, T., 2013. Management and survival rates in patients with glioma in

China (2004-2010): a retrospective study from a single-institution. *Journal of neuro-oncology*, 113(2), pp. 259-266.

YANG, Y., HAN, W., MORIN, P., CHREST, F. and PIZER, E., 2002. Activation of fatty acid synthesis during neoplastic transformation: Role of mitogen-activated protein kinase and phosphatidylinositol 3-kinase. *Experimental cell research*, 279(1), pp. 80-90.

ZAIDI, N., LUPIEN, L., KUEMMERLE, N.B., KINLAW, W.B., SWINNEN, J.V. and SMANS, K., 2013. Lipogenesis and lipolysis: The pathways exploited by the cancer cells to acquire fatty acids. *Progress in lipid research*, 52(4), pp. 585-589.

ZARUBIN, T. and HAN, J., 2005. Activation and signaling of the p38 MAP kinase pathway. *Cell research*, 15(1), pp. 11-18.

ZEISEL, S.H. and DA COSTA, K., 2009. Choline: an essential nutrient for public health. *Nutrition reviews*, 67(11), pp. 615-623.

ZHAN, X. and GUAN, K., 1999. A specific protein-protein interaction accounts for the in vivo substrate selectivity of Ptp3 towards the Fus3 MAP kinase. *Genes & development*, 13(21), pp. 2811-2827.

ZHANG, Q., CHIEU, H., LOW, C., ZHANG, S., HENG, C. and YANG, H., 2003. *Schizosaccharomyces pombe* cells deficient in triacylglycerols synthesis undergo apoptosis upon entry into the stationary phase. *Journal of Biological Chemistry*, 278(47), pp. 47145-47155.